Ph D. Thesis

Design of a material surface for rapid biofilm formation and application to a membrane-aerated biofilm reactor for simultaneous nitrification and denitrification

バイオフィルムの迅速形成を可能にする材料表面の設計と
硝化脱窒逐次反応用の膜曝気型バイオフィルムリアクターへの応用

February 2006

Akihiko TERADA

寺田　昭彦

WASEDA UNIVERSITY

JUDGING COMMITTEE

Contents

Chapter 1

General Introduction

Chapter 2

Elucidation of dominant effect on initial bacterial adhesion onto polymer surface prepared by radiation induced graft polymerization

Chapter 3

Effects of electrostatic properties of positively charged polymer surfaces on bacterial adhesion and activity

Chapter 4

Significance of electrostatic properties of positively charged polymer surfaces on biofilm formation

Chapter 5

Enhancement of biofilm formation onto surface-modified hollow-fiber membranes and its application to membrane-aerated biofilm reactor

Chapter 6

Nitrogen removal characteristics and biofilm analysis of a membrane-aerated biofilm reactor applicable to high-strength nitrogenous wastewater treatment

Chapter 7

General conclusion and perspectives

Acknowledgement

Appendix

Summary of the dissertation

Curriculum vitae

Publication lists

Chapter 1

General Introduction

Chapter 1

General Introduction

<div style="text-align: right; font-size: 3em;">**1**</div>

Biological nitrogen removal,

mechanisms of bacterial adhesion and

subsequent biofilm formation, and

development of novel biofilm reactor

Summary

Nitrogenous compounds cause eutrophication, leading to a significant negative impact to aqueous environment. Essentially, removal of nitrogenous compounds is required for preservation of the aqueous environments. Nitrogen removal in wastewater not only from sewage plant but also industrial plant, *e.g.*, wastewaters from food processing, brewery, power plant, photo processing, livestock and so on, would be necessary. Considering the fact that some industrial plants do not have enough space for wastewater treatment process, small system applicable to nitrogen removal is required. Application of biofilms for biological nitrogen removal is very useful in that biofilm itself is very compact and robust, yielding high bacterial density in a reactor. Furthermore, most natural biofilms exhibit redox stratification and the presence of strong concentration gradients of both

electron donors and acceptors, resulting in simultaneous nitrification and denitrification. An engineering challenge is how we can control biofilm stiffness and maintain such redox stratification. Essentially, we need to chase the mechanism of biofilm formation and to make robust biofilms. In this chapter, biological nitrogen removal, basics of biofilm, initial bacterial adhesion and subsequent biofilm formation, and development of novel biofilm reactor with use of a gas-permeable membrane are described.

Published in (partly): A. Terada, K. Hibiya, S. Tsuneda, A. Hirata. "Novel water treatment system with hollow-fiber membranes" *Water and Purification and Liquid Water Treatment*, 44 (4), 153-164 (2003) (in Japanese)

1.1 Origin of nitrogen pollution

Nitrogen compounds are essential for all living organisms since it is a necessary element of DNA, RNA and proteins. Although it is composed of 78% of the earth's atmosphere as nitrogen gas, almost all bacteria except a few organisms cannot utilize this form of nitrogen directly. In many situations, fixed nitrogen is the limiting nutrient because its availability is usually much smaller than the potential uptake by, for example, plants (Pynaert, 2003). Hence, the supply of protein food for the global population by agriculture is recently dependent on the use of synthetic nitrogen fertilizer generated from atmospheric N_2 by the Haber-Bosch process. The global estimation for biological nitrogen fixation is in the range of 200-240 Mt nitrogen, which indicates that the mass flows for nitrogen have a major impact on the global nitrogen cycle (Gijzen and Mulder, 2001).

The consumption of protein will yield the discharge of organic nitrogenous compounds

in wastewater (Van Hulle, 2005). Some nitrogenous compounds derived from fertilizer accumulate and end up in wastewater in the form of ammonium or organic nitrogen. Other polluting nitrogenous compounds are nitrite and nitrate. Nitrate is originally used to make fertilizers, even though it is also used to make glass, explosives and so on. Nitrite is manufactured mainly for use as a food preservative. These nitrogenous compounds, *i.e.*, organic nitrogen, ammonia, nitrite and nitrate, exist ubiquitously.

 The discharge of these nitrogenous compounds into water environment results in several environmental and health problems. Essentially, ammonia is a nutrient for plants and it is responsible for eutrophication, *i.e.*, undesirable and excessive growth of aquatic plants and algae. Such excessive growth of the aquatic vegetables would cause a depletion of oxygen since they consumes oxygen in the water, which has a significant impact on viability of fish. Additionally, the growth of the vegetables determines oxygen and pH of the surrounding water. The greater the growth of algae, the wider the fluctuation in levels of dissolved oxygen (DO) and pH will be. This affects metabolic processes in organisms seriously, leading to their death. Besides that, some blue-green algae have a potential to produce algal toxins, which fatally kill fish and livestock that drink the water (Antia *et al.*, 1991). Ammonia itself is also toxic to water environmental organisms at concentration below 0.03 g-NH_3-N/L (Solbe and Shurben, 1989). Nitrate pollution impeded the production of drinking water critically. Nitrite and nitrate in drinking water can result in oxygen shortage of newly born, which is alternatively called 'blue baby syndrome' (Knobeloch *et al.*, 2001) and, during chlorination of drinking water, carcinogenic nitrosamines may be formed by the interaction of nitrite with compounds containing organic nitrogen. Therefore, nitrogenous compounds need to be removed from wastewater. For the removal of nitrogen, a wide variety of biological removal systems are available (Henze *et al.*, 1995).

1.2 Biological nitrogen removal

Inorganic nitrogen, which comes from domestic and industrial wastewater, is normally found in most reduced form, ammonia. In wastewater treatment, nitrogen removal with microorganisms (bacteria) is most widely applied in wastewater treatment plant because biological nitrogen removal is less costly and less harmful to water environment than physicochemical counterpart. In the biological nitrogen removal, complete nitrogen removal is achieved by two successive processes: nitrification and denitrification.

1.2.1 Nitrification process

Nitrification is the aerobic oxidation of ammonia to nitrate (Rittmann and MaCarty, 2001). It is an essential process prior to the actual nitrogen removal by denitrification. The process consists of two sequential steps that are performed by tow phylogenetically unrelated groups of aerobic chemolithoautotrophic bacteria and, to a minor extent, some heterotrophic bacteria. In the first step, ammonia is oxidized to nitrite by ammonia-oxidizing bacterial (AOB) and, in the second step, nitrite-oxidizing bacteria (NOB). Sometimes AOB and NOB are summarized as nitrifiers. The stoichiometry for both reactions is given in equations 1.1 and 1.2, respectively (U.S. Environmental Protection Agency, 1975). In these cases, typical values for AOB and NOB biomass yield are used as follows:

Ammonia oxidation (nitritation)

$$55NH_4^+ + 76O_2 + 109HCO_3^- \rightarrow C_5H_7NO_2 + 54NO_2^- + 57H_2O + 104H_2CO_3 \quad (1.1)$$

Nitrite oxidation (nitrataion)

$$400NO_2^- + NH_4^+ + 4H_2CO_3 + HCO_3^- + 195O_2 \rightarrow C_5H_7NO_2 + 3H_2O + 400NO_3^-$$

$$(1.2)$$
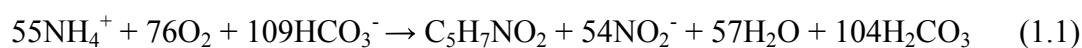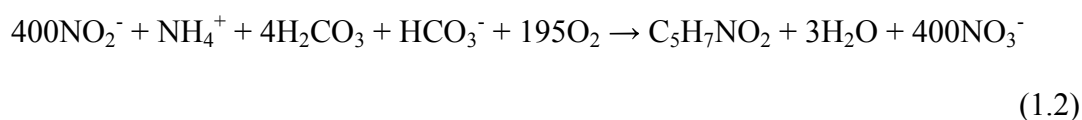
Both groups of bacteria are chemolithoautotrophic and obligatory aerobic. Autotrophic means that they definitely fix and reduce inorganic carbon dioxide (CO_2) for biosynthesis, which is an energy-expensive process. Such very unique characteristic of nitrifiers makes their yield values lower than that of aerobic heterotrophic bacteria. The fact that they utilize a nitrogen electron donor even lowers their cell yield due to less energy release per electron equivalent compared to organic electron donors. As a consequence, both AOB and NOB are considered slow growing bacteria. Molecular oxygen is utilized for endogenous respiration and conversion of reactant *i.e.,* ammonia or nitrite. It is generally known that nitrifies grow well at slightly alkaline pH (7.2-8.2) and temperature between 25-35°C (Sharma and Ahlert, 1977). At a pH below 6.5, no growth of AOB is observed probably due to limited ammonia availability at such low pH value (Burton and Prosser, 2001). The optimal DO for AOB and NOB is normally 3-4 $g\text{-}O_2/m^3$ (Barnes and Bliss, 1983), although levels of 0.5 $g\text{-}O_2/m^3$ (Hanaki *et al.*, 1990) and even 0.05 $g\text{-}O_2/m^3$ (Abeliovich, 1987) supported significant rates of ammonia oxidation but not nitrite oxidation (Bernet *et al.*, 2001).

1.2.2 Phylogeny of nitrifying bacteria

Nitrifying bacteria (nitrifiers) have minimal nutrient requirements owing to their true chemolithotrophic nature. Nitrifiers are obligate aerobes, and they use oxygen for respiration and as a direct reactant for the initial monooxygenation of ammonia (NH_4^+) to hydroxylamine (NH_2OH). The most commonly known genus of bacteria that carries out ammonia oxidation is *Nitrosomonas*; however, *Nitrosococcus, Nitrosopira, Nitrosovibrio,* and *Nitrosolobus* are also able to oxidize ammonia to nitrite. The AOB, which all have the genus prefix *Nitroso*, are genetically diverse, but related to each other in the β-subdivision of the proteobacteria (Teske *et al.*, 1994). This diversity suggests that

neither the *Nitrosomonas* genus nor any particular species within it (*e.g.*, *N. europaea*) necessarily is dominant in a given system.

Although *Nitrospira, Nitrospina, Nitrococcus*, and *Nitrocystis* are recognized as NOB to sustain themselves from nitrite oxidation, *Nitrobacter* is the most famous genus of the NOB. Within the *Nitrobacter* genus, several subspecies are distinct, but closely related genetically within the α-subdivision of the proteobacteria (Teske *et al*. 1994). Recent findings using oligonucleotide probes targeted to the 16S rRNA of *Nitrobacter*, which indicates that *Nitrobacter* is not the most important nitrite-oxidizing genus in most wastewater treatment processes. *Nitrospira* more often is identified as the dominant NOB (Aoi *et al.,* 2000). Since nitrifiers exist in water environment and wastewater treatment plants where organic compounds are present, such as in wastewater treatment plants, it might seem curious that they have not evolved to use organic molecules as their carbon source. While the biochemical reason that organic-carbon sources are excluded is not known, the persistence of their autotrophic dependence probably is related to their evolutionary link to photosynthetic microorganism (Teske *et al.*, 1994).

1.2.3 Differential behavior of AOB and NOB

Several environment conditions affects the activity AOB and NOB. Generally, the amount of nitrate defines NOB activity under aerobic conditions. By setting optimal conditions, we can theoretically achieve not nitrite but ammonia oxidation since NOB are more sensitive to detrimental environmental conditions, *e.g.*, unusual pH, low DO, temperature, solid retention time and so on, than AOB. Among the most important environmental parameters influencing ammonia and nitrite oxidation are the free ammonia (FA) and free nitrous acid (FNA) concentration, temperature, pH and DO concentration. Engineering challenge is how we can differentiate the activity of AOB

with NOB critically.

1.2.3.1 FA and FNA inhibition of nitrifiers

The uncharged nitrogen forms are considered to be the actual substrate/inhibitor for ammonia and nitrite oxidation. The amount of FA and FNA can be calculated form temperature and pH using following equilibrium equations:

$$NH_4^+ \quad \overset{K_b}{\rightleftharpoons} \quad NH_3 + H^+ \tag{1.3}$$

$$\text{With a typical } K_b \text{ value of } 5.68 \times 10^{-10} \text{ at } 25^\circ C \text{ and pH } 7$$

$$HNO_2 \quad \overset{K_a}{\rightleftharpoons} \quad NO_2^- + H^+ \tag{1.4}$$

$$\text{With a typical } K_a \text{ value of } 4.6 \times 10^{-4} \text{ at } 25^\circ C \text{ and pH } 7$$

where K_b and K_a are ionization constants of ammonia and nitrous acid, respectively. The NH_3 and HNO_2 concentrations can be calculated from equations 1.5 - 1.8 proposed by Anthonisen *et al.* (1976):

$$FAasNH_3(g/m^3) = \frac{17}{14} \times \frac{(NH_4^+ - N) \times 10^{pH}}{K_b / K_w + 10^{pH}} \tag{1.5}$$

$$K_b / K_w = e^{(6344/273+T)} \tag{1.6}$$

$$FNAasHNO_2(g/m^3) = \frac{46}{14} \times \frac{(NO_2^- - N)}{K_a \times 10^{pH}} \tag{1.7}$$

$$K_a = e^{(-2300+273+T)} \tag{1.8}$$

where NH_4^+-*N* and NO_2^--*N* are ammonia- and nitrite-nitrogen concentrations, *T* is temperature in ºC, respectively. For these equilibriums 1.5 and 1.7, *T* and *pH* of the solution will determine the concentrations of FA and FNA. The toxicity effect of this FA and FNA on the two groups of nitrifiers has been described regarding a diagram proposed by Anthonisen *et al.* (1976). The diagram (Figure 1.1), where the AOB are represented by *Nitrosomonas* and the NOB by *Nitrobacter*, indicates that inhibition of AOB by FA is likely in the rage of 10 to 150 g-N/m³ while NOB are likely inhibited at significant lower

concentrations of 0.1 to 1 g-N/m^3. In case of NOB, the key enzyme, a nitrite oxidoreductase (NOR), loses activity (Yang and Alleman, 1992). This difference in NH$_3$ sensitivity could give rise to nitrite accumulation when wastewater with high ammonia concentration is treated. However, adaptation of NOB to high FA levels is observed by Turk and Mavinic (1989). They reported that NOB appeared capable of tolerating ever-increasing levels of FA concentrations up to 40 g NH$_3$-N/m^3. At low pH less than 7, FNA affect the activity of AOB and NOB. According to Figure 1.1, a FNA concentration of 0.2-2.8 g HNO$_3$-N/m^3 inhibits NOB.
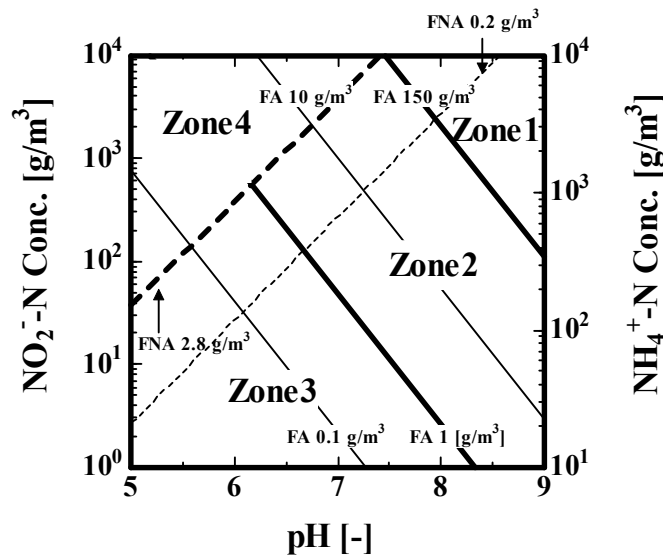
Figure 1.1 Dependence of free ammonia (FA) and free nitrous acid (FNA) on pH in the solution proposed by Anthonisen *et al.* (1976). Zone 1 shows FA inhibition of *Nitrobacter* and *Nitrosomonas*, Zone 2 shows FA inhibition of only *Nitrobacter*, Zone 3 shows complete nitrification, and Zone 4 shows FNA inhibition of *Nitrobacter*. Symbols: solid lines, FA of 0.1, 1, 10 and 150 mg l^{-1}, respectively; dotted lines, FNA of 0.2 and 2.8 mg l^{-1}.

1.2.3.2 Effect of oxygen

Both AOB and NOB require oxygen for their normal anabolism and catabolism. Low DO concentration will disrupt rates of ammonia and nitrite oxidation, leading to imbalance between the growth of AOB and NOB. The effect of DO on the specific growth rate of

nitrifiers is generally governed by the Monod equation, where affinity constant of oxygen K_{O2} is a determining parameter. Considering the report that the constant for AOB and NOB are 0.6 and 2.2 g-O_2/m^3, respectively (Wiesmann, 1994), K_{O2} value for AOB are lower than that for NOB, indicating a higher oxygen affinity of AOB than that NOB at low DO concentrations. In such oxygen-limited systems, this feature could lead to a decrease in the amount of nitrite oxidation and therefore accumulation of nitrite (Bernet *et al.*, 2001; Garrido *et al.*, 1997; Pollice *et al.*, 2002; Terada *et al.*, 2004).

Besides the direct inhibitory effect of low DO, there is also an indirect effect. AOB exposed to low DO levels have been shown to generate higher amounts of the intermediate hydroxylamine, which might be the determinant compound of nitrite build-up (Yang and Alleman, 1992). Kindaichi *et al.* (2004) clarified that the addition of hydroxylamine decreases the activity of NOB, which alternatively lead to an increase of AOB activity and changes of microbial community in an autotrophic nitrifying biofilm.

1.2.3.3 Effect of temperature

Temperature is a key parameter in the nitrification process; however, the exact influence has not been clarified because of the interaction between mass transfer, chemical equilibrium and growth rate dependency. Normally, both AOB and NOB have similar temperature ranges for their activities. Both organisms have maximum growth rates at a temperature of 35ºC (Grunditz and Dalhammar, 2001); however, they prefer moderate temperature (20-30ºC). The activities significantly decrease at temperatures below 20ºC and above 40-45ºC because of enzyme disruptions. Generally, AOB grow faster than NOB at temperatures of more than 25ºC, whereas this is reversed at lower temperatures around 15ºC. The SHARON process (Single reactor High activity Ammonia Removal Over Nitrite) employs such principle. In this process, nitritation, oxidation of ammonia to nitrite, is established in chemostat by operating under high temperature conditions (above

25ºC) and maintaining an appropriate sludge retention time (SRT), which is also a selection pressure between AOB and NOB. Such selective operation keeps AOB in the reactor, while NOB are washed out and further nitratation, oxidation of nitrite to nitrate, can be prevented. Nitrite build-up would be very useful when treating low carbon/nitrogen-containing wastewater because subsequent denitrification requires less organic carbon in case via nitrite than in that via nitrate.

Furthermore, considering the influence of temperature on microbial community between AOB and NOB, increased temperature will increase the ratio of NH_3/NH_4^+, possibly causing inhibitory effects on the NOB. Additionally, an increase of temperature decrease saturated DO concentration, leading to oxygen-limited conditions disrupting the imbalance of AOB and NOB with possible nitrite accumulation.

1.2.3.4 Effect of pH

In spite of a wide divergence of the reported effects of pH on nitrification, it is generally known that the optimum pH range for both AOB and NOB is from 7.2 to 8.2 (Pynaert, 2003). The range is also related to NH_3/NH_4^+ and NO_2^-/HNO_2 ratios, where FA and FNA can exhibit inhibitory effects starting from certain pH. Ammonia oxidation brings acidifying conditions when it occurs (see equation 1.1). If buffer capacity of this environment is too low, the pH will decrease rapidly. Below pH 7, nitrification rate decrease even though there are some reports of nitrifying activity in acidic environments (Burton and Prosser, 2001; Tarre *et al.*, 2004a, b).

1.2.4 Denitrification process

Denitrification is the dissimilatory reduction of nitrate or nitrite to mainly nitrogen gas. In other words, nitrate or nitrite is the electron acceptor used in energy generation. Denitrification normally occurs among heterotrophic and autotrophic bacteria, many of

which can shift between oxygen respiration and nitrogen respiration. Denitrifying bacteria (denitrifiers) are common among the Gram-negative *Proteobacteria*, such as *Pseudomonas*, *Alcaligenes*, *Paracoccus* and *Thiobacillus*. Some Gram-positive bacteria, including *Bacillus*, can also denitrify. Even a few halophilic Archaea, such as *Halobacterium*, are able to denitrify. The denitrifiers used in environmental biotechnology are chemotrophs that can use organic or inorganic electron donors. Those that utilize organic electron donors are heterotrophs and are widespread among the *Proteobacteria*. Inorganic electron donors also can be used and gaining popularity (Rittmann and MaCarty, 2001). Hydrogen (H_2) is an excellent electron donor for autotrophic denitrification. Its advantages include lower cost per electron equivalent compared to organic compounds, less biomass production than with heterotrophs, and absolutely no reduced nitrogen added. The main disadvantage of H2 in the past has been lack of a safe and efficient H_2 transfer system. The recent development of membrane-dissolution devices overcomes the explosion hazard of conventional gas transfer and makes H_2 a viable alternative (Lee and Rittmann, 2000, 2002). Reduced sulfur also can drive autotrophic denitrification. The most common source of reduced S is elemental sulfur, S(s), which is oxidized to SO_4^{2-}. The S normally is embedded in a solid matrix that includes a solid base, such as $CaCO_3$, because the oxidation of S(s) generates strong acid.

During biological heterotrophic denitrification, oxidized nitrogen forms are reduced and an organic electron donor is oxidized for energy conservation. This electron donor can be the organic material present in wastewater, or, in case of shortage, an externally added carbon source, *e.g.*, acetate. An example of a denitrification reaction is given in equation 1.9, where nitrate is denitrified to nitrogen gas with acetate as an electron donor.

$$CH_3COOH + 8/5\ NO_3^- + 4/5\ H_2O\ \rightarrow\ 4/5\ N_2 + 2\ H_2CO_3 + 8/5\ OH^- \quad (1.9)$$
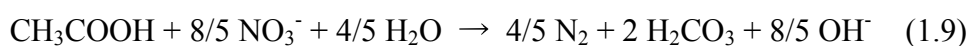
The pathways of denitrification are composed of four steps (equation 1.10). Each of the reduction steps is catalyzed by respective enzymes, *i.e.,* nitrate reductase, nitrite reductase, nitric oxide reductase and nitrous oxide reductase.

$$NO_3^- \rightarrow NO_2^- \rightarrow NO \text{ (gas)} \rightarrow N_2O \text{ (gas)} \rightarrow N_2 \text{ (gas)} \qquad (1.10)$$
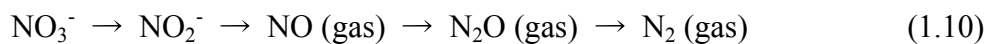
NO and N_2O are gaseous intermediates, which have to be avoided. Since the greenhouse effect of N_2O is reported to be 300 times higher than that of CO_2 (IPCC, 2001), emission of N_2O should be reduced from wastewater (Tsuneda *et al.*, 2005).

1.2.5 Application to novel nitrogen removal

1.2.5.1 Nitrogen removal via nitrite

As already mentioned in the previous chapters, nitrite is an intermediate in both nitrification and denitrification (Figure 1.2). Accumulation or discharge of nitrite should be harmful to aqueous environment; hence, nitrite should be removed properly. Normally, ammonia is converted into nitrate by AOB and NOB under aerobic conditions; subsequently the nitrate is converted into nitrogen gas by denitrifiers under anoxic conditions. Such pathway via nitrate requires more oxygen for nitrification and organic carbon for denitrification than that via nitrite. Numerous environmental engineers have been focusing on biological nitrogen removal via not nitrate but nitrite because of economical advantages. Concretely, the nitrification-denitrification via nitrite saves around 25% on oxygen input for nitrification and 40% of organic carbon for denitrification (Abeling and Seyfried, 1992; Bernet *et al.*, 1996; Eum and Choi, 2002; Oh and Silverstein, 1999; Turk and Mavinic, 1986). It also enables required hydraulic retention time (HRT) to decrease, which could achieve a small reactor volume.
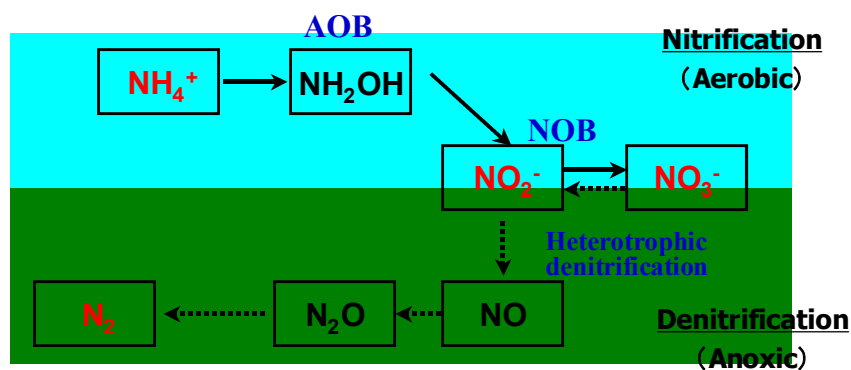
Figure 1.2 Schematic diagram of biological nitrogen removal pathway.

1.2.5.1 Simultaneous nitrification and denitrification with biofilm

Nitrification and denitrification are complementary in many ways: (1) nitrification produces nitrite or nitrate that is a reactant in denitrification; (2) nitrification reduces the pH that is raised in denitrification; and (3) denitrification generates the alkalinity that is required in nitrification (Rittmann and MaCarty, 2001). Therefore, there exists obvious advantage to carry out simultaneous nitrification and denitrification in a single reactor. In that case, it is essential to make redox stratification, *i.e.* reaction sites for aerobic and anoxic part in a single reactor. In this thesis, the author is focusing on bacterial aggregated layer on surfaces, biofilm. The Biofilms have chemical gradients because of its thickness, leading to creation aerobic and anoxic part inside; therefore, they can theoretically provide such stratification. Engineering challenges are how we can create such redox stratification in biofilms and how we can make robust biofilm. Biofilm itself and its potential toward biofilm reactor will be described in the next chapter.

1.3 Basics of biofilms and application to biofilm reactor

1.3.1 Why biofilms?

Bacteria tend to adhere onto surfaces. Once bacteria attach to a substratum surface, a multistep process starts leading to the formation of a complex and heterogeneous biofilm

(Bos *et al.*, 1999). Biofilms are layer-like aggregations of bacteria and their extracellular polymeric substances (EPSs) attached to a solid surface (Rittmann and MaCarty, 2001). Biofilms occur ubiquitously in nature and are increasingly important in engineered processes used in pollution control, *e.g.*, trickling filters, rotating biological contactors, membrane-aerated biofilm reactor and anaerobic filters. Biofilm processes are simple, reliable and stable because natural immobilization allows excellent biomass retention and accumulation without the need for separate solids-separation devices.

A biofilm can be sometimes formed by a single bacterial species, but more often biofilms consist of many species of bacteria, for instance, fungi, algae, protozoa, debris and corrosion products. The relative ratio of bacterial cells and EPS has been reported to vary significantly, from 10 to 90% of the organic matter (Nielsen *et al.*, 1997). EPS is mainly represented by polysaccharides (up to 65%) and is for this reason also known as the glycocalyx matrix. However, other substances are present, such as proteins (10-15%), nucleic acids, lipids, DNA and humic acids (Wingender *et al.*, 1999).

Here one fundamental issue about biofilm (actually, all aggregated systems) emerges: why do bacteria preferably attach to surfaces and belong to part of biofilm? Considering the issue, there are some answers as follows (Rittmann and MaCarty, 2001):

1. The biofilm create an internal environment (*e.g.*, pH, O_2, or products), which is more hospitable than the bulk liquid. In other words, the biofilm generates unique, self-created microenvironments, for example, aerobic and anoxic conditions in the same biofilm that could achieve simultaneous nitrification and denitrification (de Beer *et al.*, 1997)

2. Different bacterial species must live together in obligate consortia for substrate transport or some other synergistic relationships; the close juxtaposition of cells in a biofilm, *e.g.*, AOB and NOB, is necessary for the

exchanges (James *et al.*, 1995).

3. The surface itself creates a unique microenvironment, such as by adsorption of toxins or corrosive release of Fe^{2+}, which is an electron donor.

4. The surface triggers a physiological change in the bacterial.

5. The tight packing of cells in the aggregate alters the cells' physiology.

Possibilities 1-3 involve microenvironment effects and seem to occur in specific instances. They are forms of ecological selection, and biofilm formation is one tool for ecological control of a process. Evidence to support possibility 4 is spare for systems of relevance to environmental biotechnology, although it may by important for specific interactions between bacteria and surfaces. Possibility 5 is often called "quorum sensing", and evidence of its role in biofilms and other aggregates is just emerging (Miller and Bassler, 2001).

1.3.2 Mechanisms of biofilm formation

The formation of a biofilm in an aqueous environment is generally illustrated to proceed as follows (Bos *et al.*, 1999; Bryers, 2000) (Figure 1.3):

1. A conditioning film of adsorbed components is formed on the surface prior to the arrival of the first coming bacteria.

2. Bacteria are transported to the surface through diffusion, convection, sedimentation or active movement.

3. Initial microbial adhesion occurs From the physicochemical aspects of the bacterial adhesion phenomenon, since individual cell size is more or less 1 μm, cell surface characteristics, such as surface electric potential, hydrophobicity and surface polymer structure, play significant roles in bacterial adhesion (Bos *et al.*, 1999; Hayashi *et al.*, 2001; Hayashi, 2002;

Rutter *et al.*, 1984). This phenomenon is a reversible step.

4. Attachment of adhering microorganisms is strengthened through secretion of EPSs and unfolding of cell surface structures. This step is an irreversible step.

5. Surface growth of attached bacteria and continued secretion of EPSs.

6. Localized detachment of biofilm organisms caused by occasionally high fluid shear or other detachment forces.

Localized detachment of biofilm organisms commences after initial adhesion, although adhesion of individual bacteria is often considered irreversible. The ratio of detachment event could be dependent of interaction between bacterial cells and physicochemical surface characteristics, flow rate in the bulk and so on. The importance of the studied of the initial bacterial adhesion in biofilm formation has been questioned because the number of cells in a mature biofilm after the growth phase is several times higher that involved in the initial bacterial adhesion (Fox *et al.*, 1990; Petrozzi *et al.*, 1993). However, Busscher *et al.* (1995) proposed the significance of bacteria that initially adhere as the link between the colonized surface and the biofilm. Regarding initial bacterial adhesion onto a substratum, electrostatic force is considered to be the most important, because it is markedly influenced by the surface potentials of both bacterial cells and the substratum or the chemical properties of the solution, that is, ionic concentration and valence of ions (Terada *et al.*, 2005).
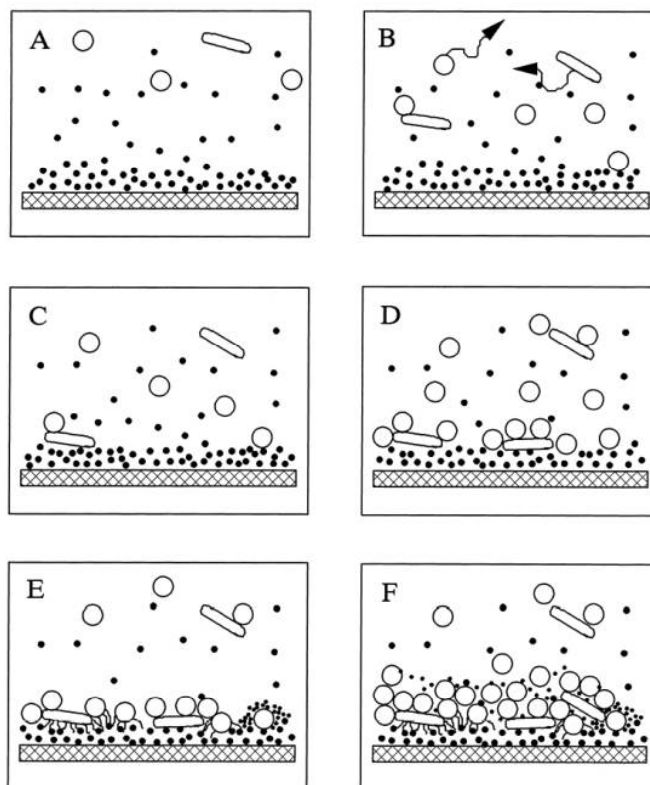
Figure 1.3 sequential illustrations of the initial steps in biofilm formation. A: Adsorption of conditioning film components; B: microbial transport and coaggregation; C: adhesion of single bacterial cells and of microbial coaggregates; D: co-adhesion between microbial pairs; E: anchoring or the establishment of firm, irreversible adhesion through secretion of EPSs; F: biofilm growth and detachment (From Bos *et al.* 1999).

1.3.3 Biofilm detachment

Detachment is an event by definition balancing the growth of a biofilm in steady state (van Loosdrecht *et al.*, 1995). It can be defined as the transport of particles from the attached solid matrix into the fluid phase. Attachment can be considered as a separate process or included in the detachment, leading to a net detachment rate. There are four different types of detachment as follows:

1. Erosion: a continuous process by which relatively small pieces of biofilm are removed from the biofilm's surface.

2. Abrasion: removal of small groups of bacterial cells from the surface as a result of collision with particles, *e.g.*, in fluidized bed or biofilm airlift reactors, or during backwash of fixed beds.

3. Sloughing: an abrupt, intermittent loss of a large section of biofilm..

4. Grazing: protozoa prey bacterial cells in a biofilm

Sloughing can result in drastic changes in the local biofilm accumulation (Rittmann and MaCarty, 2001). Considering that biofilm should be robust in a reactor for wastewater treatment, we should set a carrier, which would help bacterial cells to attach very firmly and robustly.

1.3.4 Application of fluorescence in situ hybridization (FISH) to microbial biofilms

      1.3.4.1 FISH

FISH is a powerful molecular technique, allowing for detection of phylogenetically targeted microorganisms. Advantageous points of FISH technique are reviewed by Aoi. (2003). According to the work, this technique illuminates spatial distribution of the targeted microorganisms even in a thick specimen, *e.g.* biofilm and sediment samples. Regarding bacteria and archaea, 16S rRNA gene is targeted. Oligonucleotide probe with sequences complementary to a targeted site in 16S rRNA gene is labeled with fluorochrome, each of which has inherent excitation and emission wavelengths (Amann *et al.*, 1990). According to the previous literature (Aoi, 2002), the rationales for selection of 16S rRNA gene as a target are three-fold: (i) all bacteria and archaea embrace 16S rRNA gene; (ii) the database is sufficiently provided; and (iii) the gene can be detected by either an epifluorescence microscopy or confocal laser scanning microscopy (CLSM).

      1.3.4.2 Combination of FISH technique with other methods

FISH technique has been applied to biological specimens in combination with a

sub-cloning or fingerprinting method, *e.g.* denaturing gradient gel electrophoresis (DGGE). The combination of these techniques allows one to acquire information on identification of unidentified bacteria, by a sub-cloning or fingerprinting method like DGGE, and subsequently the spatial location by FISH technique. A whole scheme of this analysis on 16S rRNA gene can be found in the previous literature (Amann *et al.*, 1995).

A microsensor with its tip diameter within the micrometer level allows attainment of *in situ* substrate profiles with rapid response time in a non-destructive manner. A Clark-type microsensor, *e.g.* DO microelectrode, is based on diffusion of oxygen through a silicon layer embedded at the edge of the microsensor tip (Kühl and Revsbech, 2001). There are several variations of Clark-type microsensors, *e.g.* N_2O, H_2S, H_2 and so on. In addition, microsensors for ionic compounds, *e.g.* NH_4^+, NO_2^-, NO_3^- and so on, can be also fabricated, allowing for these ionic concentration profiles in micrometer scale. Combination of FISH technique with microsensors has been applied to biofilms for sulfate reduction (Ramsing *et al.*, 1993), nitrification (Okabe *et al.*, 1999; Schramm *et al.*, 1996, 1988, 1999) and nitrification/denitrification (Hibiya *et al.*, 2003; Schramm *et al.*, 2000; Terada *et al.*, 2003). These studies elucidated both spatial distribution of targeted bacteria and their *in situ* activities, unveiling functions of the biofilms and potential implications for bioreactor performances (Figure 1.4).

1.3.4.3 In situ observation of nitrifying biofilms

Nitrification is generally mediated by chemolithoautotrophic bacteria, *i.e.* AOB and NOB. This means that their growth rates are not as high as those of heterotrophic bacteria. Given this point, nitrifying bacteria are potentially washed out from a bioreactor at any inconvenient operation conditions. Therefore, keeping nitrifying bacteria in a bioreactor system is a big engineering challenge. In other words, activated sludge is not always the best option to achieve organic carbon oxidation and nitrification with short hydraulic
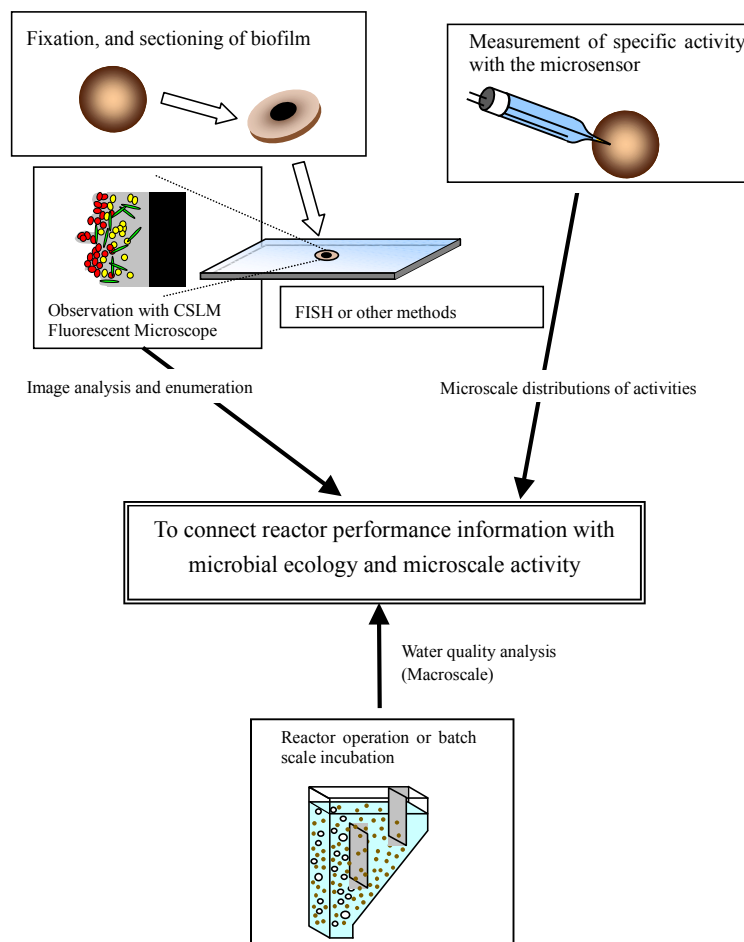
Figure 1.4 Schematic illustration of the analysis of the *in situ* organization of a biofilm community using various methods and the connection with reactor performance (partly from Aoi, 2002).

retention time. In order to ensure a certain degree of nitrification in a bioreactor system, immobilization of nitrifying bacteria is of promise. As summarized elsewhere (Aoi, 2003), several methods for immobilization of nitrifying bacteria have been proposed, *e.g.* the use of robust biofilm produced by heterotrophic bacteria as a scaffold (Tsuneda et al., 2000), a gel entrapment method (Sumino *et al.*, 1992), entrapment in a three-dimensional matrix of a fibrous material (Hayashi *et al*, 2002), and surface modified materials to electrostatistically attract bacterial cells (Hibiya et al., 2000, 2003; Terada et al., 2003). To confirm the presence of nitrifying bacteria in a biofilm, application of FISH technique can be meaningful.

By using available oligonucleotide probes, spatial distribution of even phylogenetically different AOB and NOB can be attained. Previous researches have demonstrated niche differentiation of phylogenetically different AOB and NOB in a nitrifying biofilm (Okabe *et al.*, 1999; Satoh *et al.*, 2003; Schramm *et al.*, 2000). Furthermore, combination of FISH technique with microsensor application even allowed *in situ* activity of specific AOB in the level of a single cell resolution (Schramm *et al.*, 1999). As reviewed by Aoi (2002), the attainment of *in situ* activity and spatial location of targeted bacteria leads to elucidation of unexplored biofilm functions and development of an exquisite biofilm model incorporating bacterial activities in a microscale level.

1.3.5 Surface modification by grafting method -toward enhancement of biofilm formation-

As mentioned in the chapter *1.3.3*, the sloughing from the base biofilm would be a serious problem in a biofilm reactor because almost all of the biofilm is removed from a substratum. When the biofilm has redox stratification, *i.e.*, aerobic and anaerobic part, the problem itself would become serious; all biofilm function would lose completely. Busscher *et al.* (1995) proposed that the strength between adhering bacteria and a substratum surface is determinant on biofilm strength and resistance against sloughing.

The author think consider surface modification that makes bacteria easy to attach onto the surface swiftly and robustly since initial bacterial adhesion is one of significant factor to determine biofilm property, *e.g.*, biofilm density, thickness and activity. In this study, the author is focusing on radiation induced graft polymerization (RIGP) (Figure 1.5). RIGP is one of the techniques for modifying polymeric materials with new properties. Irradiation with electron beam or gamma-rays onto a polymeric material (trunk polymer) produces radicals (reaction sites) in the polymer, Using radicals as starting sites for

polymerization, vinyl monomers that come into contact are polymerized to form polymeric brushes (polymer chains or branch polymers) (Kawai *et al.*, 2003). Although other excitation sources such as plasma and UV light can also produce radicals on the trunk polymer, RIGP is powerful in that it can introduce a high density of polymeric brushes bearing functional groups into the entire volume of the trunk polymer uniformly (Lee, 1997). The advantages of RIGP are:

1. A selectivity and chemically physically stable polymeric materials;

2. A wide application various types and shapes of polymeric materials;

3. A wide range of applicable reaction temperature; and

4. An easiness of controlling the distribution of reaction sites in the trunk polymer.

This technique can be used to maintain the physical strength and chemical stability of the trunk polymer while appending various functionalities to the trunk polymer, for instance, ion-exchange function, microbial-cell-capturing function, metal-ion-chelating function and catalytic function.

Application this method to enhancement of bacterial adhesion would be promising because of two reasons:

1. Bacterial cell surface has originally negative charges at neutral pH range.

2. By using RIGP, trunk polymer can be changed into the surface with positively charged.

Lee *et al.* (1996) reported that application of RIGP to polyethylene (PE) fiber, concretely PE was modified in order to have positively charged surface, can make *Staphylococcus aureus* cells-capturing ability increase up to 1000-fold faster than the original trunk polymer, PE. In addition, they suggested that polymer chains on the PE capture a bacterial cell softly, which remains bacterial activity (Figure 1.6). On the other hand,

Hibiya et al. (2000) reported that a nitrifying biofilm forms successfully on the surface modified sheets, which are originally made of PE, under high hydrodynamic conditions. However, there are some issues to be clarified: is there the link between initial bacterial adhesion and subsequent biofilm formation?; how is the activity of the adhering bacteria?; and can we generalize bacterial adhesion behavior statistically?.
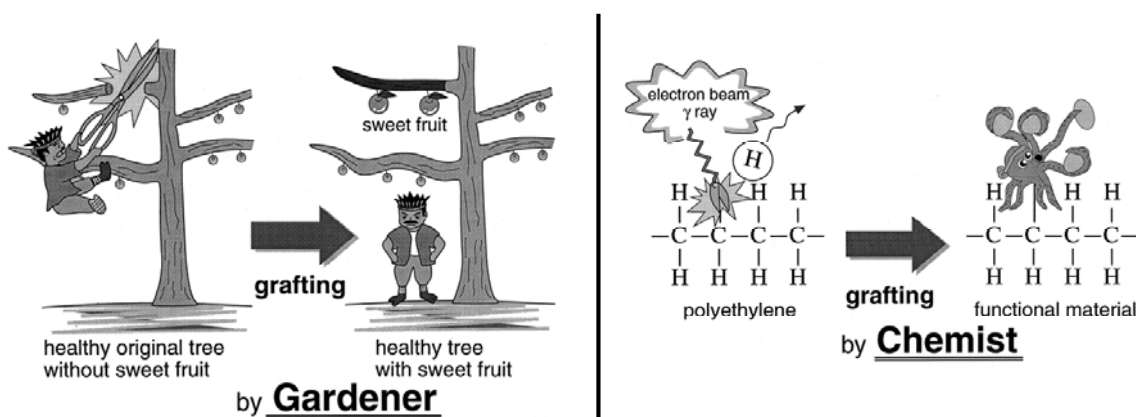
Figure 1.5 An illustration of radiation-induced graft polymerization (From Saito *et al.* 1999).
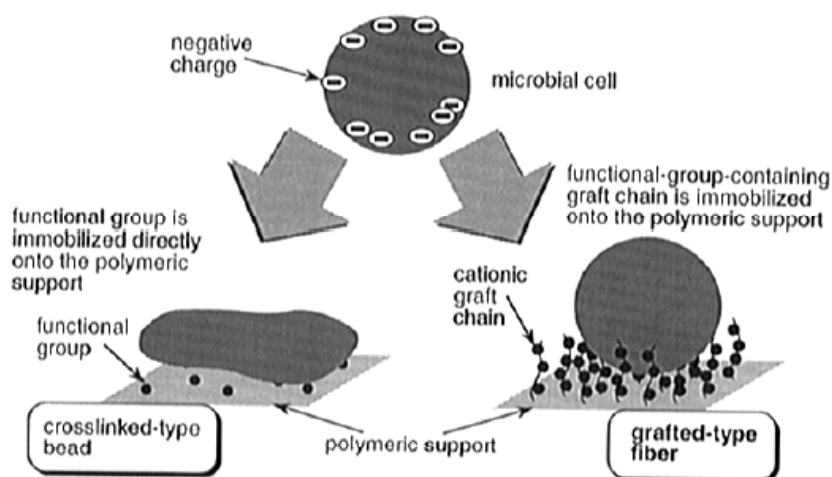
Figure 1.6 Suggested images for the adsorption of bacterial cell onto two kinds of polymers (from Lee *et al.*, 1996).

1.3.6 Novel biofilm reactor applicable to simultaneous nitrification and denitrification

-with use of membrane-aerated biofilm-

Interestingly, most natural biofilms exhibit redox stratification and the presence of strong concentration gradients of both electron donors and acceptors (Amann and Kühl, 1998; Schramm 2003). The oxygen level in most natural biofilms is modulated by external factors such as flow, light or organic loading, and consequently the redox conditions often show a pronounced spatial heterogeneity over timescales ranging from hours to days. While redox gradients can, thus, establish in natural biofilms and traditional biofilm reactors, they lack the system control measures required for precise manipulation of multiple biochemical environments within a single bioreactor unit.

Membrane-aerated biofilm reactors (MABRs) are an emerging technology that could permit a more rigorous oxygen control (Brindle et al., 1996, 1998; Casey et al., 1999; Pankhania *et al.*, 1994; Suzuki *et al.*, 1993, 2000; Yamagiwa *et al.*, 1994, 1998). Gas permeable membranes, which can be fabricated from a variety of polymers (poly (dimethylsiloxane), polyethylene and polypropylene in single or multiple layer) with different functional properties, permit bubbleless aeration and very high oxygen transfer rates (Ahmed et al., 2004; Cote et al., 1989). There are two types of aeration: flow thorough and dead-end (Figure 1.7). Such aeration type is dependent on what kind of membrane is used. Characterization of the aeration types is summarized in Table 1.1.

By growing the desired microorganisms on gas-permeable membranes, with oxygen delivered through the membrane at the base of the biofilm, and the other nutrients provided to the surface of the biofilm from the water within which the membranes are suspended, redox-stratified biofilms can be attained. Such counter diffusing fluxes of oxygen and other nutrients are, additionally, amenable to separate manipulation, yielding unprecedented opportunities for control. It is expected that MABRs would be suitable to

create the redox stratification in the biofilms, leading to simultaneous nitrification and denitrification from organic carbon-containing wastewater (Figure 1.8). Some researchers clarified that such simultaneous reaction would be feasible from mathematical modeling (Bell *et al.* 2005; Shanahan and Semmens, 2004) and from experimental work (Cole *et al.*, 2003; Hibiya *et al.*, 2003; Satoh *et al.* 2004; Semmens *et al.*, 2003; Timberlake *et al.* 1988; Terada *et al.*, 2003). Therefore, we need to verify some issues regarding MABRs, *e.g.*, whether biofilm forms on a membrane surface; whether we need to modify membrane surface to enhance biofilm formation; whether redox stratification is properly created by appropriate oxygen transfer and whether shortcut nitrogen removal via nitrite (nitrate) is feasible or not.

Table 1.1 Variation of membrane material and its characterization

	Non-porous membrane	Porous-membrane	Composite membrane
Property	Normally hydrophobic (it depends on time)		
Oxygen transfer	Dissolved	Through pores	Through pores and dissoved
Driving force of oxygen transfer	Diffusion	Diffusion or convection (it depends on operation)	Diffusion and convection
Bubbling point	High	Low	Extremely high
Cost	High	Low	High
Biofilm formation	Difficult	Easy	Easy
Specific membrane surface area	Small	Large	Large
Membrane wall	Thick	Thin	Thin
Aeration type	Cross-flow	Cross-flow/dead-end	Dead end

(a)

(b)
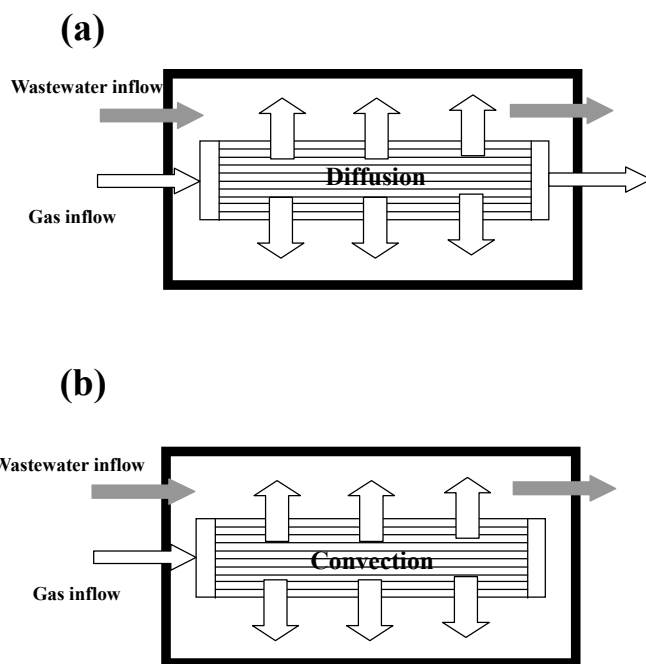
Figure 1.7 Composition of membrane module: (a) cross-flow system; (b) dead-end system.

(a) Conventional biofilm   **(b) Membrane-aerated biofilm**
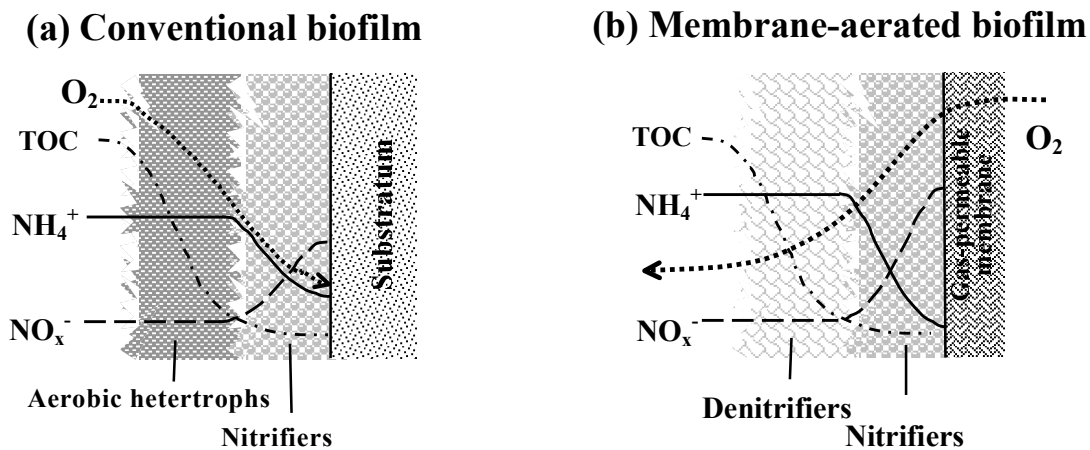
Figure 1.8 Comparison of biofilm structures for organic carbon and nitrogen removal: (a) conventional biofilm on an impermeable support; (b) proposed biofilm grown on an oxygen-permeable membrane

1.4 Objective of this study

The final objective of this study is to create stable redox stratification in a biofilm and to develop novel biofilm reactor applicable to simultaneous nitrification and denitrification. The overview of the thesis is illustrated in Figure 1.9. For achieving these goals, a challenge is how we can make swift biofilm formation and robust biofilms. Therefore, the author conducted these experiments:

1. Initial bacterial adhesion experiment: the author clarified the determinant factor on initial bacterial adhesion. Since RIGP is a very powerful method to prepare the sheets with different physicochemical properties, *e.g.*, surface roughness and surface potential, for the adhesion experiment, various membrane sheets with different properties were prepared and subsequently the initial bacterial adhesion onto the prepared surfaces were carried out (Chapter 2).

2. Bacterial adhesion and activity experiment: the relationship bacterial adhesion rates onto the surface modified sheets and their activity were investigated. And discussion whether or not the surface modified sheets would be useful for enhancement of biofilm formation is summarized in Chapter 3.

3. Biofilm formation test: the relationship between initial bacterial adhesion and the subsequent biofilm formation is linked with use of a flow cell. And some corroborative experiments were conducted to support the result of the flow cell. Through these experiment, the effectiveness of surface modified sheets was evaluated (Chapter 4).

4. Primary nitrification test: Initial adhesion of nitrifying bacteria and biofilm formation were investigated to clarify the effectiveness of the surface

modified hollow-fibers for rapid biofilm formation. Moreover, MABR, which employed the modified hollow-fiber module, was constructed and operated for nitrification test. Especially, controllability, *i.e.*, the relationship supplied oxygen and ammonia oxidation, was evaluated (Chapter 5).

5. Simultaneous nitrification and denitrification test with MABR: the MABR has been operated for one year to chase process performance from macroscale and microscale analyses. Regarding the microscale evaluation, the combination of FISH and microsensor was employed to verify the concept of membrane-aerated biofilm. Furthermore, the feasibility of simultaneous nitrification and denitrification via nitrite was discussed (Chapter 6).
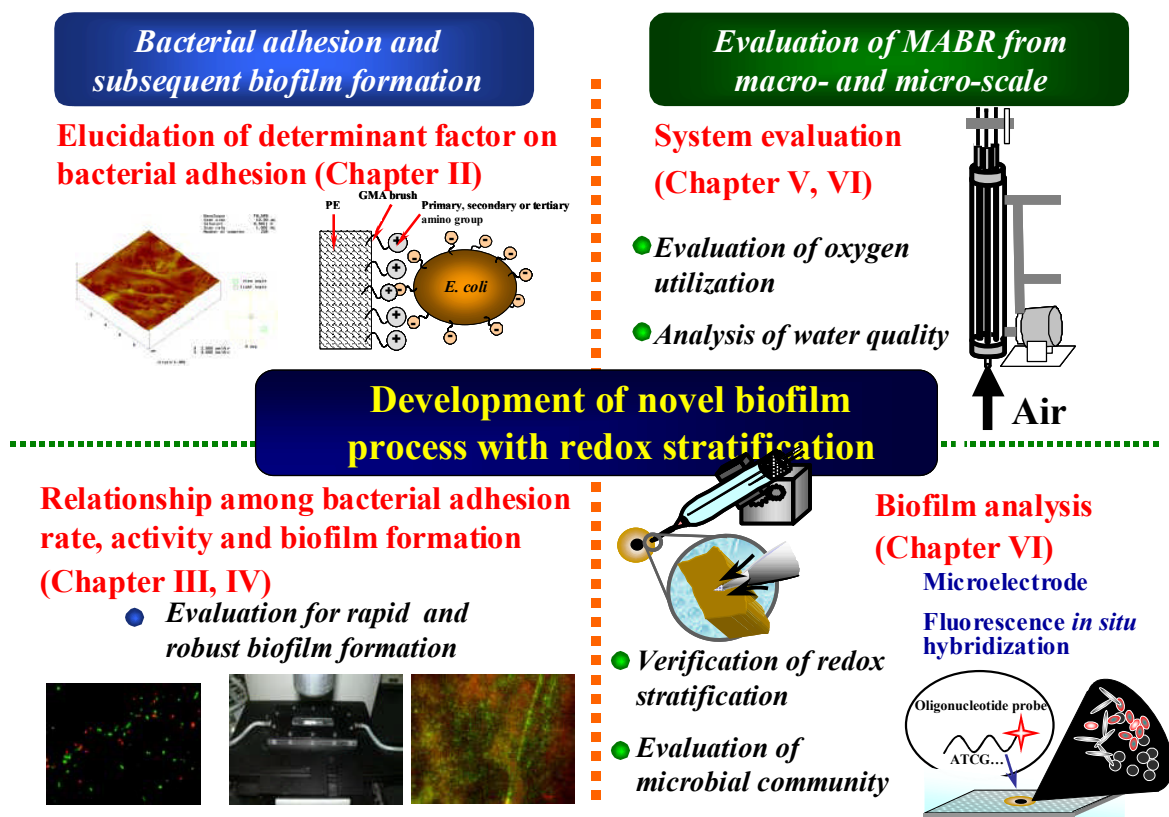
Figure 1.9 Outline of this thesis.

References

Abeling U, Seyfried CF. 1992. Anaerobic-aerobic treatment of high-strength ammonia wastewater-nitrogen removal via nitrite. Water Sci Technol 26:1007-1015.

Abeliovich A. 1987. Nitrifying bacteria in wastewater reservoirs. Appl Environ Microbiol. 53:754-760.

Ahmed T, Semmens MJ, Voss MA. 2004. Oxygen transfer characteristics of hollow-fiber, composite membranes. Adv Environ Res 8: 637-646.

Amann RI, Krumholz L, Stahl DA. 1990. Eluorescent-oligonucleotide probing of whole cells for determinative, phylogenetic, and environmental studies in microbiology. J Bacteriol 172:762-770.

Amann RI, Ludwig W, Schleifer KH. 1995. Phylogenetic identification and in situ detection of individual microbial cells without cultivation identification. Microbiol Rev 59:143-169.

Amann R, Kühl M. 1998. *In situ* methods for assessment of microorganisms and their activities. Curr Opi Microbiol 1:352-358.

Anthonisen AC, Loehr RC, Prakasam TBS, Srinath EG. 1976. Inhibition of nitrification by ammonia and nitrous acid. J Water Poll Contr Fed 48:835-852.

Antia NJ, Harrison PJ, Oliveira L. 1991. The role of dissolved organic nitrogen in phytoplankton nutrition, cell biology and ecology. Phycologia 30:1-89.

Aoi Y, Miyoshi T, Okamoto T, Tsuneda S, Hirata A. 2000. Microbial ecology of nitrifying bacteria in wastewater treatment process examined by fluorescence in situ hybridization. J Biosci Bioeng 90:234-240.

Aoi Y. 2002. In situ identification of microorganisms in biofilm communities. J Biosci

Bioeng 94:552-556.

Aoi Y. 2003. In situ identification and activities of nitrifying bacteria in biofilm communities and its application to wastewater treatment processes. Ph.D. thesis. Waseda University

Barnes D, Bliss PJ. 1983. Biological control of nitrogen in wastewater treatment. Spon Pr. London. UK.

Bell A, Aoi Y, Terada A, Tsuneda S, Hirata A. 2005. Comparison of spatial organization in top-down- and membrane-aerated biofilms: A numerical study. Water Sci. Technol 52 (7):173-180.

Bernet N, Moletta R. 1996. Denitrification by anaerobic sludge in piggery wastewater. Environ Technol 17:293-300.

Bernet N, Dangcong P, Delgène P, Steyer JP, Moletta R. 2001. Nitrification at alow oxygen concentration in biofilm reactor. J Environ Eng 127:266-271.

Brindle K, Stephenson T. 1996. The application of membrane biological reactors for the treatment of wastewaters. Biotechnol Bioeng 49:601-610.

Brindle K, Stephenson T, Semmens MJ. 1998. Nitrification and oxygen utilization in a membrane aeration bioreactor. J Membr Sci 144:197-209.

Bryers JD. 2000. Biofilms II: analysis, process, and applications. Wiley-Liss New York USA.

Bos R, van der Mei H, Busscher H J. 1999. Physico-chemistry of initial microbial adhesive interactions-its mechanisms and methods for study. FEMS Microbiol Rev 23:179-230.

Burton SAQ, Prosser JI. 2001. Autotrophic ammonia oxidation at low pH through urea hydrolysis. Appl Environ Microbiol 67: 2952-2957.

Busscher HJ, Bos R, van der Mei HC. 1995. Initial microbial adhesion is determinant for

the strength of biofilm formation. FEMS Microbiol Lett 128:229-234.

Casey E, Glennon B, Hamer G. 1999. Review of membrane aerated biofilm reactor. Res Consev Recycl 27:203-215.

Cole AC, Semmens MJ, LaPara TM. 2004. Stratification of activity and bacterial community structure in biofilms grown on membranes transferring oxygen. Appl Environ Microbiol 70:1982-1989.

Cote P, Bersillon JL, Huyard A. 1989. Bubble-free aeration using membranes: mass transfer analysis. J Membr Sci 47: 91-106.

De Beer D, Schramm A, Santegoeds CM, Kuhl M. 1997. A nitrite microsensor for profiling environmental biofilms. Appl Environ Microbiol 63:973-977.

Eum Y, Choi E. 2002. Optimization of nitrogen removal from piggery waste by nitrite nitrification. Water Sci Technol 45:89-96.

Fox P, Suidan MT, Brandy JT. 1990. A comparison of media types in acetate fed expanded-bed anaerobic reactors. Water Res 24: 827-835.

Garrido JM, van Benthum WAJ, van Loosdrecht MCM, Heijnen JJ. 1997. Influence of dissolved oxygen concentration on nitrite accumulation in a biofilm airlift suspension reactor. Biotechnol Bioeng 53:168-178.

Hanaki K, Wantawin C, Ohgaki S. 1990. Nitrification at low-levels of dissolved-oxygen with and without organic loading in a suspended-growth reactor. Water Res 24:297-302.

Hayashi H, Tsuneda S, Hirata A, Sasaki H. 2001. Soft particle analysis of bacterial cells and its interpretation of cell adhesion behaviors in terms of DLVO theory. Colloids Surf B: Biointerfaces 22:149-157.

Hayashi H, Ono M, Tsuneda S, Hirata A. 2002. Three-dimensional immobilization of bacterial cells with a fibrous network and its application in a high-rate fixed-bed

nitrifying bioreactor. J Chem Eng Jpn 35:68-75.

Hayashi H. 2002. The electrokinetic characterization of bacterial cells and its application to the biological wastewater treatment process. PhD thesis. Waseda University.

Henze M, Harremoes P, LaCour Iansen J, Arvin E. 1995. Wastewater treatment: Biological and chcemical processes. Springler-Verlag, Berlin, Germany.

Hibiya K, Tsuneda S, Hirata A. 2000. Formation and characteristics of nitrifying biofilm on a membrane modified with positively-charged polymer chains. Colloids Surf. B: Biointerfaces 18:105-112.

Hibiya K, Terada A, Tsuneda S, Hirata A. 2003. Simultaneous nitrification and denitrification by controlling vertical and horizontal microenvironment in a membrane-aerated biofilm reactor. J Biotechnol 100:23-32.

IPCC, Climate Change. 2001. The scientific basis. Contribution of working group 1 to the third assessment report of the intergovernmental panel on climate change. Chambridge University Press. Cambridge UK.

Gijzen HJ and Mulder A. 2001. The nitrogen cycle out of balance. Water 21 8:38-40.

Grunditz C, Dalhammar G. 2001. Development of nitrification inhibition assays using pure cultures of *Nitrosomonas* and *Nitrobacter*. Water Res 35:433-440.

James GA, Beudette L, Costerton JW. 1995. Interspecies bacterial interactions in biofilms. J Ind. Microbiol. 15:257-262.

Kawai T, Saito K, Lee W. 2003. Protein binding to polymer brush, based on ion-exchange hydrophobic, and affinity interactions. J Chromatography B 790:131-142.

Kindaichi T, Okabe S, Satoh H, Watanabe Y. 2004. Effects of hydroxylamine on microbial community structure and function of autotrophic nitrifying biofilms determined by in situ hybridization and the use of microelectrodes. Water Sci

Technol 48 (11-12):61-68.

Knobeloch L, Salna B, Hogan A, Postle J, Anderson H. 2000. Blue babies and nitrate-contaminated well water. Environ Health Perspectives 108:675-678.

Kühl M, Revsbech NP. 2001. Biogeochemical microsensors for boundary layer studies, pp. 180-210. *In* Boudreau BP, Jørgensen BB. (eds.), The Benthic Boundary Layer, Oxford University Press. New York.

Lee KC, Rittmann BE. 2000. A novel hollow-fiber biofilm reactor for autohydrogenotrophic denitrification of drinking water. Water Sci Technol 41:219-216.

Lee KC, Rittmann BE. 2002. Applying a novel autohydrogenotrophic hollow-fiber membrane biofilm reactor for denitrification of drinking water. Water Res 36:2040-2052.

Lee W, Furusaki S, Saito K, Sugo T, Makuuchi K. 1996. Adsorption kinetics of microbial cells onto a novel brush-type polymeric material prepared by radiation-induced graft polymerization. Biotechnol Prog 12:178-183.

Lee W. 1997. Study on charged brushes grafted in polymeric materials by radiation-induced graft polymerization and their applications as functional materials. PhD thesis Tokyo University.

Miller MB, Bassler BL. 2001. Quorum sensing in bacteria. Annual Rev Microbiol 55:165-199.

Nielsen PH, Jahn A, Palmgren R. 1997. Conceptual model for production and composition of exopolymers in biofilms. Water Sci Technol 36 (1):11-19

Oh J, Silverstein J. 1999. Acetate limitation and nitrite accumulation during denitrification. J Environ Eng 125:234-242.

Pankhania T, Stephenson T, Semmens MJ. 1994. Hollow fiber bioreactor for wastewater treatment using bubbleless membrane aeration. Water Res 28:2233-2236.

Petrozzi S, Kut OM, Dunn IJ. 1991. Protection of biofilms against toxic shocks by the

adsorption and depsorption capacity of carriers in anaerobic fluidized bed reactors. Bioprocess Eng 9:47-59.

Pollice A, Tandoi V, Lestingi C. 2002. Influence of aeration and sludge retention time on ammonia oxidation to nitrite and nitrate. Water Res 36:2541-2546.

Pynaert K. 2003. Nitrogen removal in wastewater treatment by means of oxygen-limited autotrophic nitrification-denitrfication. PhD thesis. Ghent University

Ramsing NB, Kuhl M, Jorgensen BB. 1993. Distribution of sulfate-reducing bacterial, O_2, and H_2S in photosynthetic biofilms determined by oligonucleotide probes and microelectrodes. Appl Environ Microbiol 59: 3840-3849.

Rittmann BE, McCarty PL. 2001. Environmental biotechnology: Principles and applications. McGraw-Hill Book Co. New York. USA.

Rutter P R, Vincent B, Marshall KC. 1984. Microbial adhesion and aggregation. Springer-Verlag New York USA.

Saito K, Tsuneda S, Kim M, Kubota N, Sugita K, Sugo T. 1999. Radiation-induced graft polymerization is the key to develop high-performance functional materials for protein purification. Radiation Phy Chem 54:517-525.

Satoh H, Okabe S, Yamaguchi Y, Watanabe Y. 2003. Evaluation of the impact of bioaugmentation nad biostimulation by *in situ* hybridization and microelectrode. Water Res. 37:2206-2216.

Satoh H, Ono H, Rulin B, Kamo J, Okabe S, Fukushi K. 2004. Macroscale and microscale analyses of nitrification and denitrification in biofilms attached on membrane aerated biofilm. Water Res 38: 1633-1641

Schramm A, Larsen LH, Revsbech NP, Ramsing NB, Amann R, Schleifer K. 1996. Structure and function of a nitrifying biofilm as determined by in situ hybridization and use of microelectrode. Appl Environ Microbiol. 62:4641-4647.

Schramm A, de Beer D, Wagner M, Amann R. 1998. Identification and activities of in situ of *Nitrospira* and *Nitrospira* spp. as dominant populations in a nitrifying fluidized bed reactor. Appl Environ Microbiol. 64:3480-3485.

Schramm A, de Beer D, Wagner M, Heuvel J, Ottengraf S, Amann R. 1999. Microscale distribution of populations and activities of *Nitrosospira* and *Nitrospira* spp. along a macroscale gradient in a nitrifying bioreactor: quantification by *in situ* hybridization and the use of microelectrodes. Appl Environ Microbiol. 65:3182-3191.

Schramm A, de Beer D, Gieseke A, Amann R. 2000. Microenvironments and distribution of nitrifying bacteria in a membrane-bound biofilm. Environ Microbiol 2:680-686.

Schramm A. 2003. In situ analysis of structure and activity of the nitrifying community in biofilms, aggregates, and sediments. Geomicrobiol J 20: 313-333.

Semmens MJ, Dahm K, Shanahan J, Christianson A. 2003. COD and nitrogen removal by biofilms growing on gas permeable membranes. Water Res 37:4343-4350.

Shanahan JW, Semmens MJ. 2004. Multipopulation model of membrane-aerated biofilms. Environ Sci Technol 38: 3176-3183.

Sharma B, Ahlert RC. 1977. Nitrification and nitrogen removal. Water Res 11:897-925.

Solbe JF, Shurben DG. 1989. Toxicity of ammonia to early life stages of rainbow trout (*Salmo gairdneri*). Water Res 23: 127-129.

Sumino T, Nakamura H, Mori N, Kawaguchi Y. 1992. Immobilization of nitrifying bacterial by polyethylene glycol prepolymer. J Ferment Bioeng. 73:37-42.

Suzuki Y, Miyahara S, Takeishi K. 1993. Oxygen supply method using gas-permeable film for wastewater treatment. Water Sci Technol 28: 243-250.

Suzuki Y, Hatano N, Ito S, Ikeda H. 2000. Performance of nitrogen removal and biofilm structure of porous gas permeable membrane reactor. Water Sci Technol 41:211-217.

Tarre S, Green M. 2004a. High-rate nitrification at low pH in suspended- and

attached-biomass reactors. Appl Environ Microbiol 70:6481-6487.

Tarre S, Beliavski M, Denekamp N, Gieseke A, de Beer D, Green M. 2004b. High nitrification rate at low pH in a fluidized bed reactor with chalk as the biofilm carrier. Water Sci Technol 49 (11-12):99-105.

Terada A, Hibiya K, Nagai J, Tsuneda S, Hirata A. 2003. Nitrogen removal characteristics and biofilm analysis of a membrane-aerated biofilm reactor applicable to high-strength nitrogenous wastewater treatment. J Biosci Bioeng 95:170-178.

Terada A, Yamamoto T, Hibiya K, Tsuneda S, Hirata A. 2004. Enhancement of biofilm formation onto surface-modified hollow-fiber membranes and its application to membrane-aerated biofilm reactor. Water Sci Technol 49 (11-12):263-268.

Terada A, Yuasa A, Tsuneda S, Hirata A, Katakai A, Tamada M. 2005. Elucidation of dominant effect on initial bacterial adhesion onto polymer surfaces prepared by radiation-induced graft polymerization. Colloids Surf B: Biointerfaces 43:99-107.

Tesk A, Alm E, Regan JM, Toze A, Rittmann BE, Stahl DA. 1994. Evolutionary relationships among ammonia- and nitrite-oxidizing bacteria. J Bacteriol 176:6623-6630.

Timberlake DL, Strand SE, Williamson K J. 1988. Combined aerobic heterotrophic oxidation, nitrification in a permeable support biofilm. Water Res 22:1513-1517.

Tsuneda S, Miyoshi To, Aoi Y, Hirata A. 2000. Tailoring of highly efficient nitrifying biofilms in fluidized bed for ammonia-rich industrial wastewater treatment. Water Sci Technol. 42:357-362.

Tsuneda S, Mikami M, Kimochi Y, Hirata A. 2005. Effect of salinity on nitrous oxide emission in the biological nitrogen removal process for industrial wastewater. J Hazardous Materials 119:93-98.

Turk O, Mavinic DS. 1986. Preliminary assessment of a shortcut in anitrogne removal from wastewater. Can J Civil Eng 13: 600-605.

Turk O, Mavninic DS. 1989. Maintaining nitrite buildup in a system acclimated to free ammonia. Water Res 30:1383-1388.

U.S. Environmental Protection Agency. 1975. Process design manual for nitrogen control. EPA Technology Transfer. Washington, DC. USA.

Van Hulle S. 2005. Modeling, simulation and optimization of autotrophic nitrogen removal processes. PhD thesis. Ghent University.

Van Loosdrecht MCM, Eikelboom D, Gjaltema A, Mulder A, Tijhuis L, Heijnen JJ. 1995. Biofilm structure. Water Sci Technol 32 (8):35-43.

Wiesmann U. 1994. Biological nitrogen removal from wastewater. In: Fiechter A, editor. Advances in biochemical engineering /biotechnology, Vol 5. Berlin: Springer-Verlag Berlin Heidelberg. p.113-154.

Wingender J, Neu TR, Flemming HC. 1999. Microbial extracellular polymeric substances-Characterization, structure and function. Berlin. Springer.

Yamagiwa K, Ohkawa A, Hirasa O. 1994. Simultaneous organic carbon removal and nitrification by biofilm formed on oxygen enrichment membrane. J Chem Eng Jpn 27:638-643.

Yamagiwa K, Yoshida M, Ito A, Ohkawa A. 1998. A new oxygen supply method for simultaneous organic carbon removal and nitrification by a one-stage biofilm process. Water Sci Technol 37:117-124.

Yang L, Alleman JE. 1992. Investigation of bathwise nitrite build-up by an enriched nitrification culture. Water Sci Technol 26 (5-6):997-1005.

Chapter 2

Elucidation of dominant effect on initial bacterial adhesion onto polymer surface prepared by radiation induced graft polymerization

Chapter 2

Elucidation of dominant effect on initial bacterial adhesion onto polymer surfaces prepared by radiation-induced graft polymerization

2

Abstract

Surface-modified polyethylene (PE) membrane sheets were prepared by the radiation-induced graft polymerization (RIGP) of an epoxy-group-containing monomer, glycidyl methacrylate (GMA). The epoxy ring of GMA was opened by introducing diethylamine (DEA) or sodium sulfite (SS). We examined the properties of these sheets by measuring the amount of grafting polymer, surface roughness and membrane potential, and also investigated the adhesion of five Gram-negative bacteria, *Escherichia coli, Pseudomonas aeruginosa, Pseudomonas putida, Pseudomonas fluorescens* and *Paracoccus denitrificans*, onto the prepared sheet surfaces. A linear relationship between the degree of grafting (*dg*) and surface roughness was observed. Moreover, membrane potential was dependent on the amount of DEA or SS as the ionizable group. These results indicate that RIGP enables the control of the physicochemical properties of such a

sheet surface by adjusting *dg* and the subsequent conversion of functional groups. A batch test on bacterial adhesion onto the sheets clarified that the DEA-containing sheet (DEA sheet) exhibited an adhesion rate constant, *k*, significantly greater than those of other types of sheet. Clearly, the adhesion rate constant of the DEA sheet increased with *dg*, indicating that electrostatic interaction is the most decisive factor for bacterial adhesion when it works as an attractive force. Furthermore, the densities of bacteria adhering onto the GMA-containing sheet (GMA sheet) and the SS-containing sheet (SS sheet) were almost the same as that onto a PE sheet, whereas that onto a DEA sheet significantly increased. Thus, the introduction of the GMA- and SS-containing graft chain did not have much influence on bacterial adhesion onto the surfaces, supporting the conclusion that the promotion of bacterial adhesion onto the GMA and SS sheets was due to an increase in surface area resulting from RIGP. Moreover, the scanning electron microscopy images of the sheet surfaces indicate that the conditions and morphologies of initial bacterial adhesion are dependent on surface properties, particularly membrane potential.

2. 1 Introduction

Bacteria tend to associate with surfaces. Once bacteria attach to a substratum surface, a multistep process starts leading to the formation of a complex and heterogenous biofilm

(Bos *et al.*, 1999). Biofilms are detrimental to food equipment (Dickson *et al.*, 1989), heat exchangers (Kjellerup *et al.*, 2003), ship hulls (Cooksey *et al.*, 1995), and biomaterial implants (Hendricks *et al.*, 2000), but also beneficial; for example, they degrade environmental hazardous substances in a bioreactor (Nicolella *et al.*, 2000a, b; Tsuneda *et al.*, 2003). In the former case, most research focused on how to prevent the adhesion of bacteria and therefore the formation of an infectious, pathogenic biofilm. In the latter case, an important consideration is to enhance the initial attachment of bacteria onto a substratum and maintain biofilms in an optimal spatial arrangement of different microbial species to stimulate an efficient degradation of specific substances in a bioreactor.

Bacterial adhesion leading to the formation of a coherent biofilm is a two-step process; the first step is reversible involving physicochemical forces. The second step is an irreversible chemical step, followed by the synthesis of extracellular polymeric substances cementing the film. The importance of the studies of the initial bacterial adhesion in biofilm formation has been questioned, because the number of cells in a mature biofilm after the growth phase is several times higher than that involved in the initial adhesion (Petrozzi *et al.*, 1991; Fox *et al*, 1990). From another viewpoint, however, these studies overlook the importance of bacteria that initially adhere as the link between the colonized surface and the biofilm (Busscher *et al.*, 1995). Some researchers demonstrated that the physicochemical properties of a substratum, particularly surface potential (i.e., zeta potential), affect the rate of the initial bacterial adhesion and the subsequent biofilm formation, indicating the significance of the initial bacterial adhesion onto a substratum (Harks *et al.*, 1992; Gottenbos *et al*, 1995, 1999, 2001; van Loosdrecht *et al.*, 1990).

The majority of existing models for bacterial attachment mechanisms are based on

colloidal theories. From the physicochemical aspect in the case of planktonic bacteria approaching a solid substratum in a solution, mainly van der Waals forces and electrostatic interaction due to the overlapping diffuse layer, that is, DLVO forces, comes into play initially. Then, subsequent short-range forces, such as steric interactions due to the polymeric surface structure or forces of hydrophobic nature, become dominant (Saito, 2002). Electrostatic force is considered to be the most important, because it is markedly influenced by the surface potentials of both cells and the substratum or the chemical properties of the solution, that is, ionic concentration and valence of ions.

In many surface modification methods that promote or reduce bacterial adhesion, radiation-induced graft polymerization (RIGP) has an advantage in that it enables the introduction of graft-chain-containing interfaces bearing functional groups into various polymeric backbones (Lee *et al*., 1996). Lee et al. reported that a hollow-fiber membrane modified by RIGP exhibits a significantly high capturing rate for *Staphylococcus aureus*, indicating efficient bacterial recovery for water purification (Lee *et al.*, 1996, 1997). Hibiya et al. reported that nitrifying bacteria exhibit a high adhesiveness to a membrane whose surface is modified with positively charged graft polymer chains, and nitrifying biofilms form within a short time (Hibiya *et al.*, 2000). In our previous studies, we used a positively charged hollow-fiber membrane as a bacterial support medium and as an oxygen-supplying material to develop a membrane-aerated biofilm reactor for nitrogenous wastewater treatment: we obtained a rapid immobilization of nitrifying biofilms and a high oxygen utilization efficiency of a nitrifying bacteria (Terada *et al.*, 2003, 2004). Although research on its practical applications is underway, we have to elucidate the relationship between bacteria and surfaces prepared by RIGP for the optimal design of biointerfaces.

The objective of this chapter is twofold: to examine the effect of physicochemical

properties of a surface-modified membrane sheet prepared by RIGP on the initial

bacterial adhesion and to clarify the dependence of the mechanism of adhesion onto

membrane sheet properties.

2.2 Materials and methods

2.2.1 Bacterial strains

Five Gram-negative bacteria, *Escherichia coli* (IFO-3301), *Pseudomonas aeruginosa* (IFO-3080), *Pseudomonas putida* (IFO-3081), *Pseudomonas fluorescens* (IFO-3507) and *Paracoccus denitrificans* (JSM-6892), were used in this study. These bacteria are ubiquitous and are responsible for the removal of nitrogenous and xenobiotic compounds in soil, water environments, wastewater treatment plants and so on. Prior to adhesion tests, each strain was aerobically cultured for 1 day at 30ºC in a liquid medium containing polypeptone, 10.0 g; yeast extract, 5.0 g; sodium chloride, 1.0 g; and distilled water, 1 L. Cells were harvested at their exponential growth phase by centrifugation (8000 g, 10 min) and resuspended in water. This washing procedure was repeated three times to eliminate residual substrates and extracellular polymers that bacterial cells produced during their growth. Finally, the washed cells were suspended in a 0.02 M phosphate-buffered saline (PBS) solution. Prior to the adhesion experiment, the linear relationship between cell number and optical density at 660 nm wavelength ($O.D._{660}$) was confirmed under all experimental conditions. YO-PRO-1 (Molecular Probes, Leiden, The Netherlands), which stains DNA, was used for counting cell number.

Electrophoretic mobility measurements were carried out using an electrophoretic light-scattering spectrophotometer (ELS-8000, Otsuka Electronics, Japan). Subsequently, zeta potential was calculated from obtained electrophoretic mobilities using

Smoluchowski's equation. Cell suspensions were dispersed in an ultrasonic bath for 5 min and immediately applied to the apparatus. All measurements were carried out in triplicate.

2.2.2 Fabrication of membrane sheet

A preparation scheme for diethylamino- or sulfonic acid-containing membrane sheets is shown in Figure 2.1. Firstly, a polyethylene (PE)-based membrane sheet (PE sheet) (Asahi Kasei Chemicals, Japan) was used as the stem for grafting. The longitudinal and transversal of the sheet were 10 and 7.5 cm, respectively, with a porosity of 70% and an average pore size of 0.20 μm. The sheets were irradiated with an electron beam in a nitrogen atmosphere at room temperature. The total dose of the electron beam was set at 200 kGy. Then, the irradiated sheets were immersed in a glass ampoule containing glycidyl methacrylate (GMA; 5 wt/wt% in methanol), previously sparged with nitrogen gas, and allowed to react at 313 K for a predetermined time. The obtained GMA-grafted sheets were soaked in *N, N*-dimethylformamide and then in methanol to remove residual monomers and homopolymers. They were then dried under reduced pressure. The amount of GMA grafted onto a stem sheet represented the degree of grafting (*dg*) calculated as follows:

$$dg = 100 \times \left(\frac{W_1 - W_0}{W_0} \right) \qquad [\%] \qquad (2.1)$$

,

where W_0 and W_1 are the weights of the stem sheet and GMA-grafted sheet, respectively. Then, the produced epoxy groups were converted to diethylamino groups ($-N(C_2H_5)_2$) or sulfonic acid groups ($-SO_3H$) by immersing the GMA-grafted sheet in a mixture of diethylamine (DEA)/water = 50/50 (volume ratio) or sodium sulfite (SS)/isopropyl alcohol/water = 10/15/75 (weight ratio), respectively. The conversion of the epoxy

groups to ionizable groups, that is, DEA and SS groups, was set at about 100%. Hereafter, the resultant GMA-, DEA- and SS-containing sheets are referred to as GMA, DEA and SS (X) sheets; X in parentheses represents dg.
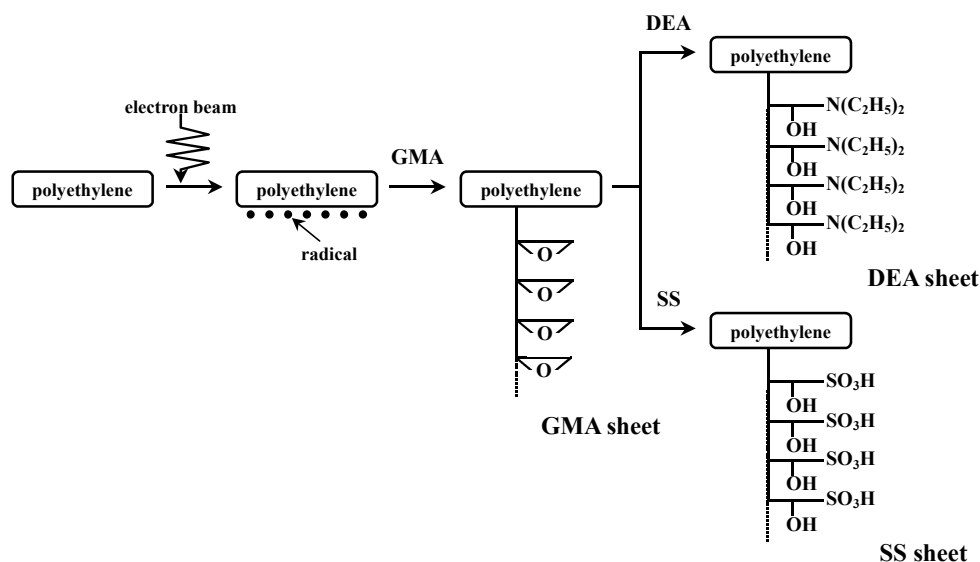
Figure 2.1 Preparation scheme for GMA, DEA and SS sheets.

2.2.3 Properties of membrane sheet

For the morphological observation of sheet surfaces fabricated by RIGP, atomic force microscopy (AFM, Nonoscope IIIa Dimersion™ 3100, Digital Instruments, USA) was carried out. For AFM, the sheets were cut in 1×1 cm sections and fixed on a microscope slide with double-sided adhesive tape. AFM was performed in the tapping mode. Height images were recorded in three dimensions at three randomly selected sites, from which the mean surface roughness and the mean three-dimensional surface area were calculated. Ten point height of roughness profile was employed for the measurement of the mean surface roughness (ISO 4287: 1997).

Membrane potential was measured following the method of Tsuru *et al.* (1990). The apparatus used in this study was a U-bend cell, which was divided into two compartments using one membrane sheet. The solute used in this study was 0.02 M PBS

(pH 7.2). The membrane sheets were rinsed in distilled water before being used for the measurements. Distilled water was supplied to one side and PBS to the other side of the cell. The temperature was maintained at 298 K. Membrane potential was measured using two reference electrodes (RE-1C, BAS Inc. Japan), which were both Ag/AgCl electrodes in a saturated potassium chloride solution, when the value became constant due to the decrease in concentration polarization. The two electrodes were connected to an electrometer (R8240, Advantest, Japan). The measurement was conducted in triplicate under the same conditions and the average value was taken.

2.2.4 Evaluation of rate of bacterial adhesion onto a membrane sheet

Forty milliliters of cell suspension prepared as described above was added to a 50 ml beaker. The concentration of the cell suspension was set at an O.D.$_{660}$ of 0.050 (5.5 ~ 9.4 × 10^9 cells/ml). Ten PE, GMA (50, 100 and 200), DEA (50, 100 and 200) and SS (50, 100 and 200) sheets were cut into 0.25 cm^2. Then, each sheet was immersed in a beaker containing a cell suspension. The rate of adhesion of five bacterial strains onto each sheet was measured in terms of the decrease in O.D.$_{660}$ of each cell suspension. The cell suspension and the prepared sheets were incubated with shaking at 200 rpm at 298 K. The cell suspension was sampled at specific time intervals. Adhesion rate was calculated from O.D.$_{660}$, two-dimensional surface area and volume. The adhesion rate constant, *k*, was defined as (Lee *et al.*, 1996):

$$V\frac{dC}{dt} = -kAC \tag{2.2}$$

where *k* can be derived as follows under an initial condition of *C=C$_0$* at *t*=0:

$$k = -\left(\frac{V}{A}\right)\left(\frac{1}{t}\right)\ln\left(\frac{C_t}{C_0}\right) \tag{2.3}$$

where V, A, t, C_t, and C_0 are the volume of cell suspension, two-dimensional sheet surface area, contact time, O.D.$_{660}$ at time t and initial O.D.$_{660}$, respectively.

2.2.5 Observation of bacterial adhesion by scanning electron microscopy

The sheets, which were immersed in cell suspensions of the five strains for 8 h at 298 K, were collected carefully and washed with distilled water. Then each sample was immediately fixed, washed with sodium cacodylic acid solution, and dehydrated with ethanol. A sample was observed by scanning electron microscope (SEM) (JSM-5600, JEOL, Japan) after the sample was mounted on a stub and coated with gold using an ion coater (JFC-1100E, JEOL, Japan).

2.3 Results

2.3.1 Membrane sheet properties prepared by RIGP

Dg for the membrane sheets increased proportionally with reaction time in 5wt/wt% GMA/methanol solution (Figure 2.2). This property allowed us to control *dg* by setting reaction time and thus to fabricate ten membrane sheets, namely, PE, GMA (50, 100 and 200), DEA (50, 100 and 200) and SS (50, 100 and 200) sheets. The relationship between surface roughness and *dg* for each sheet is shown in Figure 2.3. Whether the epoxy group of the GMA was opened to ionizable groups or not, roughness was proportional to *dg*. Surface morphological observation by AFM clarified that the sheets with a high *dg* had rough surfaces because of the introduction of GMA polymer chains to the PE sheet by RIGP (data not shown). The three-dimensional surface area of each sheet is shown in Table 2.1. These results demonstrated that RIGP produced rough sheet surfaces and larger surface areas of modified PE sheets for bacterial adhesion than that of PE sheets,

although the surface area of the modified PE sheets did not necessarily increase in proportion to the *dg* of the sheets. Representative images of the PE and DEA (200) by AFM are shown in Figure 2.4. The surface morphology of DEA (200) (Fig. 2.4 (B)) was quite different from that of PE (Fig. 2.4 (A)): the DEA (200) surface has a more complex surface compared to the PE counterpart.

Figure 2.5 shows the effects of *dg* on the membrane potential of the membrane sheets (GMA, DEA and SS sheets). The membrane potentials of GMA sheets almost remained constant (-23.4 ~ -22.5 mV) in 0.02 M PBS solution (pH 7.2) because these sheets did not have an ionizable group. In contrast, a linear relationship between membrane potential and *dg* was consistently observed for both the DEA and the SS sheets. Moreover, the absolute values of these two slopes were very similar. Therefore, we concluded that RIGP enables the control of membrane potential by adjusting reaction time in GMA/methanol solution.
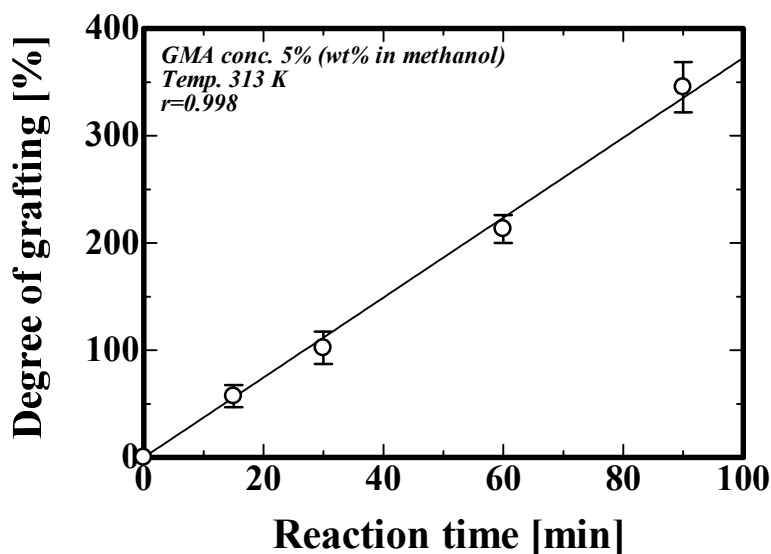
Figure 2.2 Time course of degree of grafting
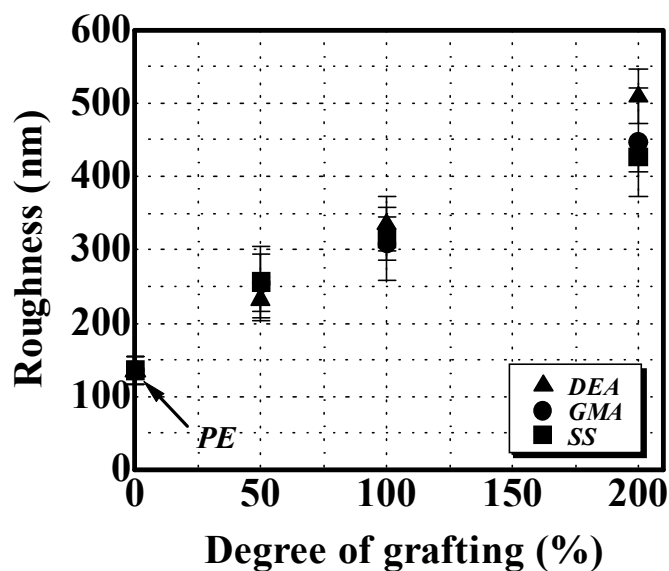
Figure 2.3 Surface roughness of membrane sheets as a function of degree of grafting.

Table 2.1 Properties of membrane sheets used in this study

	Degree of grafting (%)	Three-dimensional surface area [a] (μm^2)
PE sheet	-	2670
GMA sheet	50	3080
	100	3310
	200	3420
DEA sheet	50	2950
	100	3550
	200	3460
SS sheet	50	3660
	100	3570
	200	3690

[a] Three-dimensional surface area was measured in the range of 50×50 μm (two-dimensional area).
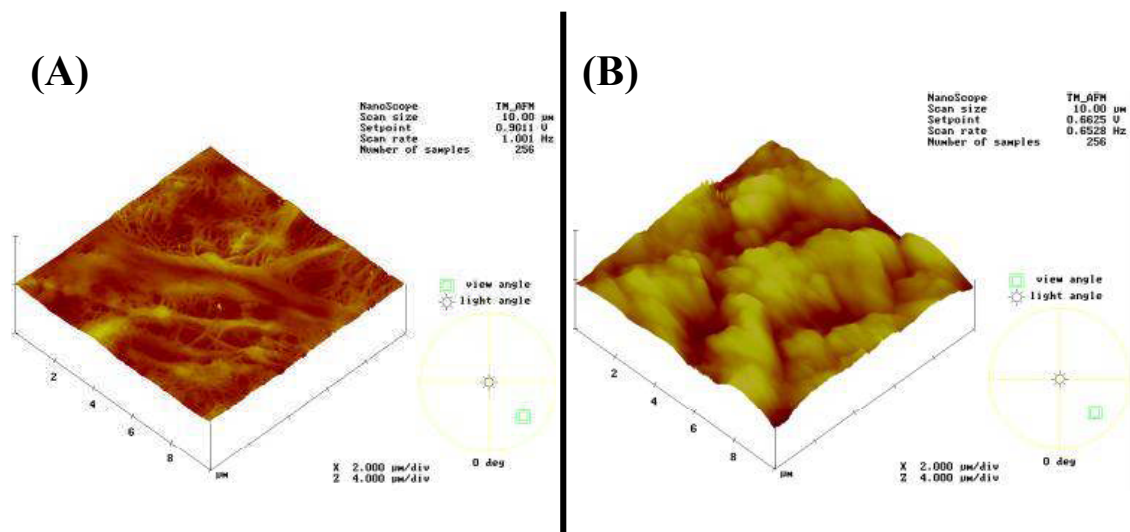
Figure 2.4 AFM images of PE (A) and DEA (200) (B).
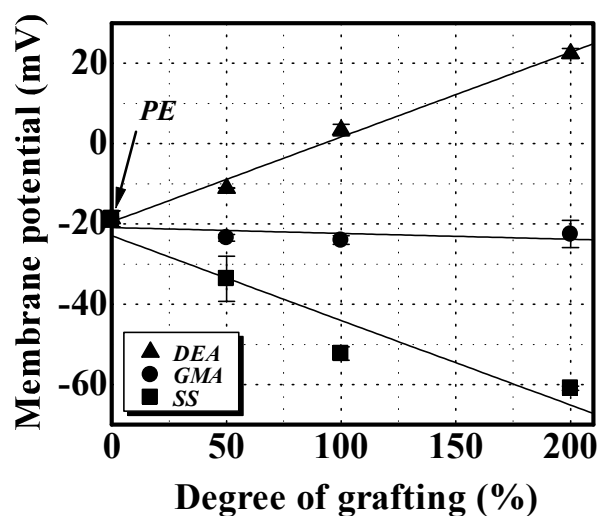
Figure 2.5 Membrane potentials of membrane sheets as a function of degree of grafting. Membrane potential was measured at 0.02 M PBS and pH 7.2.

2.3.2 Bacterial adhesion experiment

The prepared ten sheets, namely, PE, GMA (50, 100 and 200), DEA (50, 100 and 200) and SS (50, 100 and 200) sheets, were immersed in cell suspensions of five Gram-negative bacteria in the batch mode. Figure 4 shows changes in bacterial cell

concentration as representative data. As shown in Figure 2.6 (A), the adhesion of *P. aeruginosa* cells onto the PE sheet hardly occurred since O.D.$_{660}$ in the bacterial suspension was almost the same after 8 h. Slight decreases in O.D.$_{660}$ (about 15% decrease in initial O.D.$_{660}$) were observed in the case of *E. coli* and *P. denitrificans* (data not shown), which indicated that cell adhesion occurred to a small degree. On the other hand, Figure 2.6 (B) shows that the adhesion of *P. putida* onto the PE sheet rapidly occurred in a manner different from that of the three bacterial strains mentioned above. A similar trend was observed in the case of *P. fluorescens* (data not shown). These results clarified that bacterial adhesion onto the PE sheet depended on the bacterial species.

The trends of bacterial adhesion onto the GMA and the SS sheets shown in Figs. 2.6 (A) and (B) indicated that the rates of bacterial adhesion onto these sheets were slightly higher than that onto the PE sheet. In contrast, all the bacterial strains tested adhered onto the DEA sheet rapidly. These results indicate that the DEA sheet showed enhanced bacterial adhesion.
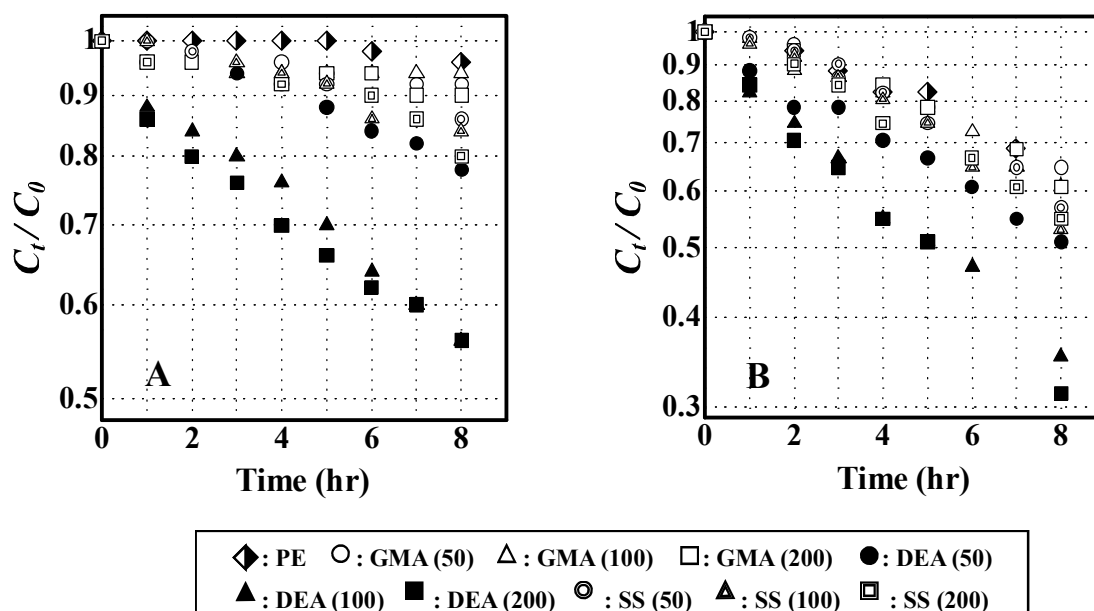
Figure 2.6 Change in concentration of bacterial cells of (A) *P. aeruginosa* and (B) *P. putida*.

2.3.3 Comparison of adhesion rate constant, k

The comparison of adhesion rate constant among the prepared sheets is shown in Figure 2.7. Figure 2.7 shows that the DEA sheet exhibited a high adhesion rate constant, *k* in all bacterial suspensions and that *k* increased with *dg*. In particular, the *k* of DEA (200) sheet in *P. aeruginosa* suspension was about 30 times higher than that of the PE sheet. These results confirmed the rapid adhesion of bacterial cells onto the DEA sheets whether or not the initial bacterial adhesion onto the PE sheet immediately occurred. On the other hand, the adhesion rate constants of GMA and SS sheets except for *P. aeruginosa* were from 1.1- to 1.9-fold greater than that of the PE sheet. Slight increases in adhesion rate constant with *dg* were observed, which was also observed in the DEA sheets. A marked difference in adhesion rate constant between the GMA and the SS sheets was not observed, although there was a considerable difference in membrane potential.
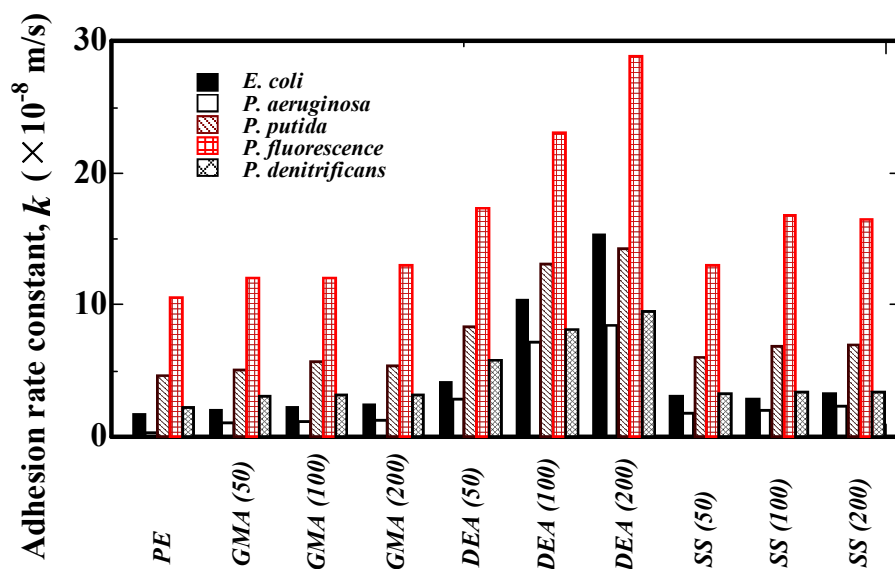
Figure 2.7 Comparison of adhesion rate constant, *k* among different sheet surfaces. Values in parentheses represent degree of grafting.

2.3.4 Observation of bacteria attached onto membrane sheet surface

Representative SEM images of *E. coli* adhesion onto the prepared sheets are shown in Figure 2.8. The forms of bacterial adhesion onto the sheets were divided into three types: adhesion onto (i) the PE sheet, (ii) the GMA and the SS sheets, and (iii) the DEA sheet. In the case of (i) (the PE sheet), it was confirmed in Figures 2.8 (A) and (E) that *E. coli* adhered unevenly in a multilayer structure: the cells were sparsely present as aggregates. Additionally, Figure 2.8 (E) shows that *E. coli* colonized the sheet with a spherical morphology, in contrast to cases (ii) and (iii), where a rod-like morphology was observed (Figures 2.8 (B), (C), (D) and (F)). In the case of (ii) (the GMA and the SS sheets), *E. coli* adhered unevenly in a monolayer structure: the cells were sparsely present on the sheets (Figures 2.8 (B) and (D)). In the case of (iii) (the DEA sheet), *E. coli* adhered evenly in a monolayer structure: the cell adhered densely onto the sheet (Figures 2.8 (C) and (F)), which exhibited a high potential for *E. coli* adhesion. Similar tendencies were confirmed by SEM for the other bacterial strains (data not shown). SEM showed clearly that the surface characteristics of a sheet significantly affected the area covered by cells, and the bacterial morphology during the initial adhesion, which seems to influence subsequent biofilm structure and activity.
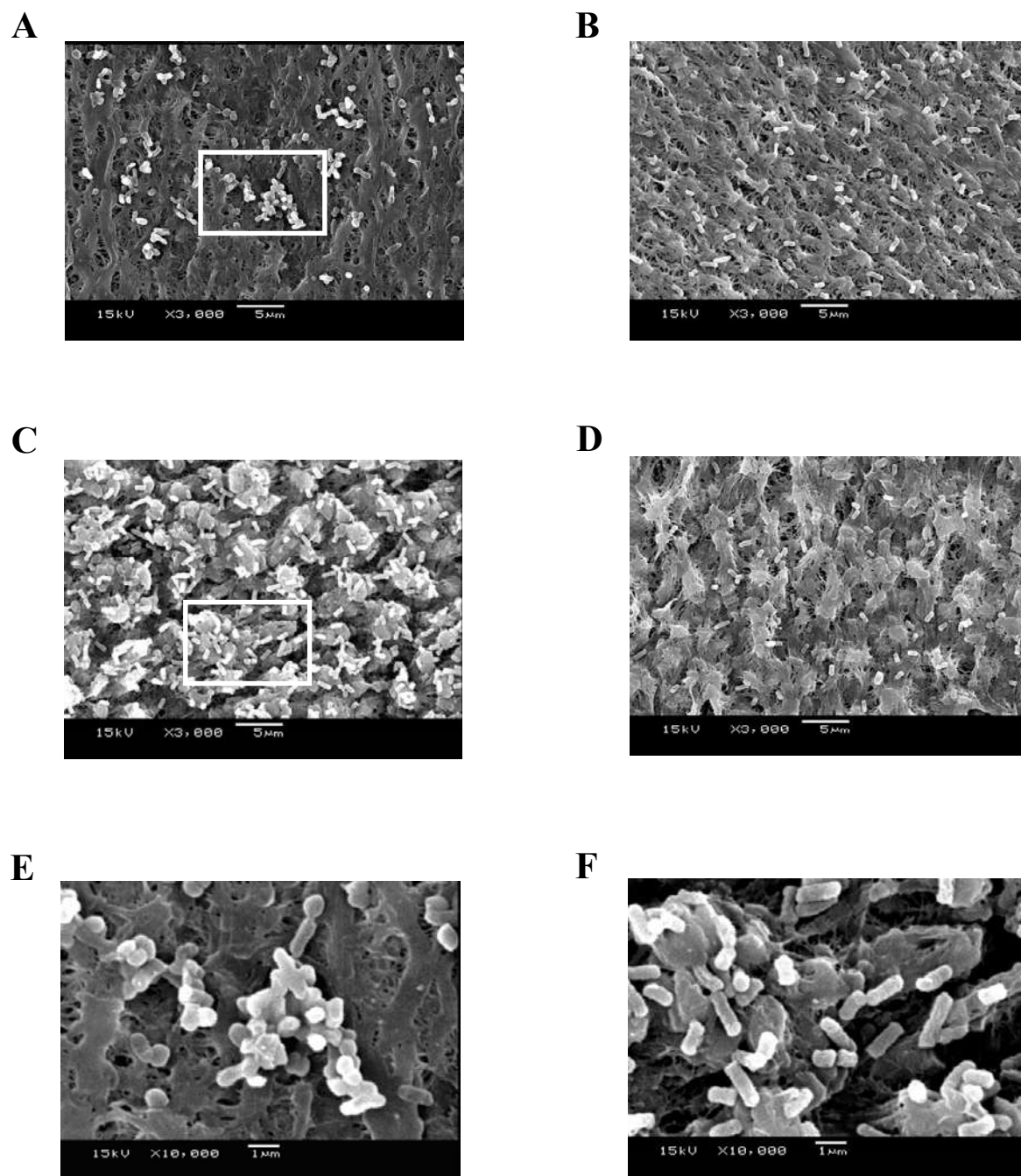
Figure 2.8 SEM images of interfaces of membrane sheets after immersion in *E. coli* suspension for 8 h. (A) PE; (B) GMA; (C) DEA; (D) SS; (E) magnified image of (A); (F) magnified image of (C). Degree of grafting of each sheet was about 100%.

2.4 Discussion

2.4.1 Effect of roughness on initial bacterial adhesion

We demonstrated a linear relationship between *dg* and the roughness of membrane sheets. Since the change in the membrane potential of the GMA sheets was negligible (-23.4 ~ -22.5 mV) compared with the change in roughness, the effect of roughness on adhesion rate constant, *k* was evaluated (Figure 2.9). Figure 2.9 confirmed that the adhesion rate constant slightly increased with *dg*, which indicated that surface roughness promoted bacterial adhesion. Morgan and Wilson clarified that the number of *Streptococcus oralis* cells adhering to surfaces increases linearly with mean surface roughness in a short period (Morgan *et al.*, 2001). Gjaltema *et al.* showed that the most important parameter of a carrier surface seems to be its roughness in a turbulent *P. putida* biofilm reactor (Gjalteman *et al.*, 1997). However, Bos *et al.* in their review stated that roughness affects biofilm formation, whereas it appears to be a minor factor with regard to the initial adhesion (1999). In our present study, although we cannot conclude that surface roughness is a major factor affecting bacterial adhesion, at least we determined that surface roughness is one of the factors promoting bacterial adhesion. Whether the promotion of bacterial adhesion caused by an increase in surface roughness is due to an increased surface area or the cleavage of surface will be discussed in *2.4.3*.
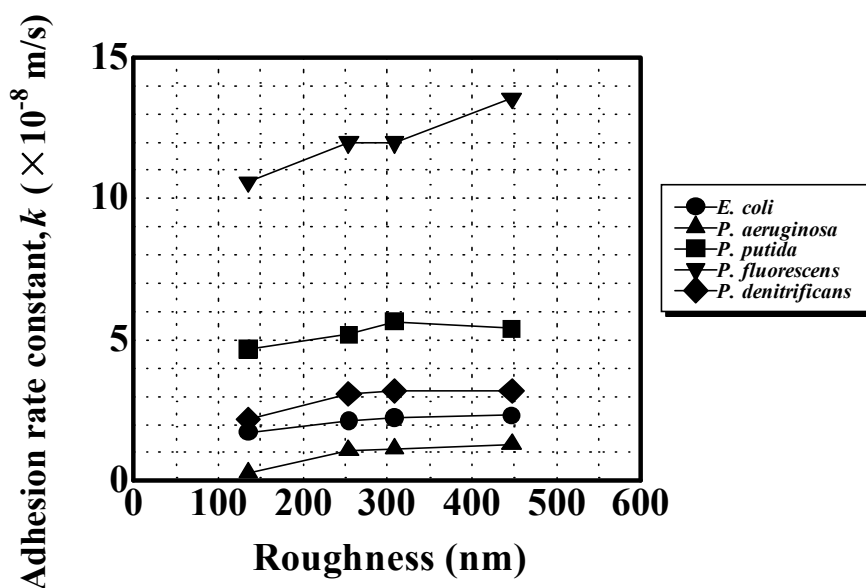
Figure 2.9 Effect of surface roughness of GMA sheet on adhesion rate constant, k

2.4.2 Effect of membrane potential on initial bacterial adhesion

Figure 2.10 shows the effect of membrane potential on adhesion rate constant, k. Considering that the zeta potentials of the five bacterial strains were negative at pH 7.2, it could be explained that electrostatic interaction between bacterial cells and the DEA sheets becomes stronger with dg, resulting in the high adhesion rate constant. Moreover, since surface roughness was a minor factor for promoting bacterial adhesion as shown in Fig. 2.9 and a linear relationship between dg and membrane potential of the DEA sheets was obtained as shown in Fig. 2.5, we can conclude that the significant increase in the rate of bacterial adhesion is attributed to the membrane potential of the DEA sheets derived from the diethylamino group. Surprisingly, the rates of bacterial adhesion onto the SS sheets did not decrease with dg in all experiments, even though their membrane potentials became more negative with dg, leading to an increase in the repulsive force between bacterial cells and the sheet surface. Furthermore, Fig. 2.7 shows that the adhesion rate constants of the GMA (50, 100 and 200) and the SS (50, 100 and 200)

sheets were approximately the same and the definite dependence of *dg* on adhesion rate constant was not observed. These results seem to be explained by Ohshima's 'soft-particle' theory (Ohshima, 1994). Considering that this theory assumes an ion-penetrable polymer layer around the core particle, the magnitudes of cell surface potential based on soft-particle theory are lower than those based on conventional zeta potential derived from Smoluchowski's theory (Morisaki *et al.*, 1999); Poortinga *et al.*, 2001; Hayashi *et al.*, 2001; Tsuneda *et al.*, 2001). Moreover, grafting materials such as the DEA and the SS sheets used in our present study may be assumed to have 'soft' surfaces because each surface has an ion-penetrable layer derived from the DEA and SS groups, respectively. Then, the energy barriers between bacterial cells and the SS sheet surfaces would be reduced significantly, leading to the observation that the adhesion rate constant is nearly the same between the GMA and the SS sheets. Kaper *et al.* analyzed the electrophoretic mobilities of poly (ethylene oxides) brushes by streaming potential measurements, yielding an electrophoretic softness (Kaper *et al.*, 2003). Therefore, future research on the dependence of the electrophoretic mobilities on the ionic strength is needed to elucidate the relationship between bacterial cells and the prepared surfaces in detail.

We can explain the obtained findings on the initial bacterial adhesion to some extent from the physicochemical aspect; however, it is difficult to generalize the findings with respect to the mechanisms of bacterial adhesion. Bakker *et al*. pointed out that taking adhesion strength and hydrodynamic conditions into consideration is necessary for the generalization of a mechanism of the initial bacterial adhesion (2004).
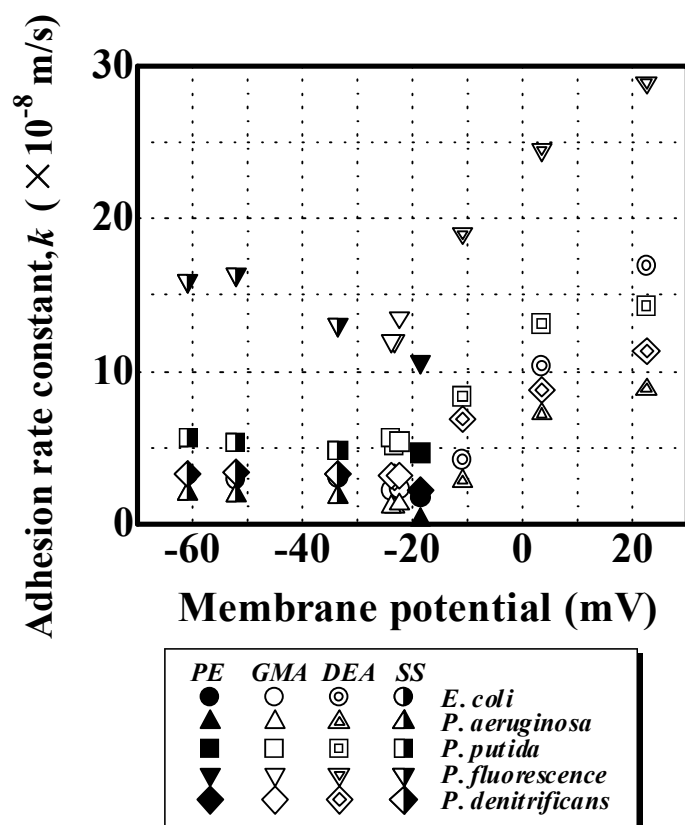
Figure 2.10 Effect of membrane potential on adhesion rate constant, *k*. Membrane potential was measured at 0.02 M PBS and pH 7.2.

2.4.3 Evaluation of bacterial density per surface area

The number of planktonic bacterial cells was calculated from a linear relationship between O.D.$_{660}$ and the number of the bacterial cells at 5 h. As a result, adhesion rate could be expressed in a first-order equation as a function of time. Then, we evaluated the number of adhering bacterial cells per surface area including the extended surface area produced by RIGP. Table 2.2 shows the estimated number of bacterial cells attached onto each sheet after a 5 h immersion in the bacterial suspension. Significant differences in the number of adhered bacterial cells were not observed among the PE, GMA and SS sheets except for *P. aeruginosa*. These results indicated that the promotion of bacterial adhesion with an increase in roughness was not due to a drastic change in the surface

physicochemical property but due to the increase in surface area for bacterial adhesion. On the other hand, the density of bacterial cells adhering onto all DEA sheets increased markedly, implying that the adhesion rate constant k of the DEA sheets increased with membrane potential as shown in Fig. 2.10. These results support the SEM observation that bacterial adhesion occurred evenly onto the DEA sheets because these sheets attract bacterial cells due to their physicochemical properties, whereas bacterial adhesion occurred unevenly onto the PE, GMA and SS sheets because these sheets repulse bacterial cells. On the basis of SEM images shown in Fig. 2.8, we can explain the mechanism of the initial bacterial adhesion onto different surfaces. These results clarified that the rate and conditions of the initial bacterial adhesion were strongly dependent on the physicochemical properties of the surface.

Table 2.2 **The estimated number of bacteria adhered onto each surface after immersion in bacterial suspension for 5 h**

Bacterial strain (Zeta potential (mV)[a])	Bacterial density per surface area including roughness [b] ($\times 10^5$ number/mm^2)									
	PE	GMA (50)[c]	GMA (100)	GMA (200)	DEA (50)	DEA (100)	DEA (200)	SS (50)	SS (100)	SS (200)
E. coli. (-38.5)	0.39	0.34	0.47	0.46	0.88	1.5	1.6	0.57	0.44	0.56
P. aeruginosa (-12.4)	0.098	0.26	0.24	0.23	0.53	1.1	1.2	0.29	0.29	0.28
P. putida (-27.0)	0.83	0.88	0.82	0.79	1.4	1.7	1.7	0.87	0.89	0.87
P. fluorescens (-30.1)	3.4	3.0	2.8	3.1	3.9	3.9	4.1	2.9	3.4	2.9
P. denitrificans (-34.5)	0.69	0.80	0.75	0.63	1.2	1.5	1.5	0.68	0.69	0.59

[a] Zeta potential was measured at pH 7.2 in 0.02 M PBS.

[b] The number of bacteria adhered onto each sheet was calculated from O.D.$_{660}$ after immersion in bacterial suspension for 5 h

[c] X in parentheses designates *dg.*

2.4.4 Relationship between bacterial adhesion and subsequent biofilm formation

Some researchers have focused on the effect of surface properties on biofilm formation. Gottenbos *et al.* reported that the adhesion of Gram-negative bacteria onto a trimethylaminoethylmethacrylate chloride material with a positive zeta potential is faster than that onto other materials with a negative zeta potential; however, the subsequent biofilm formation by Gram-negative bacteria is slower, indicating that a positively charged surface affects biofilm formation negatively (2001). On the other hand, Hibiya *et al.* showed that a nitrifying biofilm with 100 μm thickness forms on a positively charged surface within 150 days and this biofilm exhibits a much higher specific nitrification rate than other biofilms (2000). Lee *et al.* proposed that a GMA polymer grafted onto a PE polymer captures *Staphylococcus aureus* "softly" (1996). These reports support the notion that the GMA graft chain seems to have a positive influence on biofilm formation. However, the mechanism by which the GMA graft chain facilitates bacterial adhesion still remains unclear. Our ongoing research is focusing on the activity of bacterial cells adhering onto the DEA and SS sheets and on subsequent biofilm formation, which may elucidate differences in the mechanisms of a series of biofilm formation dependent on surface properties.

2.5 Conclusion

A positively charged sheet on which a DEA-group-containing graft chain was introduced by RIGP can significantly facilitate the initial bacterial adhesion mainly due to electrostatic interaction and partly due to an increased surface area. Moreover, an increase in the amount of the DEA group largely governs the rate of bacterial adhesion, which allows us to control bacterial adhesion. On the other hand, the sheets whose surfaces work as a repulsive force against bacterial adhesion (GMA and SS sheets) can

slightly facilitate the initial bacterial adhesion in comparison with the PE sheet due to an increased surface area rather than the physicochemical properties. It is obvious that the rate and activity of initial bacterial adhesion largely depend on the properties of membrane sheet surfaces produced by RIGP, leading to a possibility that these surfaces also influence subsequent biofilm formation.

References

Bakker DP, Postmus BR, Busscher HJ, van der Mei HC. 2004. Bacterial strains isolated from different niches can exhibit different patterns of adhesion to substrata, Appl Environ Microbiol 70:3758-3780.

Bos R, van der Mei H, Busscher HJ. 1999. Physico-chemistry of initial microbial adhesive interactions-its mechanisms and methods for study. FEMS Microbiol Rev 23:179-230.

Busscher HJ, Bos R, van der Mei HC. 1995 Initial microbial adhesion is determinant for the strength of biofilm adhesion. FEMS Microbiol Lett 128:229-234.

Cooksey KE, Wigglesworth-Cooksey B. 1995. Adhesion of bacteria and diatoms surfaces in the sea: a review. Aquat Microb Ecol 9:87-96.

Dickson JS, Koohmaraie, M. 1989 Cell-surface charge characteristics and their relationship to bacterial attachment to meat surfaces. Appl Environ Microbiol 55: 832-836.

Fox P, Suidan MT, Bandy JT. 1990. A comparison of media types in acetate fed expanded-bed anaerobic reactors. Water Res 24:827-835.

Gjaltema A, van der Marel N, van Loosdrecht MCM, Heijnen JJ. 1997. Adhesion and biofilm development on suspended carriers in airlift reactors: hydrodynamic conditions versus surface characteristics. Biotechnol Bioeng 55:880-889.

Gottenbos B, van del Mei HC, Busscher H J, Grijpma DW, Feijen J. 1999. Initial adhesion and surface growth of Pseudomonas aeruginosa on negatively and positively charged poly (methacrylates). J Material Sci: Mater in Medicine 10:853-855.

Gottenbos B, van der Mei HJ, Busscher J. 2000. Initial adhesion and surface growth of

Staphylococcus epidemidis and *Pseudomonas aeruginosa* on biomedical polymers. J Biomed Mater Res 50:208-214.

Gottengbos B, Grijpma DW, van der Mei HC, Feijen J, Busscher HJ. 2001. Antimicrobial effects of positively charged surfaces on adhering Gram-positive bacteria, J Antimicrob Chemotherapy 48:7-13.

Harkes G, Dankert J, Feijen J. 1992. Growth of uropathogenic *Escherichia coli* strains at solid-surfaces. J Biomater Sci-Polymer Ed 3:403-418.

Hayashi H, Tsuneda S, Hirata A, Sasaki H. 2001. Soft particle analysis of bacterial cells and its interpretation of cell adhesion behaviors in terms of DLVO theory. Collids Surf B: Biointerfaces 22:149-157.

Hendricks SK, Kwok C, Shen MC, Horbett TA, Ratner BD, Bryers JD. 2000. Plasma-deposited membranes for controlled released of antibiotic to prevent bacterial adhesions and biofilm formation. J Biomed Mater Res 50:160-170.

Hibiya K, Tsuneda S, Hirata A. 2000. Formation and characteristics of nitrifying biofilm on a membrane modified with positively-charged polymer chains. Colloids Surf B: Biointerfaces 18:105-112.

Kaper HJ, Busscher HJ, Norde J. 2003. Characterization of poly (ethylene oxide) brushes on glass surfaces and adhesion of *Staphylococcus epidermidis*. J Biomed Mater Res 14:313-324.

Kjellerup BV, Olesen BH, Nielsen JL, Frolund B, Odum S, Nielsen PH. 2003. Monitoring and characterization of bacteria in corroding district heating systems using fluorescence in situ hybridization and microautoradiography. Water Sci Technol 47 (5):117-122.

Lee W, Furusaki S, Saito K, Sugo T, Makuuchi K. 1996. Adsorption kinetics of microbial cells onto a novel brush-type polymeric material prepared by radiation-induced graft

polymerization. Biotechnol Prog 12:178-183.

Lee W, Saito K, Furusaki S, Sugo T. 1997. Capture of microbial cells on brush-type polymeric materials bearing different functional groups. Biotechnol Bioeng 53:523-528.

Morgan TD, Wilson M. 2001. The effects of surface roughness and type of denture acrylic on biofilm formation by *Streptococcus oralis* in a constant depth film fermentor. J Appl Microbiol 91:47-53.

Morisaki H, Nagai S, Ohshima H, Ikemoto E, Kogure K. 1999. The effect of motility and cell-surface polymers on bacterial attachment. Microbiology-UK 145:2797-2802.

Nicolella C, van Loosdrecht MCM, Heijnen SJ. 2000. Particle-based biofilm reactor technology. Trends Biotechnol 18:312-320.

Nicolella C, van Loosdrecht MCM, HeijnenSJ. 2000. Wastewater treatment with particulate biofilm reactors. J Biotechnol 80:1-33.

Ohshima H. 1994 Electrophoretic mobility of soft particles. J Colloid Interface Sci 163:474-483.

Petrozzi S, Kut OM, Dunn IJ. 1991. Protection of biofilms against toxic shocks by the adsorption and desorption capacity of carriers in anaerobic fluidized bed reactors. Bioprocess Eng 9:47-59.

Poortinga AT, Bos R, Busscher HJ. 2001. Electrostatic interactions in the adhesion of an ion-penetrable and ion-impenetrable bacterial strain to glass. Colloids Surf B: Biointerfaces 20:105-117.

Saito K, Tsuneda S, Kim M, Kubota N, Sugita K, Sugo T. 1999. Radiation-induced graft polymerization is the key to develop high-performance functional materials for protein purification. 54:517-525.

Terada A, Hibiya K, Nagai J, Tsuneda S, Hirata A. 2003. Nitrogen removal

characteristics and biofilm analysis of a membrane-aerated biofilm reactor applicable to high-strength nitrogenous wastewater treatment. J Biosci Bioeng 95:170-178.

Terada A, Yamamoto T, Hibiya K, Tsuneda S, Hirata A. 2004. Enhancement of biofilm formation onto surface-modified hollow-fiber membranes and its application to membrane-aerated biofilm reactor. Water Sci Technol 49 (11-12):263-268.

Tsuneda S, Jung J, Hayashi H, Aikawa H, Hirata A, Sasaki H. 2003. Influence of extracellular polymers on electrokinetic properties of heterotrophic bacterial cells examined by soft particle electrophoresis theory. Colloids Surf B: Biointerface 29:181-188.

Tsuneda S, Nagano T, Hoshino T, Ejiri Y, Noda N, Hirata A. 2003. Characterization of nitrifying granules produced in an aerobic upflow fluidized bed reactor Water Res 37:4965-4973.

Tsuru T, Nakao S, Kimura S. 1990. Effective charge-density and pore sturucture of charged ultirafiltration membranes. J Chem Eng Jpn. 23:604-610.

Chapter 3

Effects of electrostatic properties of positively

charged polymer surfaces

on bacterial adhesion and activity

Chapter 3

Effects of electrostatic properties of positively charged polymer surfaces on bacterial adhesion and activity

3

Abstract

Primary, secondary and tertiary amino groups were introduced into polymer chains grafted onto a polyethylene (PE) flat-sheet membrane to evaluate the effect of surface properties on the adhesion and viability of *Escherichia coli* cells. The characterization of the surfaces containing amino groups, *i.e.*, ammonia (AM), ethylamino (EA) and diethylamino (DEA), revealed that the membrane potentials of AM-containing sheets are constant regardless of AM group density. A high bacterial adhesion rate constant k was observed at a high membrane potential, which indicates that membrane potential could be an indicator for evaluating bacterial adhesion onto the EA and DEA sheets. The maximum *E. coli* cell adhesion rate constants of the EA- and DEA-containing sheets were 3.5-fold that of the PE sheet. The *E. coli* cell viability experiment revealed that approximately 70% of the cells adhering onto these sheets were inactivated after a contact time of 8 h, and that such viability was dependent on membrane potential.

Furthermore, *E. coli* cell viability significantly decreased at a membrane potential higher than −8 mV. Future perspectives regarding the application of these sheets to the enhancement of biofilm formation or prevention are discussed.

Submitted to: A. Terada, A. Yuasa, S. Tsuneda, A. Katakai, M. Tamada, "Effects of electrostatic properties of positively charged polymer surfaces on bacterial adhesion and activity" *Microbiology-SGM*

3.1 Introduction

The vast majority of microorganisms adhere to most surfaces and form complex and heterogeneous microbial communities termed biofilms (Bos *et al*., 1999). Although the formation of biofilms is harmful in aqueous environments and biomaterial systems (Hallam *et al*., 2001; Kjellerup *et al*., 2003; Hendricks *et al*., 2000), the application of biofilms to a wastewater treatment system can be beneficial (Lin *et al*., 2004; Nicolella *et al*., 2000; Tsuneda *et al*., 2003). In the former case, the focus of most research is how to prevent bacterial adhesion followed by the subsequent formation of harmful biofilms. In the latter case, the enhancement of the initial adhesion of bacteria onto a substratum and the formation of robust biofilms are significant for the rapid startup of biofilm reactors and the effective removal of contaminants in such reactors.

Bacterial adhesion leading to mature biofilms generally entails two steps: a reversible step involving physicochemical forces and an irreversible chemical step involving the generation of extracellular polymeric substances (EPSs). The significance of the effect of the initial bacterial adhesion on biofilm formation has been questionable because the number of bacterial cells involved in the initial adhesion is much smaller than that in

mature biofilms (Petrozzi *et al*., 1991; Fox *et al*., 1990); however, some researchers have suggested the significance of the link between the initial bacterial adhesion and the biofilms formed (Busscher *et al*., 1995). In particular, it has been reported that physicochemical properties, *e.g.*, surface potential, roughness and hydrophobicity, affect the rate of the initial bacterial adhesion and the subsequent biofilm formation (Gottenbos *et al*., 1999, 2000, 2001; Hibiya *et al*., 2000; Terada *et al*., 2005). Moreover, taking into account the fact that bacterial growth and EPS secretion after adhesion onto a solid substratum result in biofilm formation, the estimation of both bacterial adhesion and bacterial viability is essential for determining some clues to biofilm prevention and enhancement.

Many surface modification techniques, such as surface abrasion (Morgan and Wilson, 2001), chemical coating (Harris and Richards, 2004) and chemical grafting (Gottenbos *et al*., 1999, 2000, 2001; Hibiya *et al*., 2000; Terada *et al*., 2004, 2005; Park *et al*., 1998; Pasmore *et al*., 2000; Roosjen *et al*., 2003, 2004; Lee *et al*., 1996, 1997, 1998), have been developed to promote or prevent bacterial adhesion and biofilm formation. Radiation-induced grafting technology can generate highly reactive radicals and subsequently initiate the polymerization and extension of long graft chains onto common polymer materials such as polyethylene (PE). In particular, radiation-induced graft polymerization (RIGP) can control the density and length of graft chains. Each property can be varied by adjusting two set times: the time that a base material is exposed to an electron beam and the time that the treated base material is reacted with the vinyl monomer (Kawai *et al*., 2003). Another important feature of RIGP is that many monomers can be chemically modified further during a functionalization step to impart on the important properties such as the ability to attract bacterial cells. In our previous study, positively or negatively charged groups were introduced into PE membrane sheets

by the RIGP of an epoxy-group-containing monomer, glycidyl methacrylate (GMA) and subsequent epoxy-ring-opening reaction. Then, bacterial adhesion characteristics were examined. As a result, it was clarified that electrostatic interaction is the most decisive factor for bacterial adhesion (Terada *et al*., 2005). However, it is still unclear how a positively charged surface affects bacterial viability and whether the optimum point for biofilm enhancement and prevention exists.

From the above viewpoint, primary, secondary and tertiary amino groups, having different strengths of positive charges, were introduced into poly-GMA chains in this chapter. The objective of this chapter is twofold: 1) to examine the effect of the electrostatic properties of a positively charged surface prepared by RIGP on the initial bacterial adhesion statistically, 2) to evaluate the viability of bacteria adhering onto surfaces and determine the decisive factor of bacterial viability.

3.2 Materials and methods

3.2.1 Bacterial strain

As a representative bacterial strain, Escherichia coli (IFO-3301) was used in this study. Before adhesion tests, this strain was aerobically cultured for 1 day at 30°C in a liquid medium containing the following: polypeptone, 10.0 g; yeast extract, 5.0 g; sodium chloride, 1.0 g; and distilled water, 1 L. Cells were harvested in their exponential growth phase by centrifugation (8000 g, 10 min) and resuspended in water. This washing step was repeated three times to eliminate residual substrates and EPS. Finally, the washed cells were suspended in 0.02 M phosphate-buffered saline (PBS). The linear relationship between cell number and optical density at 660 nm wavelength (O.D.660) was confirmed using YO-PRO-1 (Molecular Probes, Leiden, The Netherlands).

3.2.2 Introduction of anion-exchange groups into membrane sheet

Figure 3.1 shows a preparation scheme for the amino groups into PE. PE-based membrane sheets (PE sheets) (Asahi Kasei Chemicals, Tokyo, Japan) were used as the trunk polymer for grafting. Each sheet was 10 × 7.5 cm, with a porosity of 70% and an average pore size of 0.20 μm. Technical-grade GMA was purchased from Tokyo Kasei (Tokyo, Japan) and used without further purification. Ammonia, ethylamine and diethylamine were obtained from Kanto Chemical (Tokyo, Japan). The sheets were irradiated with an electron beam from an accelerator (Dynamitron, Model IEA 3000-25-2, Radiation Dynamics Inc., Edgewood, NY) operating at a beam energy of 2.0 MeV and a current of 1 mA at ambient temperature in a nitrogen atmosphere. The total irradiation dose was 200 kGy. Then, the irradiated sheets were immersed in a glass ampoule containing GMA (5wt/wt% in methanol), previously sparged with nitrogen gas, and allowed to react at 313 K. The radicals generated on the sheets, which react with GMA, are used as starting sites for the polymerization and extension of long graft chains from the bulk towards and off the surface of the sheets. The GMA-grafted sheets (GMA sheets) obtained were immersed in *N,N*-dimethylformamide and then in methanol to remove residual monomers and homopolymers, followed by drying under reduced pressure. The amount of GMA grafted onto each stem sheet represented the degree of grafting (*dg*) calculated using

$$dg = 100 \times \left(\frac{W_1 - W_0}{W_0} \right) \tag{3.1}$$

where W_0 and W_1 are the weights of the stem and GMA sheets, respectively. The grafted sheets with a *dg* of approximately 100% were prepared by setting the grafting time at 30 min. The GMA sheets with a *dg* of 100% were then immersed in ammonia-, ethylamine-, or diethylamine-containing solution under the conditions shown in Table 3.1. The

reaction of the GMA sheets with AM, EA and DEA converts the epoxy groups of the GMA into the respective amino groups. The amino group density and molar conversion percentage are calculated using

$$\text{Amino group density} = 1000 \times \frac{\dfrac{W_2 - W_1}{M_W}}{W_2} \tag{3.2}$$

$$\text{Molar conversion percentage of amino groups} = 100 \times \frac{\dfrac{W_2 - W_1}{M_W}}{\dfrac{W_1 - W_0}{142}} \tag{3.3}$$

where W_2 and M_w are the weight of the amino-group-containing sheet and the molecular weight, respectively. Hereafter, the resultant GMA-, AM-, EA- and DEA-containing sheets are respectively referred to as GMA, AM, EA and DEA (X) sheets; X in parentheses designates the molar conversion percentage of each amino group.
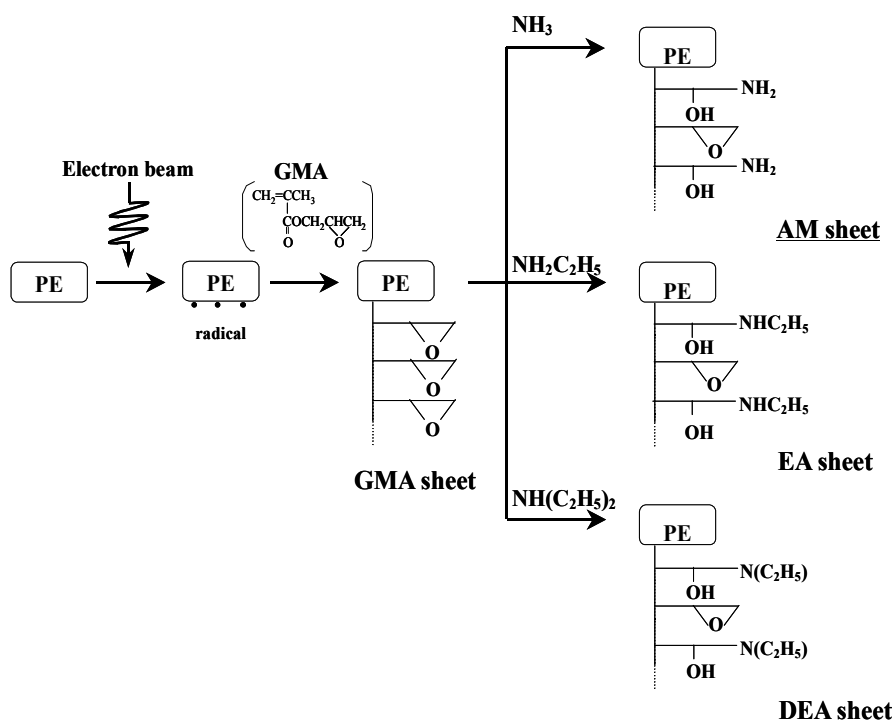
Figure 3.1 Preparation scheme of primary, secondary, or tertiary amino group-containing polymer chains grafted onto flat-sheet membranes.

Table 3.1 Conditions for Epoxy-Opening Reaction for the Preparation of Primary-, Secondary- and Tertiary-Amino-Group-Containing Flat-Sheet Membrane.

	AM sheet	EA sheet	DEA sheet
Reactant	NH_3	$NH_2C_2H_5$	$NH(C_2H_5)_2$
Dissolution constant of reactant (25°C)	1.77×10^{-5} [1]	3.98×10^{-4} [2]	6.91×10^{-4} [3]
Molecular weight (M_W) [g/mol]	17	45	73
Conc. of reactant[4] [v/v%]	28	50	50
Reaction temperature [K]	318	303	303

[1]   Bates and Pinching (1950)

[2]   Zheng and Blanchard (2000)

[3]   Perrin (1965)

[4]   Solvent: water

3.2.3 Characterization of membrane sheets prepared by RIGP

The densities of the AM, EA and DEA groups were determined from the measurements of the total ion exchange capacity by titration. The AM, EA and DEA sheets were immersed in 2 M NaOH solution to recover anion-exchange capacity. Then, 0.2 M HCl solution was used for ion exchange. Titration was performed using 0.1 M NaOH solution. A solution of methyl red and methylene blue (Kanto Chemical Co., Tokyo, Japan) was used as an indicator. Membrane potential was measured in accordance with the procedure of Tsuru *et al*. (1990). A U-bend glass cell was divided into two compartments by pinching one membrane sheet at the bottom of the cell. After rinsing in distilled water, the membrane sheets were used for the measurements. Distilled water and 0.02 M (pH 7.2) PBS were supplied to one side and the other side of the cell, respectively. Temperature was maintained at 298 K. Membrane potential was measured using two reference electrodes (RE-1C, BAS Inc., Tokyo, Japan), which were Ag/AgCl electrodes both connected to an electrometer (R8240, Advantest, Tokyo, Japan) in a saturated potassium chloride solution. The measurement was conducted in triplicate under the

same conditions. Water contact angles on each sheet were measured at 20ºC using the sessile drop technique. The sheets were fixed on a glass plate with double-sided sticky tape and the contact angle of each sample was measured by keeping the syringe in the water droplet (1.5 µL). Each contact angle was the average of at least ten different points.

3.2.4 Evaluation of rate of E. coli cell adhesion onto membrane sheets

Bacterial adhesion tests were conducted in accordance with the method of Terada *et al.* (2005). The prepared cell suspension of 40 ml was placed in a 50-ml beaker. The concentration of *E. coli* cells was set at an O.D.$_{660}$ of 0.050 that is equivalent to 5.8×10^9 cells/mL. PE, GMA, AM (*X*=26, 32, 46, 48, 58 and 100), EA (*X*=35, 37, 54, 67, 75 and 87) and DEA (*X*=11, 29, 67, 74, 95 and 100) sheets were cut into 0.25 cm^2 sections. Each sheet was immersed in a beaker containing an *E. coli* cell suspension. The cell suspension and the prepared sheets were shaken at 200 rpm and 298 K. The adhesion of the cell onto each sheet was measured from the decrease in the O.D.$_{660}$ of each cell suspension. The adhesion rate constant *k* was defined as

$$V \frac{dC}{dt} = -kAC \tag{3.4}$$

$$k = -\left(\frac{V}{A}\right)\left(\frac{1}{t}\right)\ln\left(\frac{C_t}{C_0}\right) \tag{3.5}$$

where *V*, *A*, *t*, *C$_t$*, and *C$_0$* are the volume of the cell suspension, two-dimensional sheet surface area, contact time, O.D.$_{660}$ at time *t* and initial O.D.$_{660}$, respectively.

3.2.5 Viability of E. coli cells adhering onto membrane sheet

The viability of *E. coli* cells adhering onto each sheet was evaluated with a commercially available staining kit (Live/Dead *Bac*light bacterial viability kit, Molecular Probes,

Leiden, The Netherlands). The Live/Dead kit comprised the green fluorescent DNA-binding stain SYTO 9 and the red fluorescent DNA-binding stain propidium iodide (PI), enabling the detection of bacterial viability from the difference in membrane integrity between embedded cells. Each membrane sheet was carefully removed from the beaker after immersion in *E. coli* cell suspension for 0.25, 2, 4, 6 and 8 h and was mounted onto a slide glass well. Each sheet was filled with 8 μl of 1000-fold-diluted Live/Dead kit and incubated for 15 min in the dark. After washing with distilled water, the sheets were mounted in FluoroGuard Antifade reagent (Bio-Rad, Hercules, CA), and observed by fluorescence microscopy (Axio skop2 plus, Carl Zeiss, Oberkochen, Germany) to visualize live and dead cells. Bacterial viability was calculated from the ratio of the number of live cells stained with SYTO-9 to the total number of cells (SYTO-9-positive plus PI-positive cells). Direct counting was carried out for more than 10 randomly recorded images.

3.3 Results

3.3.1 Characterization of membrane sheets prepared by RIGP

The *dg* of the membrane sheets increased proportionally to reaction time in 5wt/wt% GMA/methanol solution (r=0.998) (data not shown). The time courses of the conversion of the grafted epoxy groups to the amino groups are shown in Figure 3.2. The molar conversion percentages of the epoxy groups to the amino groups ranged from 11 to 100%. The conversion was almost completed within 1.5 h, as shown in Figure 3.2, indicating that the reaction is faster than those previously reported (Lee *et al.*, 1996, 1997; Koguma *et al.*, 2000). This difference seems to be simply because the membrane used in this study was a flat sheet, allowing for the rapid permeation of a solvent with the amino groups,

compared with hollow-fiber membranes. Figure 3.3 shows the relationship between the density of the AM, EA and DEA groups determined by titration and that determined from weight gain calculated using equation (3.2). A good agreement was observed, which indicates that the weight gain accompanying the reaction of the epoxy group with AM, EA or DEA corresponded to the intrinsic introduction of these groups. This result clearly shows that the increase in weight was due to the conversion of GMA to AM, EA or DEA, indicating the accuracy of the conversion reaction in this experiment.

Figure 3.4 shows the relationship between amino group density and membrane potential. Clearly, this figure shows that the membrane potentials of the EA and DEA sheets are proportional to their amino group densities. On the other hand, the membrane potential of the AM sheets remained constant in spite of an increase in AM group density. Obviously, these results indicate that amino group density is not necessarily dependent on membrane potential probably because the AM sheets do not have a higher degree of dissociation constant in solution than the EA and DEA sheets. Koguma *et al.* (2000) revealed that the permeability of Tris-HCl buffer through AM hollow fibers, *i.e.*, liquid flux, is constant irrespective of the occurrence of conversion, which supports our result that membrane potential was independent of AM group density. The result of contact angle is summarized in Table 3.2. The contact angle of the GMA sheet was almost the same as that of the PE sheet. On the other hand, the conversion of the GMA sheet to the AM (100), EA (87) or DEA (100) sheet slightly decreased contact angle. This decrease is probably because the amino groups have a hydroxyl group, which is generated through such conversion reaction. In summary, the contact angles after the grafting and conversion did not change dynamically compared with those in previous studies that treat the modification of polymers with grafting (Park *et al.*, 1998; Sainbayar *et al.*, 2001; Wang *et al.*, 2000).
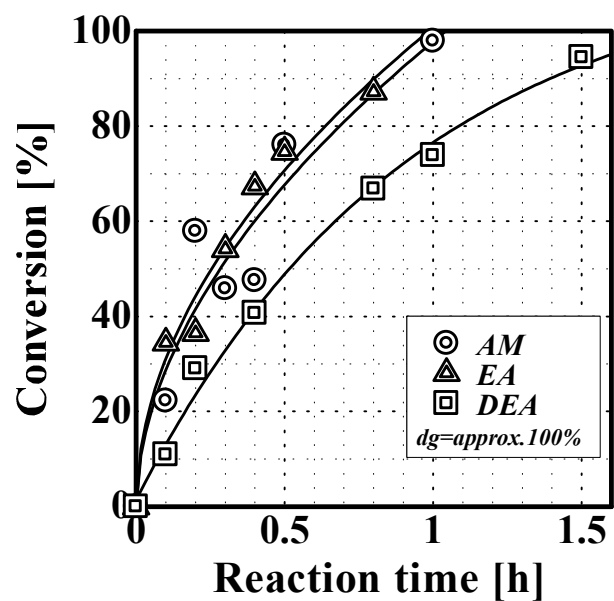
Figure 3.2 Time courses of conversion of epoxy groups to AM, EA and DEA groups.
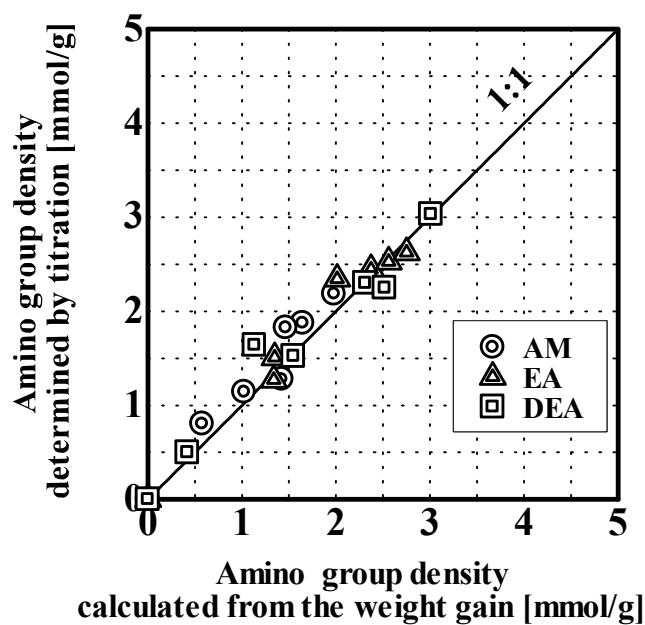
Figure 3. 3 Amino group densities determined by titration vs. those calculated from weight gain.
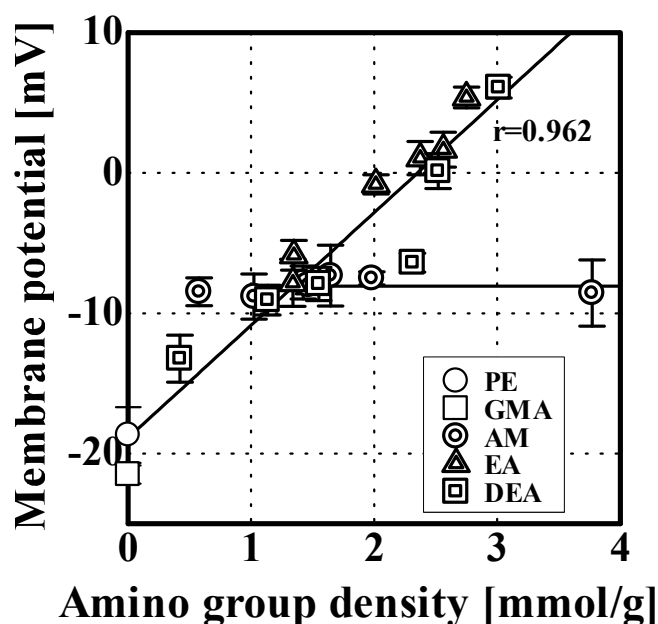
Figure 3.4 Relationship between amino group density and membrane potential.

Table 3.2 Contact Angles of PE, GMA, AM, EA and DEA sheets. Values in Parentheses Represent Conversion Percentages of Amino Groups.

	PE	GMA	AM (100)	EA (87)	DEA (100)
Contact angle [°]	92.0	93.8	79.6	80.4	83.0
Standard deviation	±0.83	±1.67	±2.87	±2.91	±3.63

3.3.2 Estimation of E. coli cell adhesion

The result of the *E. coli* cell adhesion experiments is shown in Figure 3.5. For the AM sheets (Figure 3.5 (a)), the concentration of the *E. coli* cell suspension did not decrease significantly notwithstanding conversion ratio, indicating that the AM sheets with a high conversion percentage do not enhance *E. coli* adhesion essentially. On the other hand, a marked enhancement of *E. coli* cell adhesion was observed for the EA and DEA sheets (Figures 3.5 (b-c)). Moreover, the adhesion rate of *E. coli* increased with conversion

percentage, indicating the significant effect of conversion on bacterial adhesion. Considering that the zeta potential of the *E. coli* cell surface is negative at pH 7.2 (Terada *et al.*, 2005), the electrostatic interaction between the cells and the sheet surface is a decisive factor governing bacterial adhesion. Figure 3.6 shows the effect of the membrane potential of the sheets on the bacterial adhesion rate constant k. The rate constants of the EA and DEA sheets increased with their membrane potentials. Furthermore, the slope of the rate constant increased at a membrane potential higher than -8 mV. Since the membrane potentials of the AM sheets were almost the same regardless of their densities as shown in Figure 3.4, it was approximately -8 mV. These results indicate that membrane potential is a decisive factor reflecting the adhesion behavior of *E. coli* in terms of the EA and DEA sheets. Thereafter, membrane potential is used to evaluate the viability of *E. coli* cells.

(a)

(b)

(c)
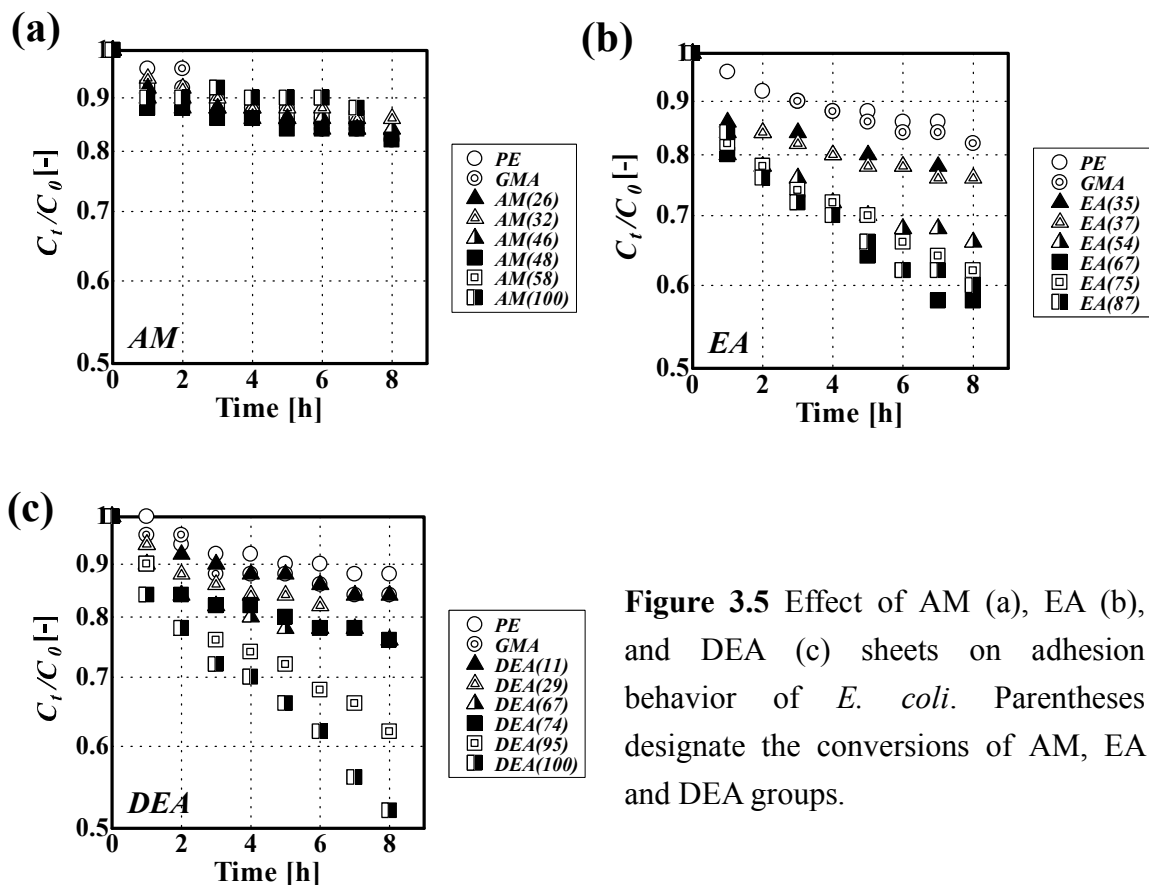
Figure 3.5 Effect of AM (a), EA (b), and DEA (c) sheets on adhesion behavior of *E. coli*. Parentheses designate the conversions of AM, EA and DEA groups.
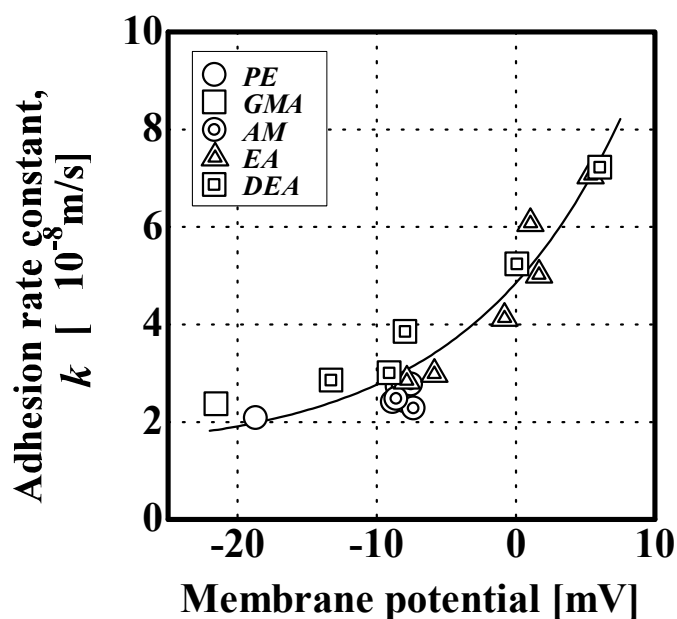
Figure 3.6 Effect of membrane potential on adhesion rate constant k.

3.3.3 Evaluation of E. coli viability

The time courses of the transition of bacterial viability on the PE, GMA, AM (100), EA (87) and DEA (95) sheets are shown in Figure 3.7. All *E. coli* cells did not aggregate in bulk liquid and any colonization on each sheet was not observed during the experiment (data not shown). The viability of planktonic *E. coli* cells remained approximately 90% after 8 h in the bulk liquid where each sheet was immersed. This result indicates that there is no dissolution of amino groups from each polymer sheet and that the effect of the bulk liquid on the viability of *E. coli* cells is negligible. Similar tendencies between the PE and GMA sheets were observed: 70-80% cells of adhering *E. coli* cells on the PE and GMA sheets were viable and the viability remained almost constant during the whole experimental period. Although bacterial activities on the PE and GMA sheets decreased to some extent, they more or less remained constant. On the other hand, the trends of *E. coli* cell viability on the AM (100), EA (87) and DEA (95) sheets were quite different from those on the PE and GMA sheets. The *E. coli* cell viability of the AM (100) sheet

gradually decreased; those of the EA (87) and DEA (95) sheets were quite low even at 0.25 h. After the 8-h immersion of these three sheets in *E. coli* cell suspension, the percentage viability decreased to 20-30% irrespective of the differences among primary, secondary and tertiary amino groups, indicating that large amounts of *E. coli* cells were inactivated after adhesion onto the AM (100), EA (87) and DEA (95) sheets. The relationship between membrane potential and *E. coli* cell viability is shown in Figure 3.8 after the 6-h immersion of the cell suspension. A critical point of *E. coli* cell viability was clearly observed; the viability decreased significantly at membrane potentials higher than −8 mV. In other sampling points (2, 4 and 8 h), sharp decreases in *E. coli* cell viability were also observed at almost the same point (data not shown), indicating that the membrane potentials of these sheets strongly affect *E. coli* cell viability. Although the exact reason for this decrease in activity remains unclear, we have demonstrated that amino-group-containing sheets, *i.e.*, the AM, EA and DEA sheets, with a membrane potential higher than −8 mV, significantly inactivate *E. coli* cells and that there exists a membrane potential threshold for the decrease in the activity of *E. coli* cells.
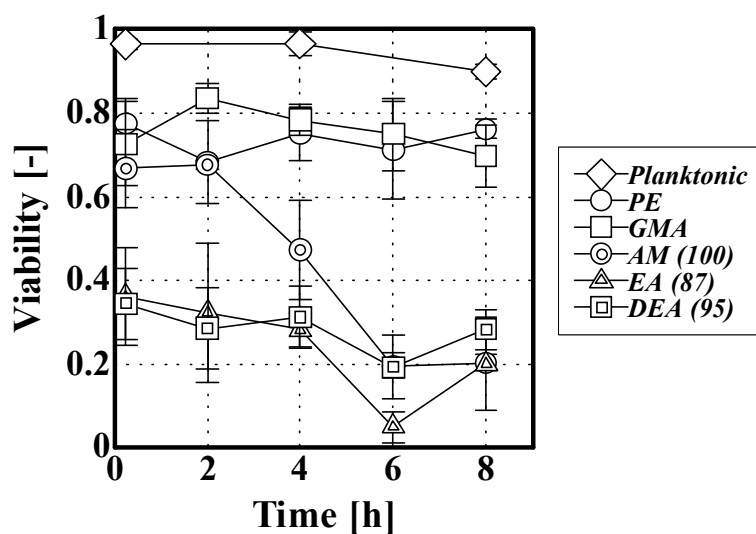
Figure 3.7 Time course *E. coli* cell viability on PE, GMA, AM (100), EA (87) and DEA (95) sheets.
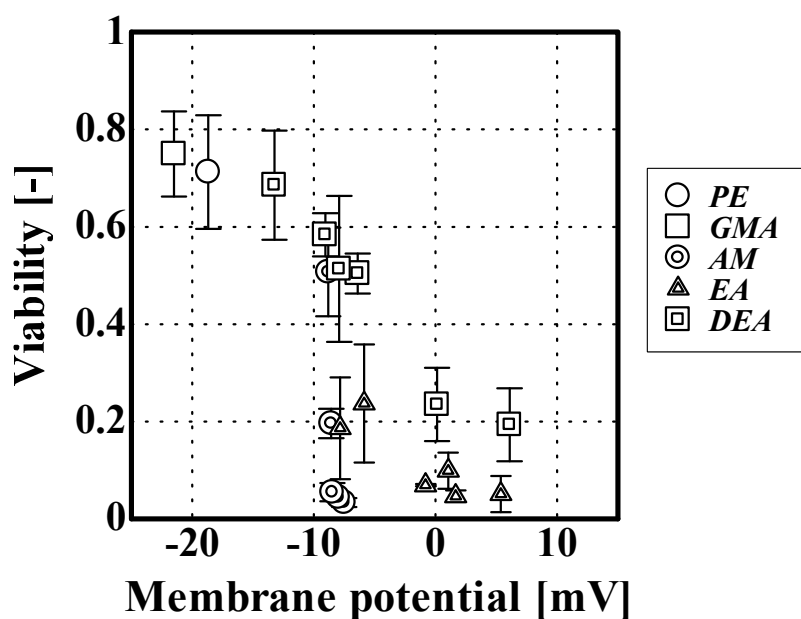
Figure 3.8 Dependence of *E. coli* cell viability on membrane potential of each sheet (6 h).

3.4 Discussion

3.4.1 Surface characterization

For measurement of the surface characteristics of the prepared sheets, X-ray photoelectron spectroscopy (XPS) or Fourier transform infrared attenuated total reflectance (FTIR-ATR) could be a powerful tool. However, these measurements were not conducted in this study because of the following two reasons. One reason is that the composition of nitrogen in the AM, EA and DEA sheets is significantly less than those of carbon and hydrogen, yielding critical error in the quantitative analyses of the sheets with different amino group densities. Using FTIR-ATR, however, Lee *et al.* (1998) qualitatively confirmed the existence of C=O stretching in the GMA fibers and its disappearance when converting the GMA fibers completely into DEA fibers. Therefore, XPS or FTIR-ATR could be useful for corroboration of the results obtained from

gravimetric method and titration. The other reason is that XPS or FTIR-ATR is conducted under completely dry conditions, whereas the adhesion and activity experiments were conducted under wet conditions: this discrepancy probably gives rise to inadequate interpretation of bacterial adhesion behavior. From the above-mentioned two reasons, it is judged that the most appropriate method, which enables the quantitative measurement of nitrogen components under the same conditions as the bacterial adhesion experiment, is the combination of the gravimetric method and titration.

3.4.2 Generalization of E. coli adhesion behavior

Considering that some physicochemical features of the membrane sheet surfaces affect *E. coli* adhesion, it is essential to clarify which parameter determines *E. coli* adhesion behavior. The contact angles of the AM, EA and DEA sheets did not decrease significantly compared with those of the PE and GMA sheets (Table 3.2), which indicates that the differences in respective surface hydrophobicity were less significant than the fluctuations of membrane potential and density (Figure 3.4). We previously investigated the relationship between the surface roughness of membrane sheets and the degree of grafting (*dg*), leading to the fact that the roughness increases linearly in *dg* irrespective of functional groups, *i.e.*, DEA and GMA (Terada *et al*., 2005). Since sheets with a *dg* of approximately 100% were used in this study, the roughnesses of all the surfaces except the PE membrane are probably the same; hence, the effect of roughness would not be significant on *E. coli* cell adhesion. In summary, it is concluded that electrostatic interaction, *i.e.*, membrane potential, would be the most significant parameter in terms of *E. coli* adhesion.

The determination of the behavior of *E. coli* adhesion onto the prepared sheets shows that the adhesion rate constant of *E. coli* increases with membrane potential and that the

slope increases at a membrane potential higher than −8 mV. Lee *et al*. (1997) clarified that there is a relationship between the conversion ratio of the DEA group to the GMA group and the capture rate constant of *Staphylococcus aureus* and that the rate constant increases with conversion ratio, *i.e.*, the density of DEA. The obtained result indicates that both the density and membrane potential of the EA and DEA sheets are good indicators for understanding the behavior of *E. coli* adhesion onto sheets. The reason the AM sheets did not have different membrane potentials is the low dissolution constant of AM (Bates *et al.*, 1950). Since the dissolution constant of AM is one order of magnitude smaller than those of EA and DEA (Table 1), the AM sheets did not have a high ion exchange capacity, leading to no difference in membrane potential among them.

3.4.3 Effect of graft chain on E. coli cell adhesion

As shown in Figure 3.7, the viability of *E. coli* cells on the AM (100) sheet decreased gradually. In contrast, more than half of the *E. coli* cells on the EA (87) and DEA (95) sheets whose adhesion rate constants were much higher than those of the PE, GMA and AM (100) sheets were inactivated after 0.25-h immersion in *E. coli* suspension. The sheets prepared by RIGP have a very unique structure, *i.e.*, they have graft chains containing amino groups with a positive charge, which attracts bacterial cells (Kawai *et al.*, 2003). Therefore, it seems to be important in elucidating how these polymer conformations influence bacterial adhesion. Kawai *et al.* (2000) reported that the DEA-containing graft chain extends with the capture of proteins due to the electrostatic repulsion between each DEA group in water and ionizable graft chains can form distinct conformational structures depending on the density of ionizable groups. Koguma *et al.* (2000) showed that two-dimensional protein adsorption occurs in AM-containing hollow-fiber membranes owing to insufficient electrostatic interaction among graft

chains, whereas three-dimensional protein adsorption occurs in EA- and DEA-containing hollow-fiber membranes, resulting in a significant difference in binding capacity. Their results support our result that the strengths of the charges of AM, EA and DEA determine bacterial adhesion rate, which is presumably related to graft chain conformation. Moreover, the behaviors of protein adsorption and bacterial adhesion are quite similar in spite of the difference in particle size between a protein molecule and a bacterial cell. Regarding the relationship between adhesion rate constant and membrane potential in Figure 3.6, the slope of the constant increases markedly at a membrane potential higher than −8 mV. This result disagrees with our previous results that the membrane potential of DEA sheets with a conversion of approximately 100% is proportional to the *E. coli* adhesion rate constant (Terada *et al.*, 2005). This difference seems to be due to the effect of graft chain conformation: the EA and DEA sheets with low degrees of conversion cannot extend graft chains, leading to low adhesion rate constants of *E. coli* cells. Additionally, our result agrees with that of Lee *et al.* (1997), in which capture rate constant increases markedly during the conversion of a DEA group higher than 80% although they used a different bacterium. Considering that the GMA sheet does not enhance *E. coli* adhesion, as shown in Figure 3.6, it can be concluded that the enhancement of bacterial adhesion is due to the favorable membrane potential of *E. coli* cells and possibly to the extension of graft chains induced by electrostatic repulsion among graft chains.

3.4.4 Is the sheet prepared by RIGP effective for biofilm prevention and formation?

The result in Figure 3.8 shows that the viability of *E. coli* cells is dependent on membrane potential irrespective of the differences among primary, secondary and tertiary amino groups. Apparently, there is a threshold around a membrane potential of −8 mV,

which governs the viability of *E. coli* cells. Therefore, the membrane potential of the sheets could be a decisive factor affecting not only bacterial adhesion rate but also bacterial viability. In general, the anion-exchange group-containing surfaces, *e.g.*, quaternary ammonium compounds (QACs), are widely used because of their antibacterial effect (McDonnel and Russell, 1999; Kügler *et al.*, 2005). The mechanism of the loss of bacterial activity has been proposed by Salton *et al.* (1968). Kügler *et al.* (2005) reported that the electrostatic interaction between a QAC surface and bacteria is a significant parameter for the control of bacterial growth. They clarified that *E. coli* cells are inactivated within less than 10 min, which is shorter than the doubling time of *E. coli*, and thus there is no possibility for biofilm formation on the QAC surface. On the other hand, our results clarified that approximately 20% of *E. coli* cells on the EA (87) and DEA (95) sheets are still active even after the 6-h immersion in the cells suspension. Figure 3.9 shows the number of adhering *E. coli* cells, which was calculated from the relationship between O.D.$_{660}$ and the number of *E. coli* cells. Seemingly, the cells adhering onto the EA (87) and DEA (95) sheets would be effective for antibacterial application; however, some cells were still alive, indicating that the growth potential to form biofilms remains on the EA (87) and DEA (95) sheets. These sheets would not be suitable for killing bacteria and biofilm prevention; however, it is possible to increase membrane potential by increasing *dg* (Terada *et al.*, 2005). Therefore, the optimum design of sheets for biofilm prevention may be possible.

Some researchers have focused on the effect of positively charged surface properties on biofilm formation. Gottenbos *et al.* (2001) clarified that bacterial adhesion onto a surface with positive zeta potential is enhanced; however, the subsequent biofilm formation is slower, indicating that a positively charged surface adversely affects biofilm formation. On the other hand, Hibiya *et al.* (2000) reported that a nitrifying biofilm,

which is difficult to obtain, forms on DEA-containing sheets successfully under high hydrodynamic conditions. This apparent controversy may be due to the fact that different surface properties, bacterial concentrations and hydrodynamic conditions have been used in these studies, and hence it seems to be difficult to summarize the decisive factors for biofilm formation systematically. Moreover, Lee *et al.* (2004) observed, by atomic force microscopy, that EPS from dead *E. coli* cells adsorbed onto glass surfaces although it is unclear how EPS works after cell death. Tsuneda *et al.* (2000) reported that the utilization of EPS excreted by heterotrophic bacteria results in a thick biofilm with large quantities of the autotrophic nitrite-oxidizing bacterium, *Nitrobacter winogradskyi*, and a high nitrite-oxidation rate. Since the EPS excreted by dead *E. coli* cells could help the biofilm adhere strongly and supply carbon component to live cells, the EA (87) and DEA (95) sheets seem to have an advantage in biofilm formation under turbulent flow conditions. Our ongoing research is focused on the long-term activity of bacterial cells adhering onto PE, GMA, AM, EA and DEA sheets and on subsequent biofilm formation with a flow chamber, which will elucidate the differences between the mechanisms of the formation of a series of biofilms dependent on surface properties. The adhesion assay used in this study is not applicable to monitoring subsequent biofilm formation because bacteria from the bulk liquid inevitably attach to the biofilm, leading to error in the estimation. Biofilm formation experiments with a flow chamber, which has been conducted by numerous researchers, probably overcome this problem and facilitate *in situ* observation of grown biofilms (Bos *et al.*, 1999; Busscher and van der Mei, 1995; Stoodley *et al.*, 2003). Through such observation, we will propose the optimum biointerface design for the enhancement or prevention of biofilm formation.
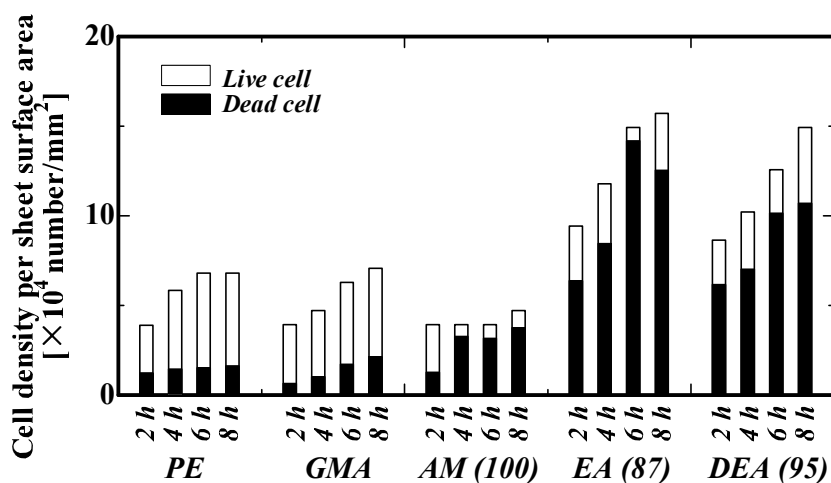
Figure 3.9 Estimated numbers of live and dead *E. coli* cells adhering onto each surface.

3.5 Conclusion

A monomer containing an epoxy group, GMA, was grafted onto a PE sheet. Three amino

groups, *i.e.*, AM, EA and DEA, were introduced into the grafted sheets with different

amino group densities. The anion exchange capacities determine the conformation of

graft chains, which reflects membrane potential. Membrane potential is a good indicator

of the rate of bacterial adhesion onto the EA and DEA sheets since *E. coli* adhesion rate

constant increases with membrane potential. Apparently, the viability of *E. coli* cells on

the anion exchange sheets, *i.e.*, the AM (100), EA (87) and DEA (95) sheets, decreases

with increasing membrane surface potential in comparison with those on the PE and

GMA sheets. Furthermore, a membrane potential threshold critically affecting *E. coli* cell

viability is observed. Considering the high bacterial adhesion potentials of the EA and

DEA sheets, these sheets do not seem to be suitable for bacterial biofilm prevention.

Although we cannot determine whether these sheets are feasible for biofilm formation

yet, the results obtained in this chapter, at least, lead to the conclusion that differences in

these surface properties apparently influence adhesion behavior and adhering bacterial activity, both of which are closely associated with biofilm formation.

References

Bates RG, Pinching GD. 1950. Dissociation constant of aqueous ammonia at 0 to 50ºC from E. m. f. studies of the ammonium salt of a weak acid. J Am Chem Soc 72:1393-1396.

Bos R, van der Mei H, Busscher HJ. 1999. Physico-chemistry of initial microbial adhesive interactions-its mechanisms and methods for study. FEMS Microbiol Rev 23:179-230.

Busscher HJ, Bos R, van der Mei HC. 1995 Initial microbial adhesion is determinant for the strength of biofilm adhesion. FEMS Microbiol Lett 128:229-234.

Busscher HJ, van der Mei HC. 1995. Use of flow chamber devices and image-analysis methods to study microbial adhesion. Methods in Enzymology 253:455-477.

Fox P, Suidan MT, Bandy JT. 1990. A comparison of media types in acetate fed expanded-bed anaerobic reactors. Water Res 24:827-835.

Gottenbos B, van del Mei HC, Busscher H J, Grijpma DW, Feijen J. 1999. Initial adhesion and surface growth of Pseudomonas aeruginosa on negatively and positively charged poly (methacrylates). J Material Sci: Mater in Medicine 10:853-855.

Gottenbos B, van der Mei HJ, Busscher J. 2000. Initial adhesion and surface growth of *Staphylococcus epidemidis* and *Pseudomonas aeruginosa* on biomedical polymers. J Biomed Mater Res 50:208-214.

Gottengbos B, Grijpma DW, van der Mei HC, Feijen J, Busscher HJ. 2001. Antimicrobial effects of positively charged surfaces on adhering Gram-positive bacteria, J Antimicrob Chemotherapy 48:7-13.

Hallam NB, West JR, Forster CF, Simms J. 2001. The potential for biofilm growth in water distribution systems. Water Res 35:4063-4071.

Hendricks SK, Kwok C, Shen MC, Horbett TA, Ratner BD, Bryers JD. 2000. Plasma-deposited membranes for controlled release of antibiotic to prevent bacterial adhesion and biofilm formation. J Biomed Mater Res 50:160-170.

Hibiya K, Tsuneda S, Hirata A. 2000. Formation and characteristics of nitrifying biofilm on a membrane modified with positively-charged polymer chains. Colloids Surf B: Biointerfaces 18:105-112.

Kawai T, Sugita K, Saito K, Sugo T. 2000. Extension and shrinkage of polymer brush grafted onto porous membrane induced by protein binding. Macromolecules 33:1306-1309.

Kawai T, Saito K, Lee W. 2003. Protein binding to polymer brush, based on ion-exchange hydrophobic, and affinity interactions. J Chromatography B 790:131-142.

Kjellerup BV, Olsen BH, Nielsen JL, Frolund B, Odum S, Nielsen PH. 2003. Monitoring and characterisation of bacteria in corroding district heating systems using fluorescence in situ hybridisation and microautoradiography. Water Sci Technol 47:117-122.

Koguma I, Sugita K, Saito K, Sugo T. 2000. Multilayer binding of proteins to polymer chains grafted onto porous hollow-fiber membranes containing different anion-exchange groups. Biotechnol Prog 16:456-461.

Kügler R, Bouloussa O, Rondelez F. 2005. Evidence of a charge-density threshold for optimum efficiency of biocidal cationic surfaces. Micobiology 151:1341-1348.

Lee SB, Koepsel RR, Morley SW, Matyjaszewski K, Sun Y, Russell AJ. 2004. Permanent, nonleaching antibacterial surfaces. 1. Synthesis by atom transfer radical polymerization. Biomacromolecules 5:877-882.

Lee W, Furusaki S, Saito K, Sugo T, Makuuchi K. 1996. Adsorption kinetics of microbial

cells onto a novel brush-type polymeric material prepared by radiation-induced graft polymerization. Biotechnol Prog 12:178-183.

Lee W, Saito K, Furusaki S, Sugo T. 1997. Capture of microbial cells on brush-type polymeric materials bearing different functional groups. Biotechnol Bioeng 53:523-528.

Lee W, Furusaki S, Saito K, Sugo T. 1998. Tailoring a brush-type interface favorable for capturing microbial cells. J Colloid Interface Sci 200:66-73.

Lin W, Yu T, McSwain BS. 2004. Biological fixed film systems. Water Environ Res. 76:1099-1154.

McDonnell G, Russell AD. 1999. Antiseptics and disinfectants: activity, action, and resistance. Clin Microbiol Rev 12:147-179.

Morgan TD, Wilson M. 2001. The effects of surface roughness and type of denture acrylic on biofilm formation by *Streptococcus oralis* in a constant depth film fermentor. J Appl Microbiol 91:47-53.

Nicolella C, van Loosdrecht MCM, Heijnen SJ. 2000. Wastewater treatment with particulate biofilm reactors. J Biotechnol 80:1-33.

Park KD, Kim YS, Han DK, Kim YH, Lee EHB, Suh H, Choi KS. 1998. Bacterial adhesion on PEG modified polyurethane surfaces. Biomaterials 19:851-859.

Pasmore M, Todd P, Smith S, Baker D, Silverstein J, Coons D, Bowman CN. 2001. Effects of ultrafiltration membrane surface properties on *Pseudomonas aerutinosa* biofilm initiation for the purpose of reducing biofouling. J Membr Sci 194:15-32.

Perrin DD. 1965. Dissociation Constants of Organic Bases in Aqueous Solution. Butterworths: London.

Petrozzi S, Kut OM, Dunn IJ. 1991. Protection of biofilms against toxic shocks by the adsorption and desorption capacity of carriers in anaerobic fluidized bed reactors.

Bioprocess Eng 9:47-59.

Roosjen A, Kaper HJ, van der Mei HC, Norde W, Busscher HJ. 2003. Inhibition of adhesion of yeasts and bacteria by poly (ethylene oxide)-brushes on glass in parallel plate flow chamber. Microbiology 149:3239-3246.

Roosjen A, van der Mei HC, Busscher HJ, Norde W. 2004. Microbial adhesion to poly (ethylene oxide) brushes: influence of polymer chain length and temperature. 20:10949-10955.

Sainbayar A, Kim JS, Jung WJ, Lee YS, Lee CH. 2001. Application of surface modified polypropylene membranes to an anaerobic membrane bioreactor. Environ Technol 22:1035-1042.

Salton, MRJ. 1968. Lytic agents, cell permeability and monolayer penetrability. J Gen Physiol. 52:252-277.

Stoodley P, Warwood BK. 2003. Use of flow cells and annular reactors to study biofilms. In *Biofilms in Medicine, Industry and Environmental Biotechnology*; Lens P, Moran AP, Mahony T, Stoodley P, O'Flaherty V (Eds); IWA Publishing. London: P197-213.

Terada A, Yamamoto T, Hibiya K, Tsuneda S, Hirata A. 2004. Enhancement of biofilm formation onto surface-modified hollow-fiber membranes and its application to a membrane-aerated biofilm reactor. Water Sci Technol 49:263-268.

Terada A, Yuasa A, Tsuneda S, Hirata A, Katakai A, Tamada M. 2005. Tamada, Elucidation of dominant effect on initial bacterial adhesion onto polymer surfaces prepared by radiation-induced graft polymerization. Colloids Surf. B: Biointerfaces 43:97-105.

Tsuneda S, Park S, Hayashi H, Jung J, Hirata. 2000. A. Enhancement of nitrifying biofilm formation using selected EPS produced by heterotrophic bacteria. Water Sci Technol 43:197-204.

Tsuneda S, Nagano T, Hoshino T, Ejiri Y, Noda N, Hirata A. 2003. Characterization of nitrifying granules produced in an aerobic upflow fluidized bed reactor Water Res 37:4965-4973.

Tsuru T, Nakao S, Kimura S. 1990. Effective charge-density and pore sturucture of charged ultirafiltration membranes. J Chem Eng Jpn. 23:604-610.

Wang Y, Kim JH, Choo KH, Lee YS, Lee CH. 2000. Hydrophilic modification of polypropylene microfiltration membranes by ozone-induced graft polymerization. J Membr Sci 169:269-276.

Zheng R, Blanchard JS. 2000. Identification active site residues in *E. coli* ketopantoate reductase by mutagenesis and chemical rescue. Biochemistry 39:16244-16251.

Chapter 4

Significance of electrostatic properties of positively charged polymer surfaces on biofilm formation

Chapter 4

Significance of electrostatic properties of positively charged polymer surfaces on biofilm formation

4

Abstract

The link between initial bacterial adhesion and the subsequent biofilm formation was investigated with use of a flow cell and the formed biofilm was observed by epifluorescence microscopy and scanning electron microscopy (SEM). Surface-modified polyethylene (PE) membrane sheets were prepared by the radiation-induced graft polymerization (RIGP) of an epoxy-group-containing monomer, glycidyl methacrylate (GMA). The epoxy ring of GMA was opened by introducing diethylamine (DEA) or sodium sulfite (SS). The activity of *E. coli* cells onto the DEA sheets loses significantly compared to those onto the PE, GMA and SS sheets. The biofilm formation experiment with a flow cell revealed that biofilm formation was facilitated on the DEA sheet although the viability of *E. coli* cell was the lowest among all the prepared sheets. In addition, the unique biofilm structure was observed on the DEA sheet: almost all of the *E. coli* cells were inactive on the base of the biofilm and active cells deposited on the

inactive cells. The SEM observation on the surface of the sheet clarified that extracellular polymeric substance (EPS) adhered on the DEA sheet, indicating that the EPSs could enhance biofilm formation onto the DEA sheet. From the above-mentioned experiments, a biofilm formation mechanism on positively charged polymer surface, *i.e.*, the DEA sheet, is proposed.

Paper in preparation: A. Terada, S. Tsuneda, A. Katakai, M. Tamada, "Significance of electrostatic properties of positively charged polymer surfaces on biofilm formation"

4. 1 Introduction

Biofilms are considered as a complex of bacteria and their extracellular polymeric substances (EPSs). The formation process of a biofilm in an aqueous environment is generally divided into three steps: initial bacterial adhesion (reversible step), secretion of EPSs (irreversible step), and subsequent biofilm formation (Bos *et al.*, 1999). In most common situations, *i.e.*, aqueous media with pH near neutrality, the microbial cells and solids substratum are negatively charged (Azeredo and Oliveira, 2003; Jucker *et al.*, 1997). This implies that surface charge normally has a repulsive effect against bacterial cell and acts contrary to adhesiveness of the bacteria. Meanwhile, bacteria adhesion is facilitated on positively charged surface (Gottenbos *et al.*, 1999, 2000, 2001; Harks *et al.*, 1991; Hayashi *et al.*, 2001; Hogt *et al.*, 1986; Terada *et al.*, 2004, 2005). The question is whether or not the positively charged surfaces are effective for enhancement of biofilm formation. Hitherto, there seems to be no definite answer: Gottenbos *et al.*, (1999, 2000, 2001) has reported that the positively charged surfaces are useful for prevention of biofilm formation on biomaterials; whereas some researchers have suggested that the

positively-charged surface prepared by radiation-induced graft polymerization (RIGP) are effective for biofilm formation for nitrification (Hibiya *et al.*, 2000; Terada *et al.*, 2004). Therefore, such question should be answered essentially.

The objective of this study was to elucidate the significance of positively charged polymer surface prepared by RIGP on bacterial activity and biofilm formation. A flow cell was employed to chase *Escherichia coli* adhesion and biofilm biofilm formation onto the prepared membrane sheets.

4.2 Materials and methods

4.2.1 Bacterial strain

As a representative bacterial strain, *Escherichia coli* (IFO-3301) was used in this study. Before activity and biofilm formation tests, this strain was aerobically cultured for 1 day at 30°C in a liquid medium containing the following: polypeptone, 10.0 g; yeast extract, 5.0 g; sodium chloride, 1.0 g; and distilled water, 1 L. Cells were harvested in their exponential growth phase by centrifugation (8000 *g*, 10 min) and resuspended in water. This washing step was repeated three times to eliminate residual substrates and EPS. Finally, the washed cells were suspended in 0.02 M phosphate-buffered saline (PBS).

4.2.2 Preparation of membrane sheets

A preparation scheme for diethylamino- or sulfonic acid-containing membrane sheets is shown in Figure 4.1. Firstly, a polyethylene (PE)-based membrane sheet (PE sheet) (Asahi Kasei Chemicals, Japan) was used as the stem for grafting. The sheet has a porosity of 70% and an average pore size of 0.20 μm. The sheets were irradiated with an electron beam in a nitrogen atmosphere at room temperature. The total dose of the

electron beam was set at 200 kGy. Then, the irradiated sheets were immersed in a glass ampoule containing glycidyl methacrylate (GMA; 5 wt/wt% in methanol), previously sparged with nitrogen gas, and allowed to react at 313 K for a predetermined time. The obtained GMA-grafted sheets were soaked in *N, N*-dimethylformamide and then in methanol to remove residual monomers and homopolymers. They were afterwards dried under reduced pressure. The amount of GMA grafted onto a stem sheet represented the degree of grafting (*dg*) calculated as follows:

$$dg = 100 \times \left(\frac{W_1 - W_0}{W_0} \right) \quad [\%] \quad , \quad (4.1)$$

where W_0 and W_1 are the weights of the stem sheet and GMA-grafted sheet, respectively. The grafted sheets with a *dg* of approximately 100% were prepared by setting the grafting time at 30 min. Then, the produced epoxy groups were converted to diethylamino groups ($-N(C_2H_5)_2$) or sulfonic acid groups ($-SO_3H$) by immersing the GMA-grafted sheet in a mixture of diethylamine (DEA)/water = 50/50 (volume ratio) or sodium sulfite (SS)/isopropyl alcohol/water = 10/15/75 (weight ratio), respectively. The conversion of the epoxy groups to ionizable groups, that is, DEA and SS groups, was set at about 100%. Hereafter, the resultant GMA-, DEA- and SS-containing sheets are referred to as GMA, DEA and SS (*X*) sheets; *X* in parentheses represents *dg*.
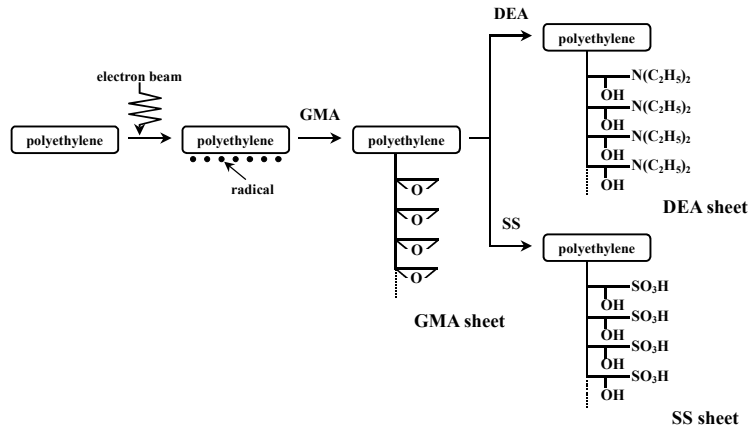
Figure 4.1 Preparation scheme for GMA, DEA and SS sheets.

4.2.3 Surface characterization of the sheets prepared by RIGP

For the measurement of roughness on the sheet surfaces fabricated by RIGP, atomic force microscopy (AFM, Nonoscope IIIa Dimersion™ 3100, Digital Instruments, USA) was employed. For AFM, the sheets were cut in 1×1 cm sections and fixed on a microscope slide with double-sided sticky tape. AFM was carried out in the tapping mode. Height images were recorded in three dimensions at ten randomly selected sites, from which the mean surface roughness was measured. Ten point height of roughness profile was employed for the measurement of the mean surface roughness (ISO 4287: 1997).

The method by Tsuru *et al.* (1990) was employed for a measurement regarding membrane potential. The experimental apparatus was a U-bend cell, which was divided into two compartments using a prepared membrane sheet. The solute was 0.02 M phosphate buffered saline (PBS) (pH 7.2). The membrane sheets were rinsed in distilled water before the measurements. Distilled water was supplied to one side and PBS to the other side of the cell. The temperature was maintained at 298 K throughout the experiment. Measurement of membrane potential was carried out by two reference electrodes (RE-1C, BAS Inc. Japan), both of which were composed of Ag/AgCl in a saturated potassium chloride solution. The two electrodes were connected to an electrometer (R8240, Advantest, Japan). The measurement was conducted in triplicate under the same conditions and the average value was taken.

4.2.4 Viability of E. coli cells adhering onto membrane sheet

Bacterial adhesion tests were conducted in accordance with the method of Terada *et al.* (2005). The prepared cell suspension of 40 ml was placed in a 50-ml beaker. The concentration of *E. coli* cells was set at an O.D.$_{660}$ of 0.050 that is equivalent to 5.8×10^9 cells/mL. PE, GMA, AM (100), EA (100) and DEA (100) sheets were cut into 0.25 cm^2

sections. Each sheet was immersed in a beaker containing an *E. coli* cell suspension. The cell suspension and the prepared sheets were shaken at 200 rpm and 298 K. The viability of *E. coli* cell adhering onto each sheet was evaluated with a commercially available staining kit (Live/Dead Baclight bacterial viability kit, Molecular Probes, Leiden, The Netherlands). Each membrane sheet was carefully removed from a beaker after the immersion in *E. coli* cell suspension for 0.25, 2, 4, 6 and 8 h and was mounted onto a slide glass well. Each sheet was filled with 8 μl of 1000-time-diluted Live/Dead kit and incubated for 15 min in the dark. After washing with distilled water, the sheets were mounted in FluoroGuard Antifade Reagent (Bio-Rad, Hercules, CA), and observed by fluorescence microscopy (Axio skop2 plus, Carl Zeiss, Oberkochen, Germany) to visualize live and dead cells. Bacterial viability was calculated from the ratio of the number of live cells stained with SYTO-9 to the total number of cells (SYTO-9-positive plus PI-positive cells). Direct counting was carried out in more than 10 randomly recorded images.

4.2.5 Biofilm formation test with a flow cell

The flow cell, which dimensions were 60 × 24 mm (length × width), image analysis system, and biofilm formation system were set up as shown in Figure 4.1. The flow cell was purchased from BioSurface Technologies (Model FC71, Montana, USA). The prepared sheet was mounted and fixed on the groove in the flow cell with double-sided sticky tape. The dimension of the groove was length, width and depth of 40.6, 11.4 and 0.203 mm, respectively. The top plate of the cell was made of glass. Before the experiment of biofilm formation, the flow cell was sterilized completely for 30 min. Prior to the experiments of initial bacterial adhesion and biofilm formation, all tubes and the flow cells were filled with 0.02 M PBS for removing all air bubbles from the system

because air bubbles would be high shears on biofilm, which made it impossible to investigate the effect of surface properties on biofilm formation. The rate of inflow was set to be 0.04 L/hr, which is equivalent to hydraulic retention time of 0.14 min and flow rate on the prepared sheet of 0.14 cm/s, respectively. After filling PBS solution, mixture of *E. coli* suspension with 0.02 M PBS (O.D.$_{660}$ of 0.1) was inoculated for 5 min. Then, 0.2 g/L Luria-Bertani (LB) broth solution, which is equal to total organic carbon (TOC) concentration of 100 g-C/m^3, was supplied at flow rate of 40 ml/hr. This solution had already been aerated in a feed tank before entering the flow cell, which produced completely aerobic condition in the cell. After 12 hr feeding of the solution, 1 mL of 1000-fold diluted BacLight solution was supplied through the bypass of the flow line for 3 min. Biofilm structure and stratification was observed by fluorescence microscopy (Axio skop2 plus, Carl Zeiss, Oberkochen, Germany) immediately after immersion of the stain.
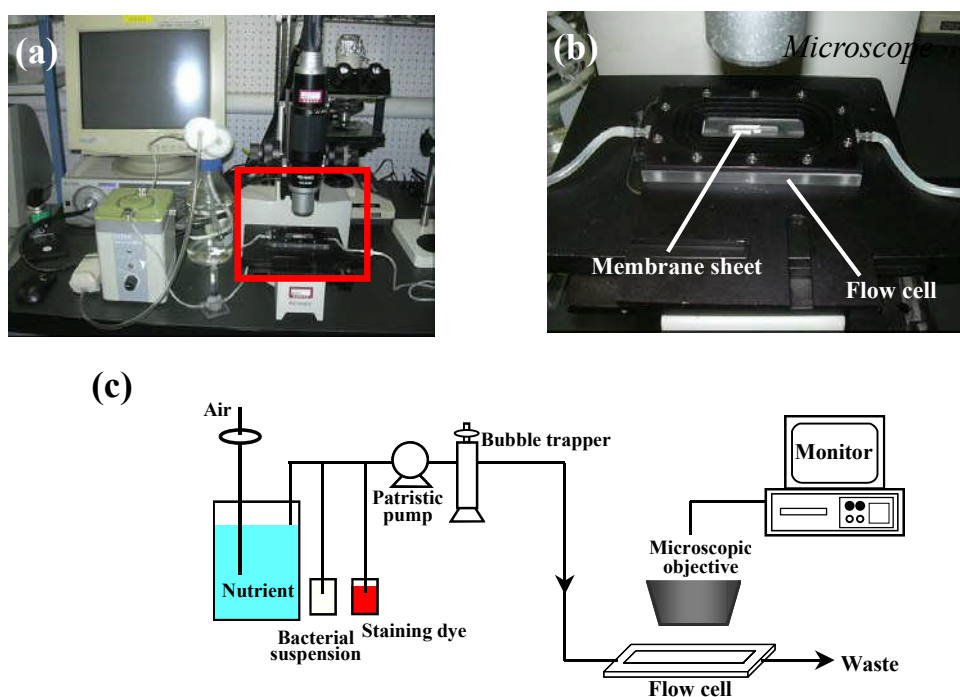
Figure 4.1 Experimental apparatus for biofilm formation; (a) picture of flow cell apparatus, (b) magnified picture of (a), (c) schematic diagram of the system.

4.2.6 Observation of biofilm by scanning electron microscopy

The PE, GMA (100), DEA (100) and SS (100) sheets, which were immersed in *E. coli* cell suspensions for 72 h at 298 K, were collected carefully and washed with distilled water. At the beginning of the experiment, Then, Luria-Bertani (LB) broth solution, which is equal to total organic carbon (TOC) concentration of 100 g-C/m^3, was supplied to make the bacterium excrete EPSs. After 73 h each sample was immediately fixed, carefully washed with sodium cacodylic acid solution, and dehydrated with ethanol. A sample was observed by scanning electron microscope (SEM) (JSM-5600, JEOL, Japan) after the sample was mounted on a stub and coated with gold using an ion coater (JFC-1100E, JEOL, Japan).

4.3 Results and discussion

4.3.1 Characterization of membrane sheets prepared by RIGP

The characterization of the prepared sheets is summarized in Table 4.1. RIGP and the subsequent epoxy-opening reaction changed dynamically electrostatic conditions; whereas they hardly changed surface roughness, indicating that the appropriate surfaces could be prepared for the subsequent experiment. Since roughnesses of the GMA (100), DEA (100) and SS (100) were almost same, the effect of surface roughness on initial bacterial adhesion and biofilm formation can be neglected.

Table 4.1 Surface characteristics of the prepared sheets.

		PE	GMA (100)[*1]	DEA (100)	SS (100)
Roughness	[nm]	135 ($\pm$19.5)[*2]	308 ($\pm$49.2)	334 ($\pm$37.0)	316 ($\pm$29.9)
Membrane potential	[mV]	-18.6 ($\pm$1.99)	-24.0 ($\pm$1.07)	3.38 ($\pm$1.41)	-52.3 ($\pm$1.70)

[*1] Values in parentheses represent *dg*.

[*2] Values in parentheses represent standard deviation.

4.3.2 Evaluation of bacterial activity on the prepared surfaces

Time course of *E. coli* cell viability onto the prepared sheets is shown in Figure 4.2. All *E. coli* cells did not aggregate in bulk liquid and any colonization on each sheet was not observed during the experiment (data not shown). The viability of planktonic *E. coli* cells kept approximately 90% after 8 h in the bulk liquid where each sheet was immersed. This result implies that there is no dissolution of DEA- or SS-group from each polymer sheet and that the possibility of the bulk liquid on the viability of *E. coli* cells is significantly low. Similar tendencies between the PE and GMA (100) sheets were observed: 70-80% cells of adhering *E. coli* cells on the PE and GMA sheets were viable and the viability remained almost constant during the whole experimental period. On the other hand, the trend of *E. coli* cell viability on the DEA (100) sheet was quite different from those on the PE and GMA sheets. After the 8-h immersion of these three sheets in *E. coli* cell suspension, the percentage viability decreased to 5%. The viability of *E. coli* cells on the SS (100) was same as that of planktonic *E. coli* cells. Considering the result of membrane potential of the respective cells, the electrostatic interaction clearly reflects the behaviors of viability of *E. coli* cells: the material which kept *E. coli* cell's viability high was in order of decreasing viability, SS (100), GMA (100), PE, and DEA (100), which order corresponds to that of increasing membrane potential.
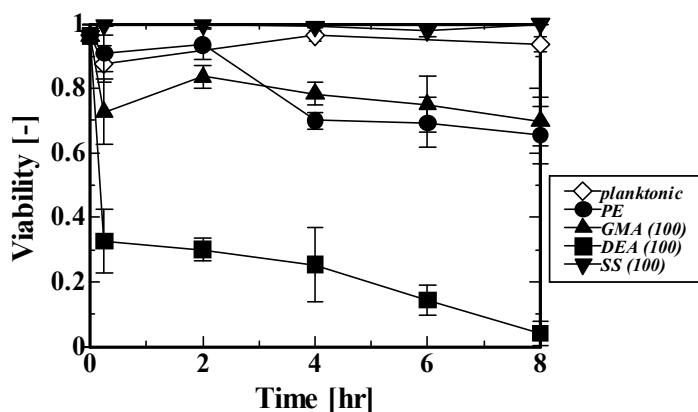
Figure 4.2 Time course of *E. coli* cell viability on the respective membrane sheets.

4.3.3 Evaluation of biofilm formation

The representative images of epifluorescence microscope were shown in Figure 4.3. The formation of *E. coli* biofilm onto the GMA (100) was not observed as shown in Figure 4.3 (a). This seems to be due to flow rate along the sheet surface, which generates high shear stress, leading to the detachment of *E. coli* cells from the sheet. The same tendencies were observed in cases of the PE and SS (100) sheets. On the other hand, biofilm formation on the DEA (100) sheet was clearly observed (Figure 4.3 (b)). Interestingly, the biofilm structure had the very unique structure where live and dead cells were mixed on the sheet. Considering the result of the initial bacterial adhesion test shown in Figure 4.2, dead cells seemed to mainly dominate on the sheet surface. It was also observed that live cells forms on the dead cells adhering on the DEA (100) sheet. Since detachment is dependent on strength of initial bacterial adhesion onto surfaces (Busscher *et al.*, 1995), the DEA (100) has a very strong interaction with *E. coli* cells. Although this result disagrees with those by some researchers, which has concluded that positively charged surfaces are very effective for prevention of biofilm formation (Gottenbos *et al.*, 1999, 2000, 2001; Kügler *et al.*, 2005), the result obtained in this study yields the conclusion that the DEA (100) would be promising for enhancement of biofilm formation. The possible reason why it does not support the results by these researchers are considered to be that the DEA sheet is introduced into tertiary amino groups, which is less strong anion-exchange potential compared to quandary amino group as a representative of quaternary ammonium compounds (QACs) (Kügler *et al.*, 2005; Lee *et al.*, 2005). The discussion indicates that to kill *E. coli* cells takes more time, as shown in Figure 4.2, than time for the growth, *i.e.*, less than one hour. Kügler *et al.* (2005) reported that the electrostatic interaction between a QAC surface and bacteria is a significant parameter for the control of bacterial growth. They clarified that *E. coli* cells are

inactivated within less than 10 min, which is shorter than the doubling time of *E. coli*, and thus there is no possibility for biofilm formation on the QAC surface. This time difference seemingly provided the formation of *E. coli* cells.
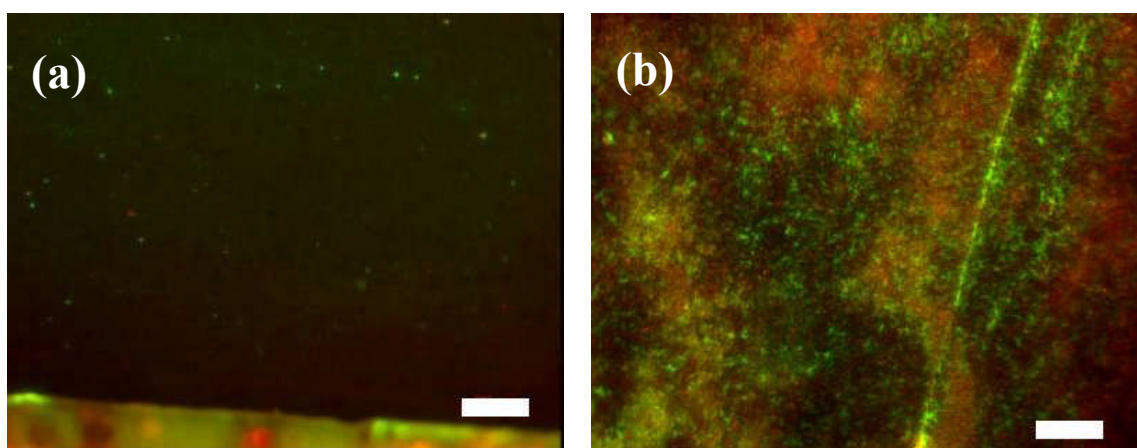
Figure 4.3 Epifluorescence microscopy images of *E. coli* biofilms onto GMA (100) (a) and DEA (100). Green and red indicate live and dead cells, respectively. Bars represent 100μm.

4.3.4 Observation of biofilm by SEM

Representative SEM images of *E. coli* biofilm onto the prepared sheets are shown in Figure 4.4. There were no biofilm formation onto surfaces of PE, GMA (100) and SS (100) (Figures 4.4 (a), (b) and (d)). This result might be due to the fact that the dewatering procedure required for SEM. However, a definite difference between the surfaces on the DEA (100) sheet and the other three sheets was observed in that some particle-like things and *E. coli* cells were simultaneously observed on the DEA (100) (Figure 4.4 (c)). These might be particles derived form bacterial lyses. Considering the definition of EPS, Geesey (1982) defined EPS as 'extracellular polymeric substances of biological origin that participate in the formation of 'microbial aggregates. Characklis and Wilderer (1989) defined that EPSs are 'organic polymers of microbial origin which

in biofilm systems are frequently responsible for binding cells and other particulate materials together (cohesion) and to the substratum (adhesion). Summarizing such definitions, the particles derived from bacterial lyses should be defined as EPSs. Since EPSs generally determines the mechanical stability of biofilm (Flemming and Wingender, 2003; Tsuneda *et* al., 2000; Wolfaardt *et al.*, 1999), EPSs secreted or lysed from *E. coli* should facilitate biofilm formation and maintain biofilm because of playing as a glue to connect each bacterial cell. The illustration of biofilm formation mechanisms onto the DEA sheet surface is shown in Figure 4.5. Although we have to clarify the amount and species of EPSs, to chase biofilm formation in detail, to investigate the strength of biofilm onto positively charged surfaces compared onto negatively charged, *i.e.*, normal, surfaces, at least it is concluded that the DEA sheet has a potential to enhance biofilm formation.

(a) **(b)**

(c) **(d)**
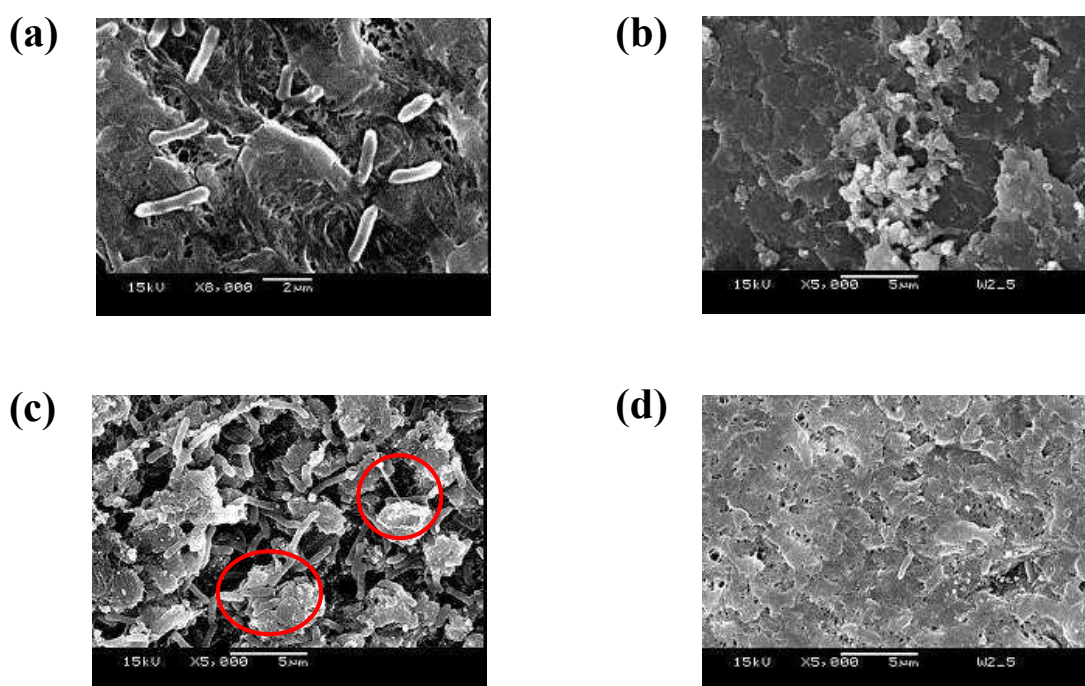
Figure 4.4 SEM imageries after 3-day immersion of *E. coli* cell suspension: (a) PE; (b) GMA (100); (c) DEA (100); (d) SS (100). Red circles show aggregates of extracellular substances.
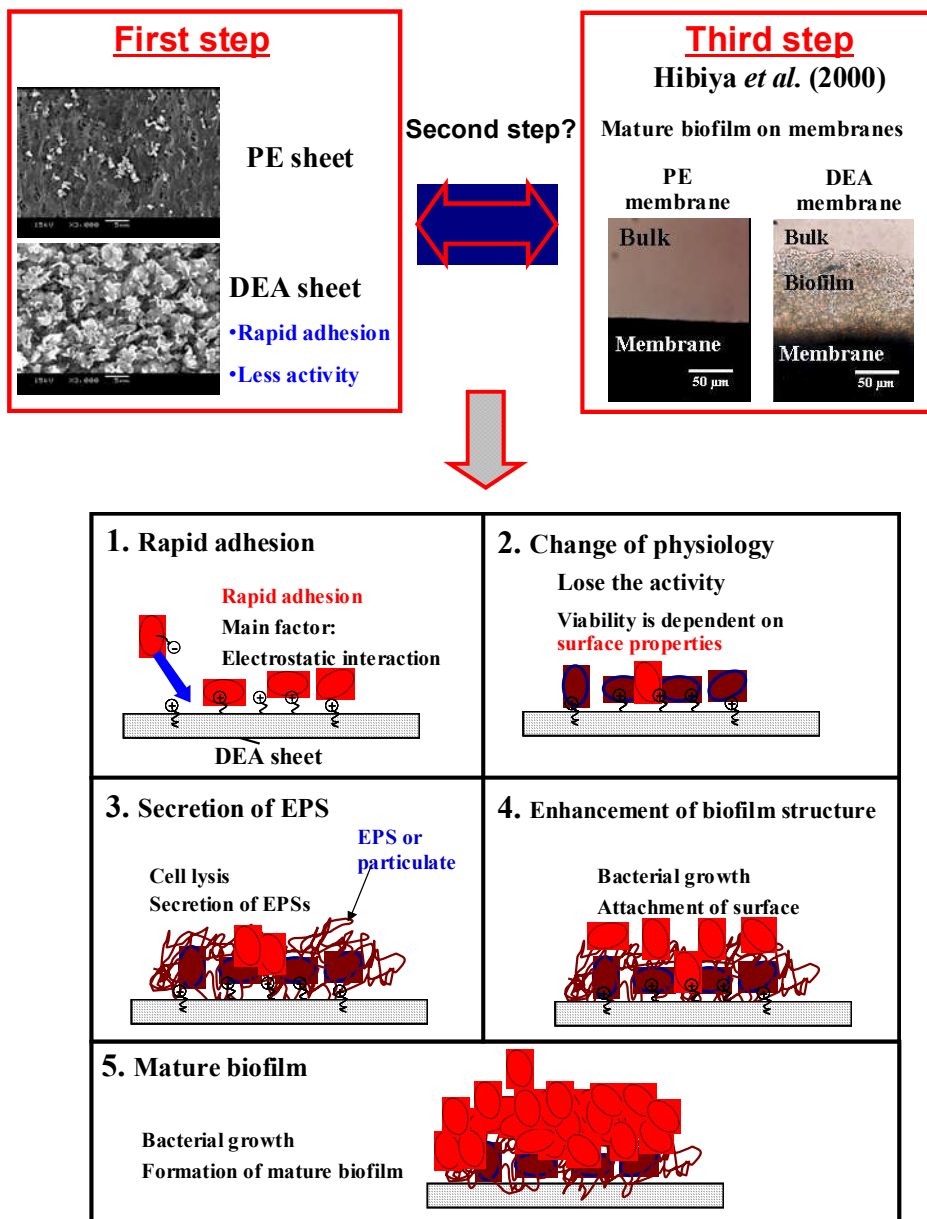
Figure 4.5 Hypothesis of biofilm formation on the DEA sheet surfaces.

4.4 Conclusion

In this chapter, the link between initial bacterial adhesion and subsequent biofilm formation was investigated. The activity of *E. coli* cells significantly decreased on the DEA (100) sheet with positively charged surface, whereas they remained almost constant on the other sheets, PE, GMA (100) and SS (100) with negatively charged surfaces. The lower the membrane potential of a surface has, the higher viability *E. coli* cells remain. Notwithstanding, the enhancement of biofilm formation was observed on the DEA (100) sheets; on the other hand, the biofilm was hardly formed on the PE, GMA (100) and SS (100) sheets, leading to the supposition that the DEA (100) surface has a potential to enhance *E. coli* biofilm. The SEM observation gives rise to the significance of EPSs, which are secreted or lysed from the live or dead cells, on biofilm formation. This result indicates that the EPSs would play an important role to retain biofilm structure. Although there are some questions to be solved, *e.g.*, how much strength does the biofilm on the DEA sheets have?; how much or what kinds of EPSs do *E. coli* cells secrete?; how are the biofilms formed under high hydrodynamic conditions?, essentially we should not judge that the positively charged surface is effective for biofilm prevention; alternatively, it would be very effective for biofilm formation.

References

Azeredo J, Oliveira R. 2003. The role of hydrophobicity and exopolymers in initial adhesion and biofilm formation. In *Biofilms in Medicine, Industry and Environmental Biotechnology*; Lens P, Moran AP, Mahony T, Stoodley P, O'Flaherty V (Eds); IWA Publishing. London: P16-31.

Bos R, van der Mei H, Busscher HJ. 1999. Physico-chemistry of initial microbial adhesive interactions-its mechanisms and methods for study. FEMS Microbiol Rev 23:179-230.

Busscher HJ, Bos R, van der Mei HC. 1995 Initial microbial adhesion is determinant for the strength of biofilm adhesion. FEMS Microbiol Lett 128:229-234.

Characklis WG, Wilderer PA. 1989. Structure and Function of Biofilms. John Wiley and Sons. Chichester UK.

Flemming HC, Wingender J. 2003. The crucial role of extracellular polymeric substances in biofilms. In *Biofilms in Wastewater Treatment-An Interdisciplinary Approach*; Wuertz S, Bishop P, Wilderer P (Eds); IWA Publishing. London UK: P.178-210.

Geesey GG. 1982. Microbial exopolymers: ecological and economic considerations. Am Soc Microbiol News 48:9-14.

Gottenbos B, van del Mei HC, Busscher H J, Grijpma DW, Feijen J. 1999. Initial adhesion and surface growth of Pseudomonas aeruginosa on negatively and positively charged poly (methacrylates). J Material Sci: Mater in Medicine 10:853-855.

Gottenbos B, van der Mei HJ, Busscher J. 2000. Initial adhesion and surface growth of *Staphylococcus epidemidis* and *Pseudomonas aeruginosa* on biomedical polymers. J Biomed Mater Res 50:208-214.

Gottengbos B, Grijpma DW, van der Mei HC, Feijen J, Busscher HJ. 2001. Antimicrobial effects of positively charged surfaces on adhering Gram-positive bacteria, J Antimicrob Chemotherapy 48:7-13.

Harks G, Feijen J, Dankert J. 1991. Adhesion of *Escherichia coli* onto a series of poly(methacrylates) differing in charge and hydrophobicity. Biomaterials 12:853-860.

Hayashi H, Nihei T, Ono M, Tsuneda S, Hirata A, Sasaki H. 2001. Rapid recovery of bacterial cells from a stable dispersion by heterocoagulation to a fibrous collector. J Colloid Interf Sci 243:109-115.

Hibiya K, Tsuneda S, Hirata A. 2000. Formation and characteristics of nitrifying biofilm on a membrane modified with positively-charged polymer chains. Colloids Surf B: Biointerfaces 18:105-112.

Hogt AH, Dankert J, Feijen J. 1986. Adhesion of coagulase-negative *staphylococci* to methacrylate polymers and copolymers. J Biomed Mater Res 20:533-545.

Jucker BA, Harms H, Hug SJ, Zehnder AB. 1997. Adsorption of bacterial surface polysaccharides on mineral oxides in mediated by hydrogen bonds. Colloids Surf B: Biointerfaces 9:331-343.

Kügler R, Bouloussa O, Rondelez F. 2005. Evidence of a charge-density threshold for optimum efficiency of biocidal cationic surfaces. Micobiology 151:1341-1348.

Lee SB, Koepsel RR, Morley SW, Matyjaszewski K, Sun Y, Russell AJ. 2004. Permanent, nonleaching antibacterial surfaces. 1. Synthesis by atom transfer radical polymerization. Biomacromolecules 5:877-882.

Terada A, Yamamoto T, Hibiya K, Tsuneda S, Hirata A. 2004. Enhancement of biofilm formation onto surface-modified hollow-fiber membranes and its application to a membrane-aerated biofilm reactor. Water Sci Technol 49:263-268.

Terada A, Yuasa A, Tsuneda S, Hirata A, Katakai A, Tamada M. 2005. Tamada,

Elucidation of dominant effect on initial bacterial adhesion onto polymer surfaces prepared by radiation-induced graft polymerization. Colloids Surf. B: Biointerfaces 43:97-105.

Tsuneda S, Park S, Hayashi H, Jung J, Hirata. 2000. A. Enhancement of nitrifying biofilm formation using selected EPS produced by heterotrophic bacteria. Water Sci Technol 43:197-204.

Tsuru T, Nakao S, Kimura S. 1990. Effective charge-density and pore sturucture of charged ultirafiltration membranes. J Chem Eng Jpn. 23:604-610.

Wolfaardt GM, Lawrence JR, Korber DR. Function of EPS. In *Microbial Extracellular Polymeric Substances*; Wingender J, Neu TR, Flemming HC (Eds); Springer. Berlin Germany: P.172-200.

Chapter 5

Enhancement of biofilm formation onto surface-modified hollow-fiber membranes and its application to membrane-aerated biofilm reactor

Chapter 5

5

Enhancement of biofilm formation onto surface-modified hollow-fiber membranes and its application to membrane-aerated biofilm reactor

Abstract

Surface-modified hollow-fiber membranes were prepared by radiation-induced grafting of an epoxy-group-containing monomer, glycidylmethacrylate (GMA), onto a polyethylene-based fiber (PE-fiber). The epoxy ring of GMA was opened by introduction of diethylamine (DEA). The bacterial adhesivity to this material (DEA-fiber) was tested by immersed into nitrifying bacterial suspension. The initial adhesion rates and the amount of attached bacteria of the DEA-fiber were 6-10-fold and 3-fold greater than those of the PE fiber, respectively. A membrane-aerated biofilm reactor (MABR) composed of DEA fibers was developed for partial nitrification with nitrite accumulation. Prior to the nitrification test, it was confirmed that the oxygen supply rate (OSR) was proportional to air pressure up to 100 kPa, allowing easy control of oxygen supply. Stable nitrite accumulation was observed in the partial nitrification test at a fixed oxygen supply

throughout the operation period, indicating that oxygen was consumed by only ammonia oxidizers. Furthermore, it was demonstrated that oxygen utilization efficiency (OUE) in the ammonia oxidation process was nearly 100% after 300 h incubation.

5. 1 Introduction

A membrane-aerated biofilm reactor (MABR) for the biodegradation of contaminated compounds is of significant interest in applications where conventional wastewater treatment systems are unsuitable (Casey *et al.*, 1999). In an MABR, a hollow-fiber membrane plays two roles: supplying oxygen and acting as the substratum for bacterial immobilization. Supplied to the inner side of a hollow-fiber membrane, oxygen penetrates through to the biofilm that has formed on the outer surface. Bacteria in the biofilm subsequently utilize the oxygen to oxidize pollutants diffusing from the bulk solution. In the latest research using the MABR, removal of chlorophenol (Wobus and Roske, 2000), nitrification (Brindle *et al.*, 1998) and simultaneous nitrification and denitrification (SND) (Suzuki *et al.*, 2000; Hibiya *et al.*, 2003; Semmens *et al.*, 2003; Satoh *et al.*, 2004; Terada *et al.*, 2003) were reported. Although control of bacterial adhesion onto the membrane outer surface is important for effective oxygen supply, the enhanced adhesion of bacterial cells, leading to rapid startup, stable operation of the MABR and development of novel reaction sites, has not been investigated. In particular,

it has been generally recognized that autotrophic bacteria such as nitrifying bacteria hardly adhered on surfaces due to low production of extracellular polymeric substances. If rigid nitrifying biofilm is formed and partial nitrification in that ammonia is not converted into nitrate but into nitrite is achieved under controlled oxygen supply, a novel SND process via not nitrate but nitrite, which is free of pH adjustment and applicable to low TOC/N ratio wastewater may be possible.

To facilitate bacterial adhesion to the membrane surface, radiation-induced graft polymerization (RIGP) was used in our previous work (Tsuneda *et al.*, 1992). This technique enables the modification of various polymeric backbones to open interfaces, which support the "grafting" of functional groups. Our groups successfully promoted bacterial adhesion via electrostatic interaction (Hibiya *et al.*, 2000). This method is expected to make the biofilm form swiftly and firmly, resulting in effective oxygen supply to specific bacteria. The objective of this chapter is three-fold: (1) to confirm the enhancement of biofilm formation owing to the introduction of tertiary amino groups onto the interface of polyethylene (PE), (2) to determine the oxygen supply rate of the surface-modified hollow fiber, and (3) to undertake a partial nitrification test with an MABR composed of the surface-modified hollow fibers.

5.2 Materials and methods

5.2.1 Hollow-fiber membranes

We prepared the surface-modified hollow-fiber membranes as follows (Figure 5.1). First of all, a polyethylene-based hollow-fiber membrane (Asahi Chemical, Japan) referred to as a PE-fiber was used as a starting material for grafting. The inner and outer diameters of the fiber were 0.8 and 1.26 mm, respectively, with a porosity of 70% and an average

pore size of 0.20 mm. The PE fibers were irradiated with an electron beam in a nitrogen atmosphere at room temperature. The total dose of the electron beam was set at 200 kGy. The irradiated PE fibers were then immersed in a glass ampoule containing glycidylmethacrylate (GMA; 5 vol/vol% in methanol), which had been previously sparged by nitrogen gas, and were allowed to react at 40ºC for a predetermined time. GMA-grafted fibers, referred to as GMA fibers, were soaked in *N.N*-dimethylformamide (DMF) followed by methanol to remove residual monomers and homopolymers, and then dried under reduced pressure. The amount of GMA grafted onto the stem fiber is represented by the degree of GMA grafting (dg) as follows:

$$dg = 100 \times \left(\frac{W_1 - W_0}{W_0} \right) \quad [\%] \tag{5.1}$$

where W_0 and W_1 are the weights of PE fiber and GMA fiber, respectively. Then, GMA fibers were reacted with diethylamine (DEA; 50 vol/vol% in water) at 30ºC overnight. The resultant DEA-containing fiber will be referred to as a DEA (*X*) fiber, where *X* in parentheses designates the degree of GMA grafting (*dg*).

PE-fiber   **GMA-fiber**   *DEA-fiber*
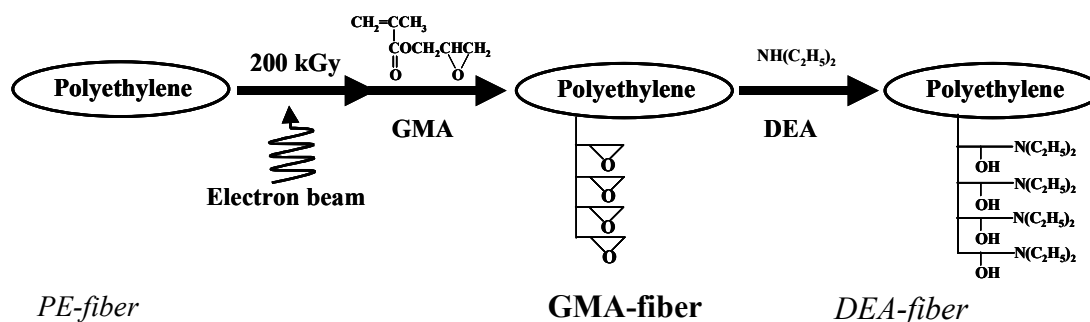
Figure 5.1 Preparation scheme of diethylamino (DEA)-group-containing hollow fiber (DEA-fibers).

5.2.2 Batch test for bacterial adhesion onto DEA fiber

Bacterial adhesion onto DEA-fiber was compared with that of virgin PE and alternative surfaces. Nitrifying bacteria acclimated with inorganic synthetic wastewater were

dispersed with a homogenizer and then centrifuged. This washing procedure was repeated twice to eliminate residual substrates and extracellular polymers produced by bacterial cells. Washed sludge was suspended in 0.02 M PBS. Nitrifying bacterial suspension with a volume of 60 ml was infused into a 100 ml flask (MLSS 1000 g/m^3). PE, DEA (23, 38, 94, 131, 160 and 270), polyacrylonitrile (PAN) and polyvinylidene fluoride (PVDF) fibers (Asahi Chemical, Japan) were immersed into the suspension, followed by shaking the flasks at 130 rpm and 25°C. Fibers of 10 cm in length were cut into 0.5 cm sections and subsequently sliced vertically in half (surface area: 2.28×10^{-3} m^2). The time course of the O.D.$_{660}$ of the bulk liquid was measured at intervals to evaluate bacterial adhesion onto the fibers. After 7 days, the cells attached onto the fibers were sonicated with a homogenizer at 100 μA for 15 min. Detached biomass was analyzed using a TOC analyzer (TOC-5000A, Shimadzu, Japan). Bacterial adhesion to membranes was confirmed by SEM (JSM-5600, JEOL, Japan) imagery.

5.2.3 Biofilm formation experiment

To evaluate the effectiveness of the surface modified fiber, *i.e.*, DEA-fiber, the biofilm formation experiments was performed. An illustration of experimental apparatus is shown in Figure 5.2. The *dg* of DEA fiber was set to be 81%. The module of DEA fibers were immersed in a nitrifying suspended solution which concentration and volume were 1000 g-SS/m^3 and 1 L, respectively. This module was composed of the three DEA fibers and made it possible to remove one of them with time for evaluation of biofilm thickness and biofilm density. Three runs were operated at different air pressures of 0, 10 and 23 kPa, respectively. The influent medium consisted of 0.236 g of $(NH_4)_2SO_4$, 0.282 g of NH_4HCO_3, 0.02 g of $MgSO_4·7H_2O$, 0.02 g of Na_2HPO_4, 0.02 g of KH_2PO_4, 0.05 g of KCl, 0.001 g of $FeSO_4·7H_2O$, and 0.84 g of $NaHCO_3$ per liter (pH 7.5±0.1). The

operation was batch mode and $(NH_4)_2SO_4$ was added to set at NH_4^+-N concentration of 100 g-N/m^3 once NH_4^+-N was depleted in the bulk. On days of 7, 14 and 28, the fiber was taken from the reactor for measurements of biofilm thickness and the amount of biomass. A 20-mm-thick biofilm section was prepared from a frozen biofilm sample embedded in OCT compound (Miles, Elkahrt, IN, USA) using a cryostat (CM 3050; Leica, Bensheim, Germany) at −20°C. The section was mount on a slide glass and biofilm thickness was measured using a digital optic microscope (Keyence, Tokyo, Japan). The amount of biomass was measured following the protocol as described in Section *5.2.2*.
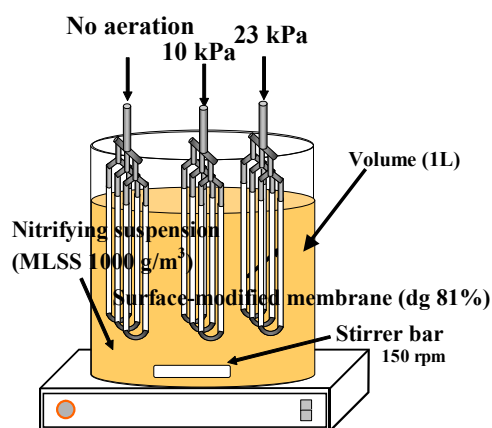
Figure 5.2 Illustration of the experimental apparatus for biofilm formation.

5.2.4 Reactor configuration

Figure 5.3 shows a schematic diagram of the laboratory-scale MABR constructed by 200 DEA (60) fibers. The working volume of the reactor vessel excluding the circulation line was 1.15 L; the reactor length, inner diameter and total volume were 600 mm, 55 mm and 1.29 L, respectively. This system had a dead-end configuration to achieve 100% oxygen transfer through inner side of the hollow-fiber membrane. The specific membrane surface area was 318 m^2/m^3. Liquid in the MABR was circulated at a flow rate of 2 cm/s to prevent the sedimentation of excess sludge. All experiments were

performed under the condition of complete mixing.
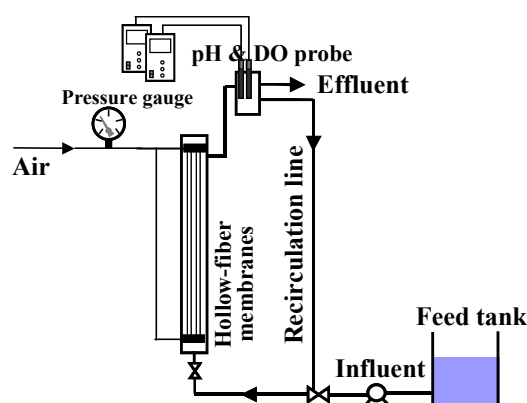
Figure 5.3 Schematic diagram of the membrane-aerated biofilm reactor (MABR)

5.2.5 Oxygen mass transfer test

The oxygen supply rate (OSR) was evaluated by calculating the oxygen transfer rate from the membrane and gas-bulk interface to the bulk; this was accomplished by looking at the time course of dissolved oxygen (DO) under different air pressure conditions at 25, 50, 75, 100 and 125 kPa. The 200 DEA (60) fiber was used to evaluate OSR. First, distilled water was poured into the MABR. After nitrogen gas was sparged into the reactor to decrease DO concentration to 0 g/m^3, aeration through the hollow-fiber membrane began. The OSR was obtained from the linear regions of the time course of DO concentration. From the relationship between air pressure and the OSR, we judged whether or not oxygen supply was controllable.

5.2.6 Partial nitrification test

The influence of air pressure on nitrite accumulation was also studied in the MABR. Inorganic artificial wastewater (NH_4^+-N 130 g-N/m^3, alkalinity 1000 g-CaCO$_3$/m^3, pH 7.5 ± 0.1, temp. 25°C) was continuously fed to the MABR with an effective volume of 1.15 l. At startup, a seed sludge of nitrifying bacteria was inoculated. Continuous

operation began when bacterial attachment was completed and the bulk liquid was free from suspended solid. The air pressure was set at 50 kPa and the required flow rate to achieve 100% partial nitrification, in that ammonia is not converted into nitrate but into nitrite, was calculated from the results of the oxygen mass transfer test. The oxygen utilization rate (OUR) and oxygen utilization efficiency (OUE) was calculated as follows (Schroeder, 1985; Brindle *et al.*, 1998):

$$OSR = r_{O2(a)} + r_{O2(m)} \qquad \text{[g-O}_2\text{/day]} \qquad (5.2)$$

$$OUR = Q(3.43 \times C_{NO2} + 4.57 \times C_{NO3}) \qquad \text{[g-O}_2\text{/day]} \qquad (5.3)$$

$$OUE = \frac{OUR}{OSR} \times 100 \qquad \text{[\%]} \qquad (5.4)$$

where $r_{O2(a)}$ and $r_{O2(m)}$ are the oxygen dissolution rates from the atmosphere and from the inner side of the membrane, Q is the volumetric flow rate, and C_{NO2} and C_{NO3} are NO_2^--N and NO_3^--N concentrations in the effluent, respectively. All samples were filtered through a glass filter (GF/F; Whatman, UK) before water quality analysis. Ammonia-nitrogen (NH_4^+-N) was measured using ion chromatography (DX-120; Dionex, Japan). Nitrite-nitrogen (NO_2^--N) and nitrate-nitrogen (NO_3^--N) were measured using a high-performance liquid chromatography (HPLC) (column: IC-Anion-PW; Tosoh, Japan). The pH and the DO were measured using a pH meter (TPX-90i, Toko, Japan) and a DO meter (TOX-90i, Toko, Japan), respectively.

5.3 Results and discussion

5.3.1 Batch test for bacterial adhesion onto DEA fiber

PE, DEA (23, 38, 94, 131, 160 and 270), PAN and PVDF fibers were brought into contact with the nitrifying suspension. Figure 5.4 shows the relationship between the

ratio of initial adhesion rates of the DEA, PAN and PVDF fibers to that of the PE fiber. The adhesion rates of nitrifying bacteria onto PE, PAN and PVDF were lower than those of the DEA fibers, indicating that bacterial adhesion could be promoted by introduction of the RIGP method (Figure 5.4). Although there is no clear difference in adhesion rates among DEA fibers whose dg were more than 38%, the initial adhesion rates were 6-10-fold greater than that of the PE fiber. In addition, the amount of nitrifying bacteria that adhered onto the DEA fiber was about 3-fold greater than that onto the PE fiber (Figure 5.5). These results indicated that nitrifying bacteria exhibited a high degree of adhesion onto the DEA fibers, suggesting that nitrifying biofilms might be easy to form onto the DEA fibers

Figure 5.6 shows SEM images of the surface of PE and DEA (131) fibers before and after contact with the nitrifier suspension for 7 days. With the application of the RIGP method to the membrane surface, the rough and complex surface formed. Nitrifying bacteria adhered onto the DEA (131) fiber, while they hardly adhered onto the PE fiber, supporting the conclusion that the DEA-group-containing graft chains could provide a favorable interface for adhesion of nitrifying bacteria.
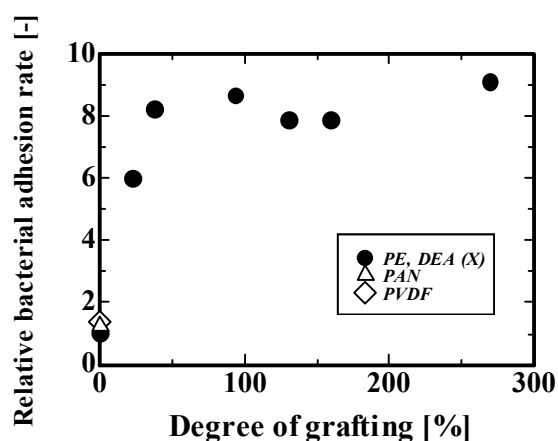
Figure 5.4 Relationship between the ratio of initial adhesion rates to the rate of the PE, and degree of grafting of respective membranes
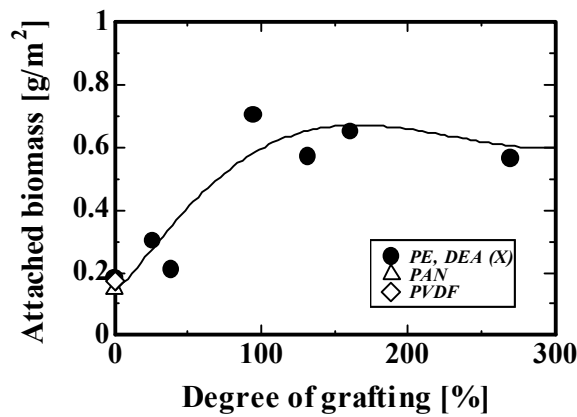
Figure 5.5 Comparison of effect of degree of grafting on bacterial attachment (on day 7)
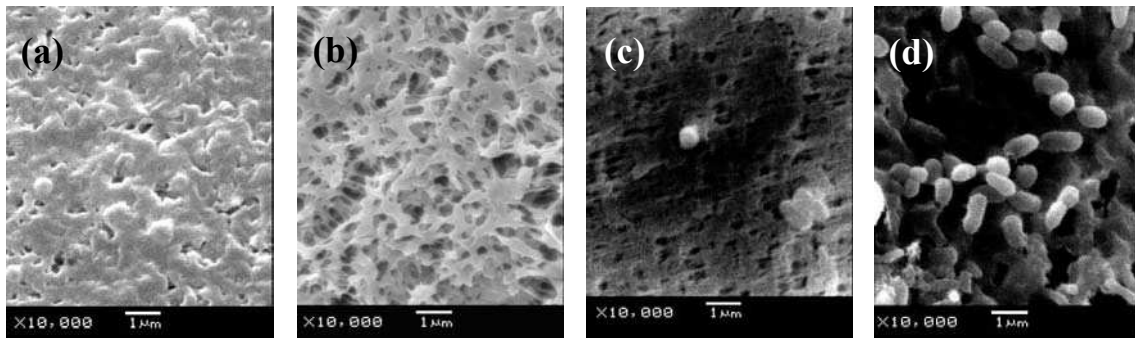
Figure 5.6 SEM images of the interfaces of PE and DEA (131) fibers before adsorption (a and b) and after exposure to nitrifying bacterial suspension for 7 days (c and d).

5.3.2 Estimation of biofilm formation

Uniform biofilm formation onto the DEA (81) was observed (Figure 5.7). Although it has been generally documented that biofilm has a mushroom-like structure (Beyenal and Lewandowski, 2002; Stoodley *et al.*, 1994), the biofilm in this study was not because of surface modification with RIGP: alternatively initial bacterial adhesion seems to be significant on subsequent biofilm formation. Time course of biofilm thickness was shown in Figure 5.8. The result clarified that the rate of biofilm formation is dependent on air pressure, *i.e.*, oxygen flux through membrane. The amount of biomass on the fibers

showed that biofilm density increased up to 61-83 kg/m^3 in one month. This value was comparable to those under high shear conditions by other researches (Staudt *et al.*, 2004; Zhang and Bishop, 1994.). Since, the experiment in this study was conducted under low shear conditions compared to those were, leading to the conclusion that the biofilm onto the DEA (81) was very compact and robust. This result supports that by Hibiya *et al.* (2000), which clarifies that formation of nitrifying biofilm is facilitated with DEA sheets prepared by RIGP, indicating that the application of surface-modified material for enhancement of initial bacterial adhesion would be very promising.
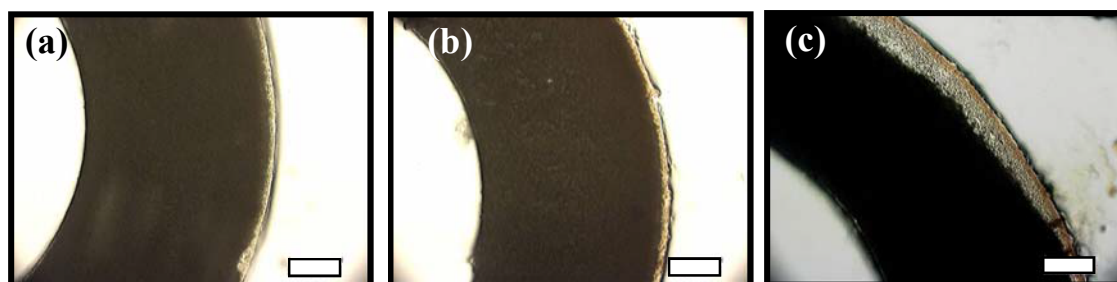
Figure 5.7 Pictures of biofilm on the DEA fibers (81) on days 7, 14 and 29, respectively. The air was supplied through the lumen of the fiber at 23 kPa. Bars represent 50 μm.
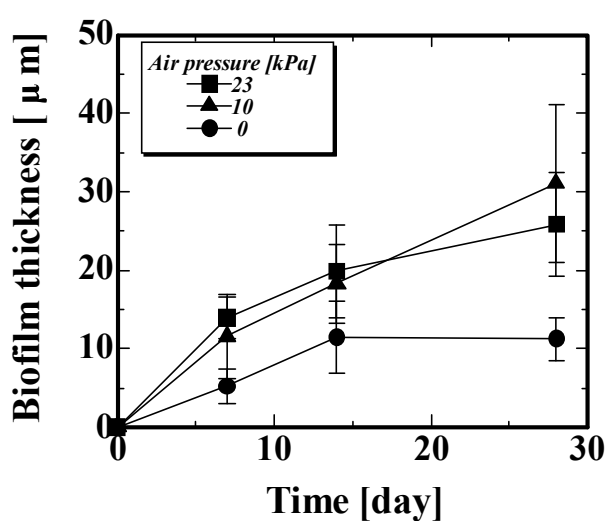
Figure 5.8 Time course of biofilm thickness on the DEA (81).

5.3.3 Estimation of oxygen supply rate (OSR)

The relationships of air pressure with $k_{L}a$ and OSR are shown in Figure 5.9. OSR increased with an increase in air pressure applied to the system. An approximate first-order relationship between OSR and air pressure was obtained up to 100 kPa, indicating that the applied air pressure can be used to control OSR. However, bubbles began to form on the membrane surface at air pressures higher than 100 kPa. This phenomenon decreases oxygen mass transfer by reduction of the liquid-gas boundary area; thus, the membrane used in this study was not effective when such high air pressures were applied.
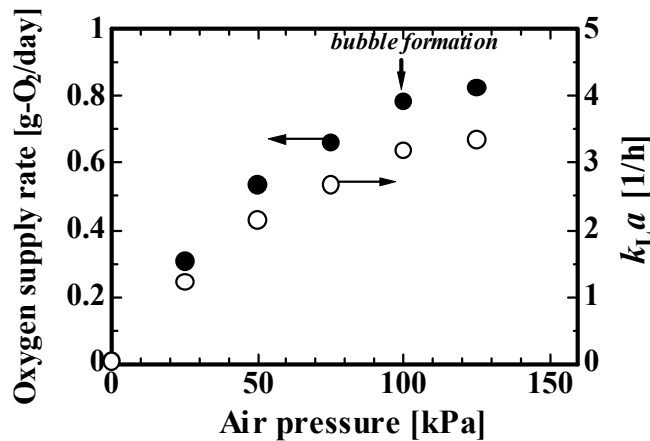
Figure 5.9 Oxygen supply rate (OSR) and $k_{L}a$ as a function of air pressure

5.3.4 Partial nitrification test

A partial nitrification test was undertaken with the MABR module constructed by DEA fibers. The time courses of water quality and nitrification rate are shown in Figure 5.10 (a). At startup, adhesion of nitrifying bacteria onto the membrane surface occurred immediately. As the nitrifiers were acclimated, more stable ammonia removal efficiency was observed. Furthermore, suspended solids were not detected, suggesting that the

nitrifying biofilm formed on the membrane surface rigidly. Obviously, the possibility that nitrification might occur in the bulk liquid was negligible since the bulk liquid was free from DO and suspended solids (Figure 5.10 (b)). The nitrogenous compounds derived from ammonia oxidation in the MABR were not nitrate but entirely nitrite throughout the operational period. The free ammonia concentration calculated from the formula advocated by Anthonisen *et al*. (1976) was less than the level in which the activity of nitrite-oxidizing bacteria (NOB) was inhibited (data not shown). Therefore, these data alone do not confirm partial nitrification; but at least support possibility.

The oxygen utilization efficiency (OUE) of the ammonia oxidizing bacteria (AOB) is shown in Figure 5.11. OUE increased gradually and reached 100% after 336 h, indicating that oxygen supplied from the inner side of the membrane was completely utilized by the nitrifying biofilm. Taking it into account that nitrate was not detected in the effluent, these results demonstrates that partial nitrification with an inactive state of NOB could be achieved if the equivalent amount of oxygen utilized by AOB is supplied to MABR. Furthermore, the MABR system would be expected to achieve SND via not nitrate but nitrite when applied to low TOC/N wastewaters.
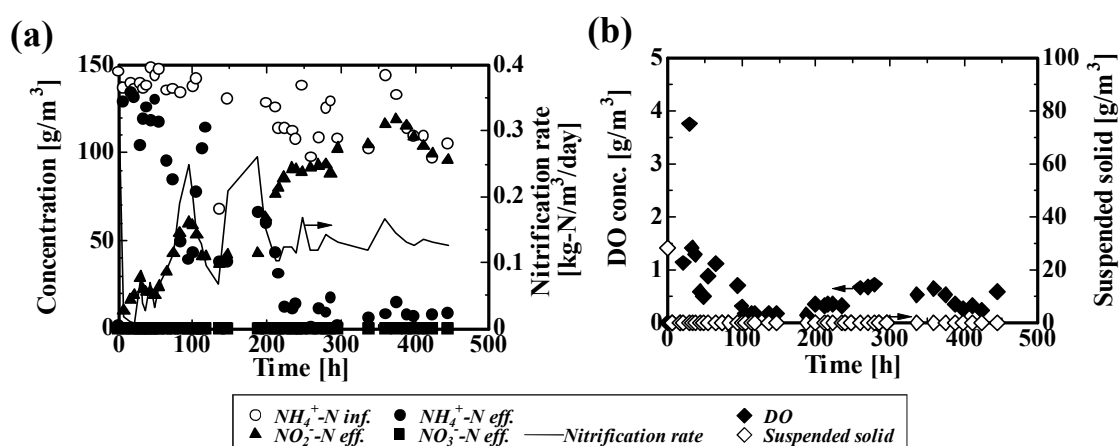
Figure 5.10 Time course results of partial nitrification experiment with the MABR: (a) Water quality and nitrification rate; (b) DO and suspended solid in the effluent
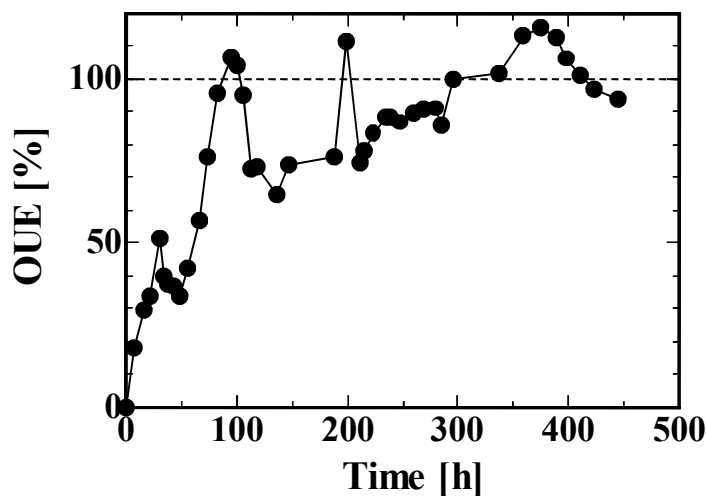
Figure 5.11 Time course of oxygen utilization efficiency (OUE)

5.4 Conclusion

The electrostatic interaction between bacterial cells and PE hollow-fiber membrane surface was successfully enhanced by the introduction of DEA-group-containing graft chains using RIGP method, to allow for rapid biofilm formation in an MABR system. Appropriate oxygen control allowed for partial nitrification with 100% OUE in the MABR system. Hereafter SND via nitrite would be expected to become viable with this system.

References

Anthonisen AC, Loehr RC, Prakasam TBS, Srinath EG. 1976. Inhibition of nitrification by ammonia and nitrous acid. J Water Poll Contr Fed 48:835-852.

Beyenal H, Lewandowski Z. 2002. Internal and external mass transfer in biofilms grown at various flow velocities. Biotehnol Prog 18:55-61.

Brindle K, Stephenson T, Semmens MJ. 1998. Nitrification and oxygen utilization in a membrane aeration bioreactor. J Membr Sci 144:197-209.

Casey E, Glennon B, Hamer G. 1999. Review of membrane aerated biofilm reactor. Res Consev Recycl 27:203-215.

Hibiya K, Tsuneda S, Hirata A. 2000. Formation and characteristics of nitrifying biofilm on a membrane modified with positively-charged polymer chains. Colloids Surf B: Biointerfaces 18:105-112.

Hibiya K, Terada A, Tsuneda S, Hirata A. 2003. Simultaneous nitrification and denitrification by controlling vertical and horizontal microenvironment in a membrane-aerated biofilm reactor. J Biotechnol 100:23-32.

Satoh H, Ono H, Rulin B, Kamo J, Okabe S, Fukushi K. 2004. Macroscale and microscale analyses of nitrification and denitrification in biofilms attached on membrane aerated biofilm. Water Res 38: 1633-1641.

Scheroeder ED. 1985. Nitrification in activated sludge processes. In *Comprehensive biotechnology*: Moo-Young M, Robinson CW, Howell JA (eds.) vol. 4 1st edn, Pergamon Press Oxford, p871-880.

Semmens MJ, Dahm K, Shanahan J, Christianson A. 2003. COD and nitrogen removal by biofilms growing on gas permeable membranes. Water Res 37:4343-4350.

Staudt C, Horn H, Hempel DC, Neu TR. 2004. Volumetric measurements of bacterial

cells and extracellular polymeric substance glycoconjugates in biofilms. Biotechnol Bioeng 88:585-592.

Stoodley P, de Beer D, Lewandowski Z. 1994. Liquid flow in biofilm systems. Appl Environ Microbiol 60:2711-2716.

Suzuki Y, Hatano N, Ito S, Ikeda H. 2000. Performance of nitrogen removal and biofilm structure of porous gas permeable membrane reactor. Water Sci Technol 41:211-217.

Terada A, Hibiya K, Nagai J, Tsuneda S, Hirata A. 2003. Nitrogen removal characteristics and biofilm analysis of a membrane-aerated biofilm reactor applicable to high-strength nitrogenous wastewater treatment. J Biosci Bioeng 95:170-178.

Tsuneda S, Saito K, Furusaki S, Sugo T., Ishigaki I. 1992. Water/acetone permeability of porous hollow-fiber membrane containing diethylamino groups on the grafted polymer branches. J Membr Sci 71:1-12.

Wobus A, Roske I. 2000. Reactors with membrane-grown biofilms: Their capacity to cope with fluctuating inflow conditions and with shock loads of zenobiotics. Water Res 34:279-287.

Zheng X, Bishop P. 1994. Density, porosity and pore structure of biofilms. Water Res 28:2267-2277.

Chapter 6

Nitrogen removal characteristics and biofilm analysis of a membrane-aerated biofilm reactor applicable to high-strength nitrogenous wastewater treatment

Chapter 6

Nitrogen removal characteristics and biofilm analysis of a membrane-aerated biofilm reactor applicable to high-strength nitrogenous wastewater treatment

6

Abstract

A membrane-aerated biofilm reactor (MABR) capable of simultaneous nitrification and denitrification in a single reactor vessel was developed to investigate the characteristics of nitrogen removal from high-strength nitrogenous wastewater, and biofilm analysis using microelectrodes and the fluorescence in situ hybridization (FISH) technique was performed. Mean removal percentages of total organic carbon (TOC) and nitrogen were 96% and 83% at removal rates of 5.76 g-C/m^2/day and 4.48 g-N/m^2/day, respectively. For stable removal efficiency, constant washing of the biofilm was needed. Dissolved oxygen microelectrode measurement revealed that the biofilm thickness was about 1600 μm, and that oxygen penetrated about 300 to 700 μm from the outer surface of the membrane.

Furthermore, FISH analysis revealed that ammonia-oxidizing bacteria (AOB) were located near the outer surface of the membrane, whereas other bacteria were located from the inner to the outer part of the biofilm. Combining these results demonstrated that simultaneous nitrification and denitrification occurred in the biofilm of the MABR system. In addition, stoichiometric analysis revealed that after 130 days the free ammonia (FA) concentration ranged within the concentration causing inhibition of the growth of nitrite oxidizing bacteria (NOB) and that AOB consumed 86% of the oxygen supplied through the intra-membrane. These results indicate that nitrogen removal not via nitrate but via nitrite was mainly achieved in the MABR system.

6. 1 Introduction

The discharge of nitrogen and phosphorus from domestic effluent and animal farms causes eutrophication, algal blooms and groundwater pollution. Particularly, since animal wastes contain high concentrations of nitrogen and phosphorus as well as organic carbon, the removal of organic carbon and nutrients is very important for water environment conservation. To treat animal wastes, activated sludge and modified activated sludge systems (i.e., sequencing batch reactors (SBRs)) have been widely used because of the high concentration of organic compounds (Bernet *et al.*, 2000; Biscudo *et al.*, 1995; Kim *et al.*, 1999; Osada *et al.*, 1991; Ra *et al.*, 2000). However, there is a major drawback: the

presence of organic compounds results in competition for dissolved oxygen (DO) between nitrifying bacteria which oxidize nitrogenous compounds and heterotrophic bacteria which oxidize organic compounds under aerobic conditions. Even in conventional biofilm processes that facilitate the immobilization of larger amounts of bacteria in the reactor vessel than activated sludge processes, nitrifying bacteria are usually outcompeted by heterotrophic bacteria due to lower growth rates and yields in the competition for DO. The outcome of these interspecies competitions is usually deterioration in nitrification efficiency (Okabe *et al.*, 1996). Thus, when applying these processes to high-strength nitrogenous wastewater treatment, a large amount of water is needed for dilution. For that reason, the reactor volume would be too large to be set up in small swine farms, particularly in Japan. Furthermore, in the case of conventional activated sludge or biofilm reactor systems, complicated system operation, large space requirement and pH adjustment in the respective vessels are unavoidable due to the necessity of vessels for two respective reactions: nitrification and denitrification. Therefore, the development of a compact and maintenance-free reactor system is desirable.

As a solution to these problems in small swine farms, the application of a membrane-aerated biofilm reactor (MABR) to the wastewater treatment process is proposed in this chapter. The MABR is composed of porous hollow-fiber membranes the outer surface of which is covered with biofilm. In the MABR, a membrane plays two roles: one is as a carrier to immobilize bacteria and the other is as an oxygen supplying material. Oxygen penetrates through the membrane into the biofilm that forms on the outer surface of the membrane. Bacteria in the biofilm subsequently consume the oxygen to oxidize pollutants diffusing from the bulk solution (Timberlake *et al.*, 1988). An MABR has previously been applied to nitrification (Brindle *et al.*, 1998; Hsieh *et al.*,

2002), simultaneous organic carbon removal and nitrification (Suzuki *et al.*, 1993, 2000; Yamagiwa *et al.*, 1994, 1998) and the treatment of high-strength food processing wastewater (Brindle *et al.*, 1999; Pankhania *et al.*, 1994; Wilderer *et al.*, 1985). Furthermore, when applying an MABR to wastewater containing organic carbon and ammonia, the aerobic zone close to the biofilm-membrane interface would support nitrification; the anoxic zone close to the biofilm-liquid interface would allow denitrification (Casey *et al.*, 1999; Hibiya *et al.*, 2002). Therefore, an MABR can be used for simultaneous nitrification and denitrification in a single reactor vessel without pH adjustment and is a compact reactor system. However, there is no report in which an MABR is applied to the treatment of high-strength nitrogen-containing wastewater from animal farms with the aim of simultaneous nitrification and denitrification, and in which the biofilm structure in the MABR is analyzed in detail.

The biofilm structure in an MABR system used for simultaneous nitrification and denitrification would be more complicated than a conventional biofilm structure because two reactions occurring under different conditions are achieved in a single reactor vessel. To elucidate the physical and microbial characteristics of the biofilm and to control the microenvironment in the biofilm are of importance for optimum operation of MABRs. Particularly, a combination of microelectrodes with a tip diameter of 3-20 mm for the measurement of substrate distribution in the biofilm (Lewandowski *et al.*, 1989) and the FISH method which is capable of detecting specific bacterial cells using 16S rRNA-targeted oligonucleotide probes labeled with a fluorescent compound provides direct information regarding microenvironments and distribution of substrates in MABRs, as previously demonstrated for biofilm reactors (Okabe *et al.*, 1999; Schramm *et al.*, 1997).

In this chapter, we developed an effective MABR system capable of simultaneous

nitrification and denitrification for high-strength nitrogenous wastewater such as swine wastewater and investigated the removal characteristics of nitrogen. Then, the DO concentration that seemed to result in substrate limitation in most biofilms and the microbial population in the biofilm were investigated using DO microelectrodes and the FISH method, respectively. Furthermore, using the experimental data of the nitrogen removal rate, oxygen supply rate, and biofilm structure, nitrogen removal characteristics and stoichiometric analysis in terms of oxygen utilization are discussed.

6.2 Materials and methods

6.2.1 Hollow-fiber membranes

As mentioned in the Introduction, in an MABR the membrane plays two roles, *i.e.*, as an oxygen supplying material and a carrier for bacterial immobilization. To promote bacterial attachment to the membrane, we used a surface-modified polyethylene membrane. This material was prepared by the radiation-induced graft polymerization (RIGP) method as described by Tsuneda *et al.* (1995). A commercially available polyethylene membrane (Asahi Kasei, Tokyo) was used as the base polymer for grafting. A vinyl monomer, glycidylmethacrylate (GMA), was grafted onto the polyethylene membrane by applying the RIGP method. The degree of GMA grafting (*dg*) defined by Eq. 6.1, was set at 100%,

$$dg = \{(W_1 - W_0)/W_0\} \times 100 \qquad [\%] \qquad (6.1)$$

where W_0 and W_1 are the weights of unmodified and GMA-grafted membranes, respectively. Subsequently, the GMA-grafted membrane was reacted with 50 %

diethylamine aqueous solution for the introduction of diethylamino (DEA) groups. Table 6.1 shows the characteristics of the DEA-grafted membrane. Nitrifying bacteria exhibited a high degree of adhesion to this DEA-grafted membrane, which resulted in the formation of nitrifying biofilms of sufficient thickness within a short time (Hibiya *et al.*, 2000).

Table 6.1 Characteristics of the DEA-grafted membrane

Material	Polyethylene
Membrane outer diameter [mm]	3.0
Membrane thickness [mm]	0.15
Membrane length [mm]	240
Pore size [μm]	0.2
DEA group density [mol/kg-resin]	3.1

6.2.2 Reactor system

A laboratory-scale MABR contained three DEA-grafted hollow-fiber membranes. Figure 6.1 shows a schematic diagram of the MABR used in this study. The working volume of the reactor vessel except for the circulation line was 0.15 L, with a reactor length, inner diameter and total volume of 280 mm, 26 mm and 0.2 L, respectively. This system adopted a dead-end configuration whereby the fiber ends furthest from the oxygen source were individually sealed. The specific membrane surface area was 50 m^2/m^3 and the dead space was about 3% of the total volume of the reactor vessel. Liquid in the MABR was circulated at a flow rate of 5 cm/s to prevent the sedimentation of excess sludge. All experiments were performed under the condition of complete mixing.
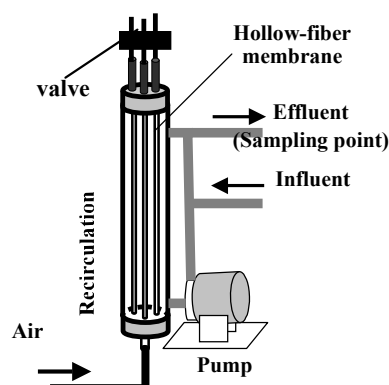
Figure 6.1 Schematic diagram of the membrane-aerated biofilm reactor (MABR).

6.2.3 Target wastewater

The target wastewater in this study was non-diluted swine liquid waste discharged from a process separating excrement and urine. Excrement does not contain nitrogen to a large extent but consists almost completely of suspended solid and organic compounds. The artificial wastewater comprising basal medium (7.93 g of dextrin, 0.91 g of peptone, 1.85 g of meat extract, 0.1 g of urea, 0.688 g of $(NH_4)_2SO_4$, 17.13 g of NH_4HCO_3, 0.64 g of KH_2PO_4, 1.483 g of KCl, 0.709 g of $MgSO_4 \cdot 7H_2O$, 0.441 g of $CaCl_2 \cdot 2H_2O$, 20 mg of $MnSO_4 \cdot 4H_2O$, 30 mg of $FeSO_4 \cdot 7H_2O$, 1 mg of $CuSO_4 \cdot 5H_2O$, and 1 mg of $ZnSO_4 \cdot 7H_2O$ per liter) was used as an inlet solution for the MABR. Table 6.2 shows the characteristics of the artificial wastewater.

Table 6.2 Characteristics of the artificial high-strength nitrogenous wastewater

Parameter		Mean value
TOC	$[g/m^3]$	4500
NH_4^+-N	$[g/m^3]$	3000
NO_2^--N	$[g/m^3]$	0
NO_3^--N	$[g/m^3]$	0
Org-N	$[g/m^3]$	1000
T-N	$[g/m^3]$	4000
T-P	$[g/m^3]$	300
pH	[-]	7.5
Salinity	[%]	1.3

6.2.4 Reactor operational conditions

First, a seed sludge of nitrifying bacteria acclimated in ammonia-rich inorganic wastewater at a nitrogen volumetric loading rate of 1.5 kg-N/m^3/day for a period of one year was inoculated. After 3 weeks of operation, the attachment of nitrifying bacteria to the DEA-grafted membrane was visually confirmed. Next, a seed sludge of heterotrophs acclimated in artificial municipal wastewater at TOC and nitrogen volumetric loading rates of 1.92 kg-C/m^3/day and 1.20 kg-N/m^3/day, respectively, over a period of three years was inoculated and the artificial swine wastewater was fed. Considering the fact that the actual swine wastewater was discharged once a day, the artificial swine wastewater was fed intermittently in the same manner. The TOC and nitrogen volumetric loading rate were set at 0.30 kg-C/m^3/day and 0.27 kg-N/m^3/day, respectively. The water temperature was 25±3°C. The oxygen was supplied through the inner side of the membrane at an air pressure of 20 kPa. The hydraulic retention time (HRT) throughout the MABR system was 15 day. For cleaning out excess sludge in the bulk liquid and biofilm during the reactor operation, washing at a flow rate of 18 cm-reactor/s was performed for 1 min on days 98, 115, 165, 213, 235, 269 and 330. Then, the suspended solids were separated by precipitation and the solid pellet was removed. Periodically, the dead end configuration was changed into flow-through configuration just in case to remove water in the membrane lumen by opening the valve on the top of the reactor.

6.2.5 Analytical method

Water for treatment was sampled just before substrate feeding. All samples were filtered through a glass filter (GF/C; Whatman, Springfield Mill, UK) before water quality analysis. Total organic carbon (TOC) was measured using a TOC analyzer (TOC-5000A; Shimadzu, Kyoto). Ammonia-nitrogen (NH$_4^+$-N) was measured using ion

chromatography (DX-120; Dionex, Osaka). Nitrite-nitrogen (NO_2^--N) and nitrate-nitrogen (NO_3^--N) were measured using high performance liquid chromatography (HPLC) (column: IC-Anion-PW; Tosoh, Tokyo). The analysis of total nitrogen (T-N) was conducted according to standard methods (APHA *et al.*, 1992). The pH was measured using a pH meter (B-211; Horiba, Kyoto).

6.2.6 Preparation of microelectrodes

A Clark-type DO microelectrode with a 90% response time of less than 5 s was prepared to measure the concentration profiles of the biofilm according to the preparation protocol described by Revsbech (1989). The tip diameter of the microelectrode was made to be ca. 10 μm by utilizing micropipette tension (MPT-1, Shimadzu, Kyoto). A two-point calibration of the microelectrodes was made with 100% oxygen-saturated water at 24°C of 8.34 g/m^3 and oxygen-free water of 0 g/m^3 by the addition of 1 M sodium sulfite.

6.2.7 Measurement of oxygen concentration profiles in the biofilm

The membrane and bulk solution in the MABR were immediately transferred to a column-type cell for microelectrode analysis (Hibiya *et al.*, 2003). Air was supplied in the same way as during MABR operation. The DO microelectrode was inserted into the biofilm using a micromanipulator (MMO-223; Narishige, Tokyo) at depth steps of 20 to 100 μm until the microelectrode was attached to the membrane outer surface the position of which was defined as 0 μm in biofilm depth. In this study, since the wastewater was fed once a day, the concentration profiles of DO within the biofilm at substrate feeding (0 h) and just before substrate feeding (24 h), were measured with a DO microelectrode. The biofilm on day 332 was immediately transferred to the column-type cell, and then the DO microelectrode was inserted into the biofilm without disrupting the biofilm.

6.2.8 Sample preparation for FISH analysis

Sample preparation for FISH analysis was performed according to the protocol described

by Aoi *et al*. (2000). Biofilm samples attached to the membrane were immediately fixed

in freshly prepared paraformaldehyde solution (4% paraformaldehyde in

phosphate-buffered saline (PBS), pH 7.2) at 4°C for 18 h and were subsequently washed

in PBS. A 20-μm-thick biofilm section was prepared from a frozen biofilm sample

embedded in OCT compound (Miles, Elkahrt, IN, USA) using a cryostat (CM 3050;

Leica, Bensheim, Germany) at –20°C. Each slice was placed in hybridization wells on a

gelatin-coated microscopic slide and immobilized by air drying and dehydrating in a

graded series of 50, 80 and 96% ethanol.

6.2.9 Oligonucleotide probes

Two 16S rRNA-targeted oligonucleotide probes were used for in situ detection of

ammonia-oxidizing bacteria (AOB) and other bacteria: first, NSO1225 (labeled with

Cy3) (Mobarry *et al*., 1996): a specific probe for a region of the 16S rRNA of AOB

belonging to the β-subclass of Proteobacteria; and second, EUB338 (labeled with FITC)

(Amann *et al.*, 1990): a probe for targeting all bacteria except Archaea. In this study,

NSO1225 and EUB338 were used at formamide concentrations of 35% and 20%,

respectively.

6.2.10 In situ hybridization and microscopic observation

Hybridization of the biofilm sections on the slide was performed according to the

standard hybridization protocol described by Amann (1995). Subsequently, the slides

were examined by fluorescence microscopy (Axio skop2 plus; Carl Zeiss, Oberkochen,

Germany) to visualize the microbial population. The image combining, processing and

analysis were performed using personal computer software packages.

6.3. Results

6.3.1 Organic carbon removal characteristics

Figure 6.2 shows the time courses of effluent TOC concentration and TOC removal efficiency during a period of approximately one year. The average TOC removal efficiency reached above 96% at a TOC loading rate of 0.30 kg-C/m^3/day. From the results of a TOC volumetric removal rate based on 50 m^2/m^3 of the specific surface area being available for the biofilm attachment and oxygenation, a TOC specific removal rate per membrane surface area was estimated to be 5.76 g-C/m^2/day. However, in some cases, the TOC concentration in the effluent exceeded more than 100 g-C/m^3, particularly after 150 day. Increasing biomass in the MABR with an increase in the biofilm thickness was clearly observed. Therefore, it was assumed that an increase in biomass in the biofilm brought about detachment and self-digestion of bacteria, and consequently the TOC concentration in the effluent was raised.
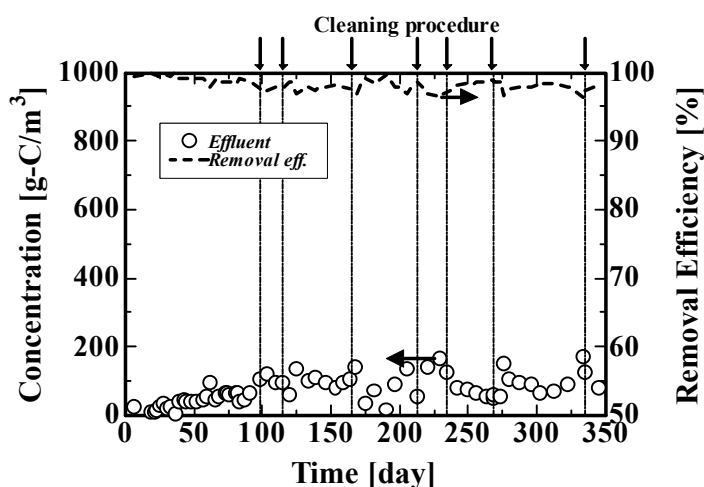
Figure 6.2 Time courses of TOC concentration in the effluent and TOC removal efficiency.

6.3.2 Nitrogen removal characteristics

Figure 6.3 shows the time courses of T-N, NH_4^+-N, NO_2^--N, and NO_3^--N concentrations in the effluent. Additionally, Figure 6.4 shows the composition of residual nitrogen compounds in the effluent and the nitrogen removal efficiency. As can be seen in Figs. 6.3 and 6.4, nitrite and nitrate were detected up to 70 days, indicating that denitrification was limited. Thin biofilms growing at the early stage of biofilm development promoted oxygen penetration to the bulk liquid, which inhibited denitrification in the bulk liquid where the DO concentration ranged from 1 to 3 g/m^3. Since a thick biofilm was observed after 70 day, nitrite and nitrate were hardly detected and a nitrogen removal efficiency of more than 85% was stably achieved. However, after 150 day, the nitrogen removal efficiency was less than 80%. In this period, inhibition of nitrification was observed and consequently ammonia in the effluent reached about 1000 mg/L and the pH reached 8.5. As shown in Fig. 6.4, after the washing procedure, the deterioration in the removal efficiency was not observed. Furthermore, since excess sludge was not observed in the reactor vessel during the entire operation period, the contribution of excess sludge to denitrification seemed to be negligible compared with that of the biofilm. In summary, during the entire operation period, the mean percentage of nitrogen removal was 83%. Furthermore, from this result, the nitrogen specific removal rate per membrane surface area was estimated to be 4.48 g-$N/m^2/day$.
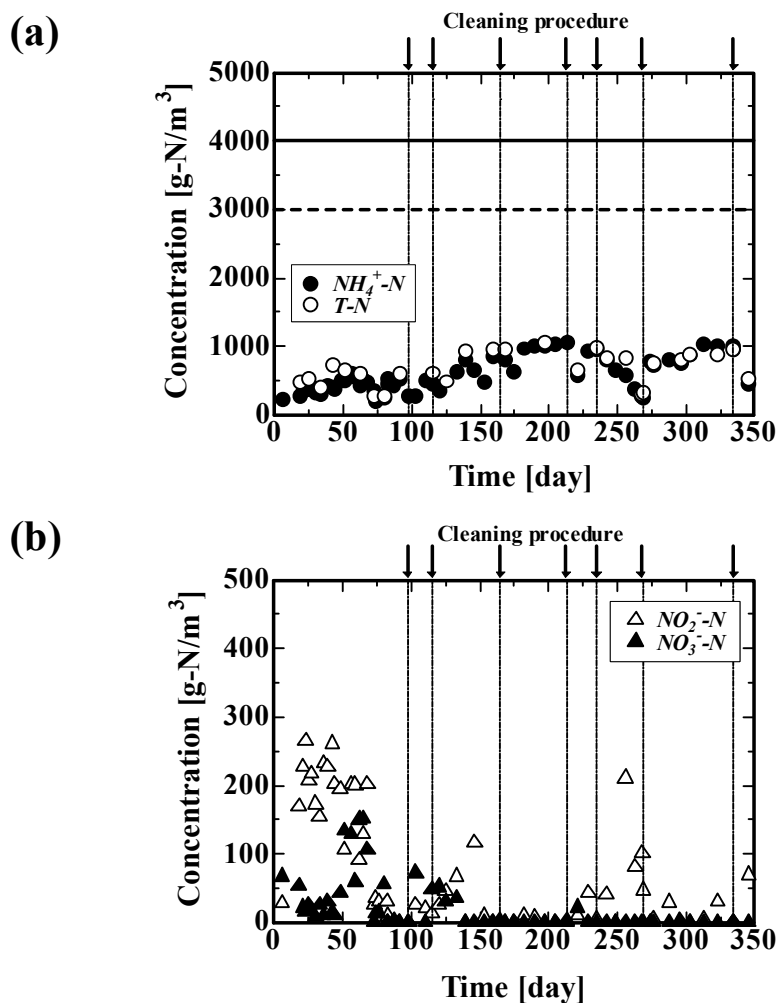
Figure 6.3 Time course of respective nitrogen concentrations in the effluent. (a) T-N and NH$_4^+$-N, (b) NO$_2^-$-N and NO$_3^-$-N. Symbols: solid line, average T-N in the influent; dotted line, average NH$_4^+$-N in the influent.
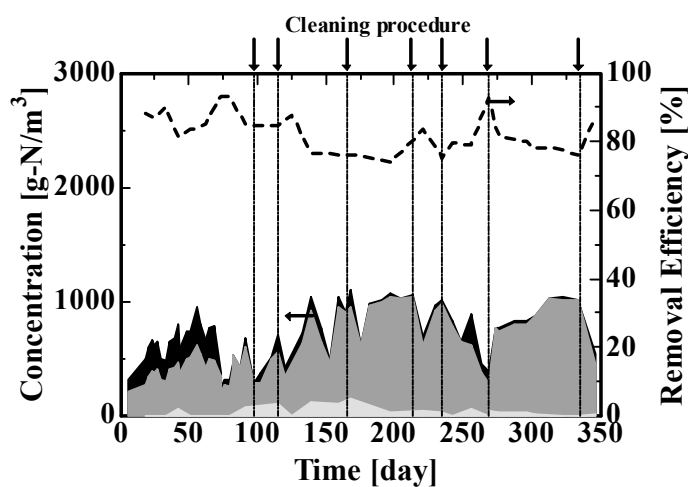
Figure 6.4 Time courses of residual nitrogen compounds in the effluent and nitrogen removal efficiency. Symbols: pale gray area, organic-N; gray area, NH$_4^+$-N; black area, NO$_x^-$-N; dotted line, T-N removal efficiency.

6.3.3 Measurement in the biofilm

Figure 6.5 shows the DO concentration profile in the biofilm. It was revealed that the biofilm thickness was about 1600 μm and the DO penetration depths at substrate feeding (0 h) and just before substrate feeding (24 h) were approximately 300 μm and 700 μm, respectively. From this result, it was suggested that the aerobic zone in the biofilm was quite limited, whereas the anoxic and anaerobic zones were relatively wide. Moreover, throughout each 24-h period, the DO in the bulk liquid was always 0 g/m^3, where denitrification by denitrifying bacteria could occur. As a result, 100% oxygen utilization efficiency was achieved owing to the dead-end configuration and bubbleless mass transfer through the membrane wall directly to the biofilm.
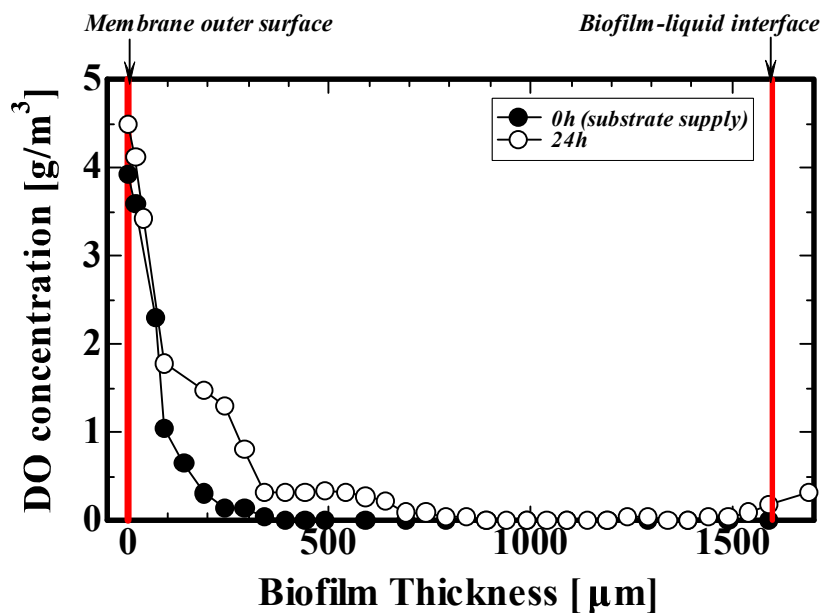
Figure 6.5 Dissolved oxygen concentration profile in a biofilm on day 334. Mean biofilm thickness was 1600 μm. Membrane outer surface was defined as having a depth of 0 μm.

6.3.4 FISH analysis

On day 346, the membrane was collected for FISH analysis. Due to the inoculation of nitrifying bacteria for 3 weeks, clusters of AOB could be detected with the Cy3-labeled NSO1225 probe throughout the aerobic region ranging from 0 to 300 μm from the outer surface of the membrane, as shown in Figures 6.6 a and b. In addition, other bacteria could be also detected with the FITC-labeled EUB338 probe in the same region. In contrast, only bacteria other than AOB were present at the interface of the biofilm and the bulk liquid as shown in Figure 6.6 c. Since the biofilm prepared for FISH was separated during the fixation procedure in the prepared paraformaldehyde solution, it was impossible to draw a clear boundary line between the biofilm outer surface and the bulk liquid in Fig. 6 c. Combining the results obtained with the DO microelectrodes with those obtained using FISH analysis, AOB mainly inhabited the oxic zone (up to 300 μm from the membrane surface). These results indicated that the ecology of AOB was dependent upon the DO concentration and that AOB converted ammonia into nitrite at the outer surface of the membrane.
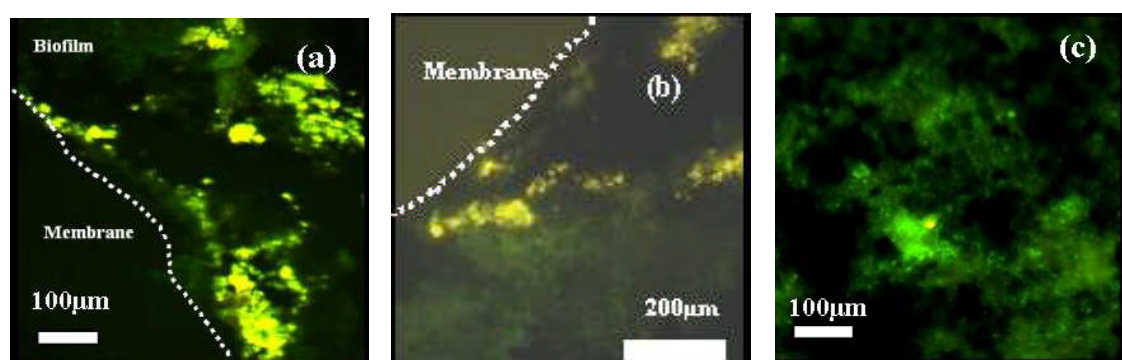
Figure 6.6 FISH images of the membrane-biofilm interface (a) (b) and biofilm-bulk liquid interface (c) with Cy3-labeled NSO1225 probe and FITC-labeled EUB338 probe. Eubacterial cells are green and ammonia-oxidizing cells are yellow.

6.4 Discussion

6.4.1 Biofilm thickness

During the entire operation period, the mean percentage of nitrogen removal was 83%. Furthermore, the nitrogen removal rate per membrane surface area reached 4.48 g-N/m^2/day. Table 6.3 summarizes the specific ammonia or nitrogen removal rates per unit membrane surface area that have been attained with biofilm reactors by other research groups. Although an exact comparison of these results might be superficial, the value obtained in this study demonstrated that the present MABR system had high nitrogen removal potential in a single reactor vessel. This can be attributed to the start-up procedure whereby nitrifying bacteria were inoculated by priority. Moreover, the RIGP method is effective for the attachment of nitrifying bacteria to the membrane surface evenly and rapidly as indicated by Hibiya *et al.* (2000). The start-up procedure and the introduction of the RIGP method resulted in a long period of effective oxygen uptake by nitrifying bacteria and a high ammonia removal rate. However, the biofilm thickness, which was measured with a DO microelectrode in this study, was about 1600 μm, also implying that substrate diffusion into the entire biofilm might be limited. Casey *et al.* (2000) reported that liquid flow velocity on the biofilm surface had an effect on mass transfer by diffusion through the boundary layer, on the detachment rate, and on the maximum biofilm thickness in the MABR system. Moreover, according to their report, when the biofilm thickness was higher than 1000 μm, substrate diffusion limitation occurred and the removal rate was reduced. On the other hand, Tsuneda *et al.* (2000) showed that utilization of extracellular polymeric substances (EPS) excreted by heterotrophic bacteria resulted in a thick biofilm that included large quantities of *Nitrobacter winogradskyi* and a high nitrite-oxidation rate. Therefore, the biofilm formed in this study was suitable for retaining large amounts of nitrifying bacteria as shown in

Figures 6.6 a and b. In addition, the result that AOB were not detected near the bulk liquid-biofilm interface as shown in Fig. 6.6 c, demonstrated that the biofilm structure in this study had another advantage; preventing AOB detachment due to liquid flow at the bulk liquid-biofilm interface. In future work, the concentration profiles of ammonia and DO will be precisely determined with respective microelectrodes; and then the optimum biofilm thickness must be determined and a thickness control technique established. Moreover, in this study, the washing procedure of the biofilm was conducted irregularly; however, periodical washing of the biofilm and withdrawal of the excess sludge in the bulk liquid was necessary to keep the TOC and nitrogen removal efficiency high, as described by Suzuki *et al.* (1993), Pankhania *et al.* (1994), and Brindle *et al.* (1999).

Table 6.3 Comparison of specific removal rate per unit membrane surface area.

References		NH_4^+-N removal rate (Nitrogen removal rate) [g-N/m^2/day]	Wastewater (Artificial)
Biofilm reactor	Matsumura *et al.* (1997)	4.0×10^{-2}	Inorganic
	Araki *et al.* (1999)	9.6×10^{-2}	Inorganic
Membrane-aerated biofilm reactor	This study	4.48[a]	High-strength nitrogenous
	Suzuki *et al.* (1993)	4.0[b]	Municipal
	Yamagiwa *et al.* (1994)	2.2	Municipal
	Yamagiwa *et al.* (1998)	1.9	Municipal
	Hibiya *et al.* (2002)	3.0[a, b]	Municipal
	Brindle *et al.* (1998)	5.4[c]	Inorganic
	Hsieh *et al.* (2002)	1.97	Inorganic

[a] Representing nitrogen removal value.
[b] Representing maximum value.
[c] Utilizing pure oxygen.

6.4.2 Ammonia accumulation

In this study, deterioration of nitrogen removal efficiency was mainly due to ammonia

accumulation. A possible reason for deterioration of the nitrogen removal efficiency would be an increase in free ammonia (FA) and free nitrous acid (FNA). FA is inhibitory to both AOB and NOB, and FNA rather than NH4+ and NO2- is inhibitory to only NOB (Anthonisen *et al.*, 1976). Figure 3.7 shows the relationship between pH and FA or FNA described by Anthonisen *et al.* (1976). When all the data of effluent NO_2^--N and NH_4^+-N concentrations in our continuous experiment were plotted on this graph, it was found that the FA concentration was as high as 150 g/m^3 from day 180 to 240 (closed circles in Fig. 3.7). It was reported that a high FA concentration (Zone 1) in the bulk liquid inhibited not only NOB such as Nitrobacter species, but also AOB such as *Nitrosomonas* species (Anthonisen *et al.,* 1976). One advantage of the MABR system is that there is no need for pH adjustment because of the simultaneous nitrification (oxidation) and denitrification (reduction) occurring in a single reactor vessel. However, when the FA concentration reached as high as 150 g/m^3, the activities of both AOB and NOB were inhibited, resulting in deterioration of nitrification efficiency. In association with this phenomenon, the pH was never lowered but was raised by ammonification and denitrification. Therefore, monitoring and adjustment of pH were desirable when high-strength nitrogenous wastewater such as that from livestock was treated. Ammonium nitrogen did not exceed 1000 g-N/m^3 probably because adaptation of AOB to the high FA concentration occurred. Turk and Mavinic (1989) reported that NOB appeared capable of tolerating ever-increasing levels of FA concentrations up to 40 g NH_3-N/m^3. Thus, AOB as well as NOB might exhibit such the tolerance, resulting in the occurrence of ammonia oxidation despite the high FA concentration. On the other hand, after 70 day, the FA concentration, ranging from 10 to 150 g/m^3, was sufficiently high to inhibit NOB activity. Inhibition by FNA was negligible throughout the experimental run, as indicated in Fig. 3.7 in which all plots (open triangles) were below FNA concentration

of 2.8 g/m^3.
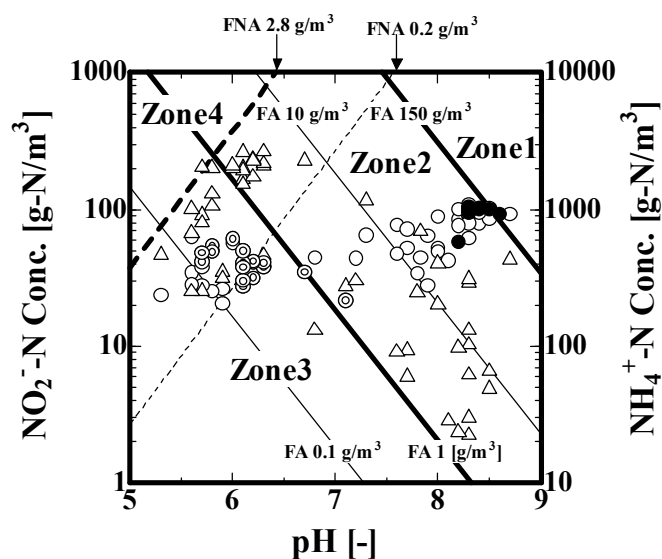
Figure 6.7 Dependence of free ammonia (FA) and free nitrous acid (FNA) on pH in the solution described by Anthonisen *et al.* (1976). Zone 1 shows FA inhibition of *Nitrobacter* and *Nitrosomonas*, Zone 2 shows FA inhibition of only *Nitrobacter*, Zone 3 shows complete nitrification, and Zone 4 shows FNA inhibition of *Nitrobacter*. Symbols: open circles, NH$_4^+$-N; double circles, NH$_4^+$-N from 0 to 70 d; closed circles, NH$_4^+$-N from 180 to 240 day; open triangles, NO$_2^-$-N; solid lines, FA of 0.1, 1, 10 and 150 g/m^3, respectively; dotted lines, FNA of 0.2 and 2.8 g/m^3.

6.4.3 Biofilm structure

Previous studies on MABRs focused only on the overall removal efficiencies without paying any attention to what happened in the biofilm. In this study, however, the combination of the in situ detection of specific bacteria in the membrane-attached biofilm using the FISH method and determination of the DO microprofiles using a DO microelectrode made it possible to confirm the microbial ecology in the biofilm; AOB were located near the membrane and bacteria other than AOB near the biofilm-bulk liquid interface. It was clearly proved that simultaneous nitrification and denitrification occurred in the same biofilm of MABR system. However, we did not investigate either

the activity of sulfate-reducing bacteria (SRB) in the biofilm or the competition for organic carbon between denitrifying bacteria and SRB. As reported by Okabe *et al.* (1998) and Santegoeds *et al.* (1998), it was possible that SRB were present extensively in the biofilm of the MABR. In this study, the production of hydrogen sulfide was not detected throughout the incubation period (data not shown), indicating that the oxygen reduction potential (ORP) of the effluent was suitable not for sulfate reduction but for denitrification. However, if the ORP decreases, the competition for organic carbon between denitrifying bacteria and SRB might occur, leading to a lack of organic carbon for denitrification and the deterioration of nitrogen removal efficiency. Therefore, future research, *i.e.*, on the production of hydrogen sulfide and the competition for organic carbon between denitrifying bacteria and SRB, is needed to better understand biofilm function and structure, and to promote overall removal efficiency of the MABR.

6.4.4 Oxygen utilization

One of the advantages of the MABR is that the amount of oxygen supplied through the intra-membrane can be easily controlled. In our previous study, it was clarified that the amount of transferred oxygen was proportional to air pressure (Hibiya *et al.*, 2002), which indicated the possibility of controlling the DO concentration in the MABR system by adjusting air pressure. According to the relationship between air intrapressure and the oxygen transfer rate obtained in our previous study (Hibiya *et al.*, 2003), the oxygen mass transfer rate in the present MABR system was calculated to be 1.17×10^{-1} g-O$_2$/day. The mean ammonia removal rate per membrane surface area from 130 day was 4.32 g-N/m^2/day, when nitrate in the effluent was not detected and the DO concentration in the bulk was 0 g/m^3. The total amount of ammonia removed in the MABR was 3.18×10^{-2} g-N/day by calculating from the membrane surface area. The stoichiometric formula of

microbial ammonia oxidation with AOB growth was previously defined as Eq. 6.2 (U.S. Environmental Protection Agency, 1975).

$$55NH_4^+ + 76O_2 + 109HCO_3^- \rightarrow C_5H_7NO_2 + 54NO_2^- + 57H_2O + 104H_2CO_3 \quad (6.2)$$
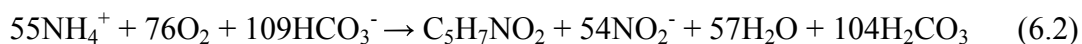
By using this formula, the amount of oxygen utilized by AOB was estimated to be 1.00×10^{-1} g-O_2/day. Since the oxygen mass transfer rate was 1.17×10^{-1} g-O_2/day as mentioned above, considering the ammonia removal rate per membrane surface area and the oxygen supplied through the intra-membrane it was revealed that 86% of supplied oxygen was used by AOB and the remaining 14% by bacteria other than AOB. If the remaining 14% of supplied oxygen, 1.70×10^{-2} g-O_2/day, was utilized by NOB, the stoichiometric formula of microbial nitrite oxidation with NOB growth was previously defined as Eq. 6.3 (U.S. Environmental Protection Agency, 1975).

$$400NO_2^- + NH_4^+ + 4H_2CO_3 + HCO_3^- + 195O_2 \rightarrow C_5H_7NO_2 + 3H_2O + 400NO_3^- \quad (6.3)$$
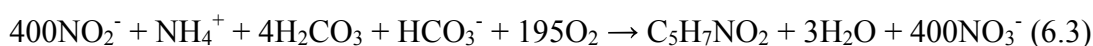
By using this formula, the amount of nitrate produced was estimated to be 1.49×10^{-2} g-N/day by depletion of oxygen, whereas the nitrite produced would be 1.62×10^{-2} g-N/day. In other words, the NO_3^--N/NO_x^--N ratio would be 0.48. In addition, taking into account FA and FNA inhibition and the competition for DO between NOB and aerobic heterotrophic bacteria in the biofilm, this ratio would be lower. Consequently, this calculation revealed that more than the half of the nitrogen was removed not via nitrate but via nitrite ($NH_4^+ \rightarrow NO_2^- \rightarrow N_2$). In previous research by Oh and Silverstein (1999), when the TOC/NO_3^--N ratio was as low as 1.00, denitrification occurred insufficiently due to TOC depletion, resulting in nitrite accumulation in the SBR. On the other hand, Bernet and Moletta (1996) reported that denitrification was complete even when the TOC/NO_2^--N ratio was 1.08 using volatile fatty acids in batch tests for denitrification. In this study, although the TOC/N ratio was as low as 1.13, nitrogen removal was attained in the MABR system where nitrogenous compounds were removed not only via nitrate

denitrification but also via nitrite denitrification. This nitrogen removal path ($NH_4^+ \rightarrow$ $NO_2^- \rightarrow N2$) could lead to denitrification at low TOC/N ratios as shown in the previous study (Bernet and Moletta, 1996). Many researchers demonstrated that the short-cut process ($NH_4^+ \rightarrow NO_2^- \rightarrow N_2$) can save on tank volume, the oxygen requirement for nitrification, and the organic carbon requirement for denitrification (Abeling and Seyfried,1992; Eum and Choi, 2002; Turk and Mavnic, 1986). In particular, in the treatment of swine wastewater, although the separation of excrement and urine results in a decrease in the TOC/N ratio and leads to a lack of organic carbon that is necessary for denitrification, elimination of excrement can prevent the biofilm from clogging. Therefore, the short-cut process would be effective when treating low-TOC/N-ratio wastewater such as swine wastewater in terms of stable removal efficiency as well as cost performance. As mentioned above, use of the MABR facilitated the generation of more detailed information regarding the biofilm, particularly bacterial activity with an oxygen requirement. Therefore, use of an MABR would be effective in the treatment of low-TOC/N-ratio wastewater, because oxygen could be supplied for specific bacterial species populating the region close to the membrane surface. Nevertheless, direct measurements with microelectrodes are necessary to clarify the nitrogen removal path in the biofilm and prove the effectiveness of the short-cut process.

6.4.5 Improvement of removal rate

The MABR system in this study exhibited lower volumetric removal rates of TOC and nitrogen because of the smaller specific surface of the membrane per reactor volume; 50 m^2/m^3 in comparison with the MABR system used in other research groups. For example, Brindle *et al.* (1999) and Pankhania *et al.* (1994) set a specific membrane surface per reactor volume of 447 m^2/m^3 and 5100 m^2/m^3 and achieved removal rates of 27

kg-COD/m^3/day and 8.94 kg-COD/m^3/day, respectively. Moreover, Brindle *et al.* (1998) concluded that the volumetric nitrification rate was limited only by the specific membrane surface area available for biofilm attachment under conditions whereby the oxygen supply was sufficient for complete nitrification. Therefore, to attain a high volumetric removal rate of nitrogen, it is necessary to use membrane modules that increase the specific surface area per reactor volume.

6.5 Conclusion

The nitrogen removal characteristics of the MABR were investigated using artificial swine wastewater as a representative high-strength nitrogenous wastewater. Although there was concern regarding substrate diffusion limitation owing to the formation of a thick biofilm on the membrane, a high nitrogen removal rate per membrane surface area, 4.48 g-N/m^2/day, was achieved. A constant washing procedure is necessary for stable removal efficiency. Combining the results obtained using the DO microelectrode and the FISH method revealed that the DO was completely consumed in the biofilm and AOB inhabited the membrane outer surface and not the biofilm-bulk liquid interface. Therefore, heterotrophic bacteria such as denitrifiers located at the biofilm-bulk liquid interface resulted in the immobilization of large amounts of AOB in the biofilm. From stoichiometric analysis, 86% of the supplied oxygen was consumed by AOB and nitrite but not the nitrate denitrification seemed to be the main path of nitrogen removal. The MABR takes advantage of the easy control of oxygen mass transfer, and thus it is useful when removing nitrogen from low-TOC/N-ratio wastewater.

References

Abeling U, Seyfried CF. 1992. Anaerobic-aerobic treatment of high-strength ammonia wastewater-nitrogen removal via nitrite. Water Sci Technol 26:1007-1015.

Amann RI, Krumholz L, Stahl DA. 1990. Fluorescent-oligonucleotide probing of whole cells for determinative, phylogenetic, and environmental studies in microbiology. J Bacteriol 172:762-770.

Amann RI. *In situ* identification of micro-organism by whole cell hybridization with rRNA-targeted nucleic probes, p. 1-15. *In* Akkerman ADC, van Elsas JD, de Bruijin FJ (eds) Molecular microbial ecology manual. Kluwer Academic Publishers; Dordrecht.

Anthonisen AC, Loehr RC, Prakasam TBS, Srinath EG. 1976. Inhibition of nitrification by ammonia and nitrous acid. J Water Poll Contr Fed 48:835-852.

Aoi Y, Miyoshi T, Okamoto T, Tsuneda S, Hirata A. 2000. Microbial ecology of nitrifying bacteria in wastewater treatment process examined by fluorescence in situ hybridization. J Biosci Bioeng 90:234-240.

APHA, AWWA, WEF. 1992. Standard methods for the examination of water and wastewater, 18th ed. American Public Health Association, Washington, DC. USA.

Araki, N., Yazawa, K., and Harada, H. 1999. Quantitative monitoring of ammonia oxidizing bacteria in PVA-immobilized pellets by fluorescent *in situ* hybridization (FISH). J Jpn Soc Water Environ 22:600-607 (in Japanese).

Bernet N, Moletta R. 1996. Denitrification by anaerobic sludge in piggery wastewater. Environ Tech 17:293-300.

Bernet N, Delgenes N, Akunna JC, Delgenes JP, Moletta R. 2000. Combined anaerobic-aerobic SBR for the treatment of piggery wastewater. Water Res

34:611-619.

Bicudo JR, Svoboda IF. 1995. Intermittent aeration of pig slurry-farm scale experiments for carbon and nitrogen removal. Water Sci Technol 32:83-90.

Brindle K, Stephenson T, Semmens MJ. 1998. Nitrification and oxygen utilization in a membrane aeration bioreactor. J Membr Sci 144:197-209.

Brindle K, Stephenson T, Semmens MJ.1999. Pilot-plant treatment of a high-strength brewery wastewater using a membrane-aeration bioreactor. Water Environ Res 71:1197-1204.

Casey E, Glennon B, Hamer G. 1999. Review of membrane aerated biofilm reactor. Res Consev Recycl 27:203-215.

Casey E, Glennon B, Hamer G. 2000. Biofilm development in a membrane-aerated biofilm reactor: effect of flow velocity on performance. Biotechnol Bioeng 67:476-486.

Eum Y, Choi E. 2002. Optimization of nitrogen removal from piggery waste by nitrite nitrification. Water Sci Technol 45:89-96.

Hsieh YL, Tseng SK, Chang YJ. 2002. Nitrification using polyvinyl alcohol-immobilized nitrifying biofilm on an O_2-enriching membrane. Biotechnol Lett 24:315-319.

Hibiya K, Tsuneda S, Hirata A. 2000. Formation and characteristics of nitrifying biofilm on a membrane modified with positively-charged polymer chains. Colloids Surf. B: Biointerfaces 18:105-112.

Hibiya K, Terada A, Tsuneda S, Hirata A. 2003. Simultaneous nitrification and denitrification by controlling vertical and horizontal microenvironment in a membrane-aerated biofilm reactor. J Biotechnol 100:23-32.

Kim J, Sakamura T, Chiba N, Nishimura O, Sudo R. 1999. Carbon and nitrogen removal in sequencing batch reactor treating piggery wastewater-pilot scale experiment. J Jpn

Soc Water Environ 22:990-996.

Lewandowski Z, Lee WC, Characklis WG, Little B. 1989. Dissolved oxygen and pH microelectrode measurements at water immersed metal surfaces. Corrosion 45:92-98.

Matsumura M, Yamamoto T, Wang P, Shinabe K, Yasuda K. 1997. Rapid nitrification with immobilized cell using macro-porous cellulose carrier. Water Res 31: 1027-1034.

Mobarry BK, Wagner M, Urbain B, Rittmann BE, Stahl DA. 1996. Phylogenetic probes for analyzing abundance and spatial organization of nitrifying bacteria. Appl Environ Microbiol 62:2156-2162.

Oh J, Silverstein J. 1999. Acetate limitation and nitrite accumulation during denitrification. J Environ Eng 125:234-242.

Okabe S, Hirata K, Ozawa Y, Watanabe Y. 1996. Spatial microbial distribution of nitrifiers and heterotrophs in mixed-population biofilms. Biotechnol Bioeng 50:23-35.

Okabe S, Itoh T, Satoh H, Watanabe Y. 1998. Analysis of spatial distributions of sulfate-reducing bacteria and their activity in aerobic wastewater biofilms. Appl Environ Microbiol 65:5107-5116.

Okabe S, Satoh H, Watanabe Y. 1999. *In situ* analysis of nitrifying biofilms as determined by *in situ* hybridization and the use of microelectrodes. Appl Environ Microbiol 65:3182-3191.

Osada T, Haga K, Harada Y. 1991. Removal of nitrogen and phosphorus from swine wastewater by the activated sludge units with the intermittent aeration process. Water Res 25:1377-1388.

Pankhania T, Stephenson T, Semmens MJ. 1994. Hollow fiber bioreactor for wastewater

treatment using bubbleless membrane aeration. Water Res 28:2233-2236.

Ra CS, Lo KV, Shin JS, Oh JS, Hong BJ. 2000. Biological nutrient removal with an internal organic carbon source in piggery wastewater treatment. Water Res 34:965-973.

Revsbech NP. 1989. An oxygen microsensor with a guard cathode. Limnol Oceanogr 34:474-478.

Santegoeds CM, Ferdelman TG, Muyzer G, de Beer D. 1998. Structural and functional dynamics of sulfate-reducing populations in bacterial biofilms. Appl Environ Microbiol 64:3731-3739.

Schramm A, Larsen LH, Revsvech NP, Amann RI. 1997. Structure and function of a nitrifying biofilm as determined by microelectrodes and fluorescent oligonucleotide probes. Water Sci Technol 36:263-270.

Suzuki Y, Miyahara S, Takeishi K. 1993. Oxygen supply method using gas-permeable film for wastewater treatment. Water Sci Technol 28: 243-250.

Suzuki Y, Hatano N, Ito S, Ikeda H. 2000. Performance of nitrogen removal and biofilm structure of porous gas permeable membrane reactor. Water Sci Technol 41:211-217.

Timberlake DL, Strand SE, Williamson K J. 1988. Combined aerobic heterotrophic oxidation, nitrification in a permeable support biofilm. Water Res 22:1513-1517.

Turk O, Mavinic DS. 1986. Preliminary assessment of a shortcut in anitrogne removal from wastewater. Can J Civil Eng 13: 600-605.

Turk O, Mavninic DS. 1989. Maintaining nitrite buildup in a system acclimated to free ammonia. Water Res 30:1383-1388.

Tsuneda S, Saito K, Furusaki S, Sugo T. 1995. High-throughput processing of proteins using a porous and tentacle anion exchange membrane. J Chromatogr 678:211-218.

Tsuneda S, Park S, Hayashi H, Jung J, Hirata A. 2000. Enhancement of nitrifying biofilm

formation using selected EPS produced by heterotrophic bacteria. Water Sci Technol 43:197-204.

US Environmental Protection Agency. 1975. Process design manual for nitrogen control. EPA Technology Transfer. Washington, DC. USA.

Wilderer PA, Brautigam J, Sekoulov I. 1985. Application of gas permeable membranes for auxiliary oxygenation of sequencing batch reactors. Conserv Recycl 8:181-192.

Yamagiwa K, Ohkawa A, Hirasa O. 1994. Simultaneous organic carbon removal and nitrification by biofilm formed on oxygen enrichment membrane. J Chem Eng Jpn 27:638-643.

Yamagiwa K, Yoshida M, Ito A, Ohkawa A. 1998. A new oxygen supply method for simultaneous organic carbon removal and nitrification by a one-stage biofilm process. Water Sci Technol 37:117-124.

Chapter 7

General conclusion and perspectives

Chapter 7

General conclusion and perspectives

7

7. 1 General conclusion

Essentially novel wastewater treatment system is required for removal of nitrogenous compounds since they would cause eutrophication. The nitrogenous compounds, mainly ammonia, are changed into nitrogen gas through two biological successive reactions, *i.e.*, nitrification and denitrification. These two reactions take place under two different conditions: aerobic and anoxic conditions, respectively, this means normally we have to construct two reactors separately for complete nitrogen removal.

Meanwhile, most natural biofilms exhibit redox stratification and the presence of strong concentration gradients of both electron donors and acceptors. If we can control such stratification in the biofilm, simultaneous nitrification and denitrification can be achieved in a single biofilm, leading to the development with low operational costs and extreme small footprint. The engineering challenges for that are the elucidation of physicochemical property of a substratum, which has an advantage to form biofilm, and the development of a novel biofilm reactor.

In this dissertation, the author considered that the relationship between the

physicochemical properties of a substratum and initial bacterial adhesion is essential for rapid biofilm formation and construction of robust biofilm; therefore, the surfaces with various physicochemical properties were designed and evaluated for initial bacterial adhesion. Radiation-induced graft polymerization (RIGP) method was employed for such design and evaluation since this method can facilitate to modify surface roughness and electrostatic condition of a substratum. In addition, the link between initial bacterial adhesion and the subsequent biofilm formation, *i.e.*, a series of biofilm formation mechanism, was investigated. Finally, a novel biofilm reactor, a membrane-aerated biofilm reactor (MABR), was designed and developed with the use of surface modified hollow-fiber membrane. Since membranes are used both as an oxygen-supplying material and a bacterial carrier in this system, oxygen can be supplied through membrane apart from supply of other substrates, which is expected to create redox stratification in a biofilm easily over conventional biofilms. Simultaneous nitrification and denitrification was demonstrated with the MABR from the considerations of both macro- and micro-scale analyses of the biofilms.

This dissertation is composed of seven chapters.

In **Chapter 1**, the author summarizes basics of biological nitrogen removal, the mechanism of bacterial adhesion and biofilm formation, surface modification techniques and novel biofilm reactors applicable simultaneous carbon and nitrogen removal in a single reactor. Furthermore, the objective of this dissertation is mentioned.

In **Chapter 2**, surface-modified polyethylene (PE) membrane sheets were prepared by RIGP of an epoxy-group-containing monomer, glycidyl methacrylate (GMA). The epoxy ring of GMA was opened by introducing diethylamine (DEA) or sodium sulfite (SS). The

obtained results indicate that RIGP enables the control of the physicochemical properties of such a sheet surface by adjusting the degree of grafting (*dg*) and the subsequent conversion of functional groups. A batch test on bacterial adhesion onto the sheets clarified that the DEA-containing sheet (DEA sheet) exhibited an adhesion rate constant, *k*, significantly greater than those of other types of sheet. Clearly, the adhesion rate constant of the DEA sheet increased with *dg*, indicating that electrostatic interaction is the most decisive factor for bacterial adhesion when it works as an attractive force. Furthermore, the densities of bacteria adhering onto the GMA-containing sheet (GMA sheet) and the SS-containing sheet (SS sheet) were almost the same as that onto a PE sheet, whereas that onto a DEA sheet significantly increased. Thus, the introduction of the GMA- and SS-containing graft chain did not have much influence on bacterial adhesion onto the surfaces, supporting the conclusion that the promotion of bacterial adhesion onto the GMA and SS sheets was due to an increase in surface area resulting from RIGP.

In **Chapter 3**, Primary, secondary and tertiary amino groups were introduced into polymer chains grafted onto a PE flat-sheet membrane to evaluate the effect of surface properties on the adhesion and viability of *Escherichia coli* cells. The characterization of the surfaces containing amino groups, *i.e.*, ammonia (AM), ethylamino (EA) and diethylamino (DEA), revealed that a high bacterial adhesion rate constant *k* was observed at a high membrane potential, which indicates that membrane potential could be an indicator for evaluating bacterial adhesion onto the EA and DEA sheets. The maximum *E. coli* cell adhesion rate constants of the EA- and DEA-containing sheets were 3.5-fold that of the PE sheet. The *E. coli* cell viability experiment revealed that approximately 70% of the cells adhering onto these sheets were inactivated after a contact time of 8 h, and that such viability was dependent on membrane potential. Furthermore, *E. coli* cell viability

significantly decreased at a membrane potential higher than –8 mV. Future perspectives regarding the application of these sheets to the enhancement of biofilm formation or prevention are discussed.

In **Chapter 4**, the relationship between initial bacterial adhesion and the subsequent biofilm formation was investigated with a flow cell and observation of epifluorescence microscopy and scanning electron microscopy (SEM). Surface-modified PE sheets were prepared by RIGP for grafting GMA on the PE. The epoxy ring of GMA was opened by introducing DEA or SS. The activity of *E. coli* cells onto the DEA sheets decreased significantly. The experiment with a flow cell revealed that biofilm formation was facilitated on the DEA sheet although the viability of *E. coli* cell was the lowest among all the prepared sheets. In addition, unique biofilm structure was observed on the DEA sheets: almost all of the *E. coli* cells were inactive on the base of the biofilm and active cells deposited on the inactive cells. The SEM observation clarified that extracellular polymeric substance (EPS) adhered on the DEA sheet, indicating that the EPSs could be enhance biofilm formation onto the DEA sheet. From the above-mentioned experiments, the DEA (100) has a potential to enhance not only initial bacterial adhesion but also biofilm formation.

In **Chapter 5**, surface-modified hollow-fiber membranes were prepared by radiation-induced grafting of GMA onto a PE-based fiber (PE-fiber). The epoxy ring of GMA was opened by introduction of DEA. The bacterial adhesivity to this material (DEA-fiber) was tested by immersed into nitrifying bacterial suspension. The initial adhesion rates and the amount of attached bacteria of the DEA-fiber were 6-10-fold and 3-fold greater than those of the PE fiber, respectively. Biofilm formation was also

facilitated through a biofilm formation experiment, yielding that the DEA-fiber is superior for rapid startup and stable biofilm formation to PE-fiber. A membrane-aerated biofilm reactor (MABR) composed of DEA fibers was developed for partial nitrification with nitrite accumulation. Prior to the nitrification test, it was confirmed that the oxygen supply rate (OSR) was proportional to air pressure up to 100 kPa, allowing easy control of oxygen supply. Stable nitrite accumulation was observed in the partial nitrification test at a fixed oxygen supply throughout the operation period, indicating that oxygen was consumed by only ammonia oxidizers. Furthermore, it was demonstrated that oxygen utilization efficiency (OUE) in the ammonia oxidation process was nearly 100% after 300 h incubation.

In **Chapter 6**, an MABR capable of simultaneous nitrification and denitrification in a single reactor was developed to investigate the characteristics of nitrogen removal from high-strength nitrogenous wastewater, and biofilm analysis using microelectrodes and the fluorescence in situ hybridization (FISH) technique was performed. Mean removal percentages of total organic carbon (TOC) and nitrogen were 96% and 83% at removal rates of 5.76 g-C/m^2/day and 4.48 g-N/m^2/day, respectively. Dissolved oxygen microelectrode measurement revealed that the biofilm thickness was about 1600 μm, and that oxygen penetrated about 300 to 700 μm from the outer surface of the membrane. Furthermore, FISH analysis revealed that ammonia-oxidizing bacteria (AOB) were located near the outer surface of the membrane, whereas other bacteria were located from the inner to the outer part of the biofilm. These results demonstrated that simultaneous nitrification and denitrification occurred in the biofilm of the MABR system. In addition, stoichiometric analysis revealed AOB consumed 86% of the oxygen supplied through the lumen of the membrane. The result supports the main nitrogen removal pathway not via

nitrate but via nitrite in the MABR system.

7.2 Future perspectives

7.2.1 Effect of hydrophobicity on bacterial adhesion

Radiation-induced graft polymerization is a powerful tool since surface physicochemical property, *e.g.*, surface roughness and membrane potential. Hydrophobicity can also be changed if DEA membrane can be hydrophilized by ethanolamine to obtain coexisting hydroxyl groups. One of the factors to determine initial bacterial adhesion is hydrophobicity. Since the effect of hydrophobicity was not conducted in the dissertation in detail (actually its effect was evaluated a little in chapter 3), its significance on initial bacterial adhesion should be clarified.

7.2.2 Biofilm formation experiment

The biofilm formation with a flow cell was monitored with epifluorescence microscopy. The microscopy was very easy to operate; hence it would be useful to chase initial bacterial adhesion onto surfaces. However, there is a limitation when it comes to mature biofilm formation with some thickness. A confocal laser scanning microscopy (CLSM) can overcome such limitation, which will provide with more clear information, *i.e.*, three-dimensional biofilm structure on surface modified sheets. The accumulation of biofilm structure with CLSM will help us to have significant information, which leads to optimum design for biointerface of biofilm formation or prevention.

7.2.3 Introduction of mathematical modeling

To corroborate the MABR technology and allow maximum extensibility of this process to

other reactor configurations and microbial transformations, a mechanistic biofilm model should be constructed by employing the simulation program of AQUASIM. This program provides one-dimensional multisubstrate and multispecies biofilm model, which is suited best to model situations where competition between the microbial fractions of the biofilm matrix is significant. Since a uniform and robust biofilm structure can be created by applying RIGP on the PE sheet, such structure can be assumed to be one-dimensional biofilm, which facilitates to model explicitly. From engineering field, one-dimensional modeling enables us to reduce time for calculation. Essentially, the applicability of the MABR, *e.g.*, extensibility of C/N ratio, possibility of shortcut nitrogen removal and elucidation of optimum biofilm thickness for the highest nitrogen removal efficiency, should be clarified with the AQUASIM. In particular, membrane aerated biofilm has a unique biofilm structure: the region, where nitrifying bacteria is active, exists near the base of biofilm, which is opposite of conventional biofilm geometry. Ammonia, which is the substrate for nitrifying bacteria, has to pass the anaerobic and anoxic regions. Such regions play as a diffusive barrier. Too thick biofilm plays as a diffusive resistance of ammonia in the membrane-aerated biofilm, leading to deterioration of nitrogen removal efficiency. On the other hand, too thin biofilm does not produce the anoxic region for denitrification, which yields a decrease of nitrogen removal efficiency also. Therefore, the clarification of optimum biofilm thickness with use of mathematical modeling is definitely required.

7.2.4 Biofilm thickness control

In this research (especially in Chapter 6), the author indicated the significance of biofilm thickness control for stable nitrogen removal in the MABR. There are some operations to detach excess biofilm on the membrane, *e.g.*, high liquid flow rate and direct aeration to

the biofilm on the membrane; however, it would be difficult to control biofilm thickness precisely with those operations. Future study will address the elucidation of appropriate method to control biofilm thickness for maintenance of removal efficiency. The finding of the appropriate method to control the thickness will lead to validation of mechanistic model and construction of more controllable process in water environmental field, and additionally some clues to detach harmful biofilm observed in industrial and medical fields.

7.2.5 Selection of suitable membrane material

In this thesis, PE-based membrane was used as a base material through the entire experiments; however, gas-permeable membranes with higher oxygen permeability compared to PE should have been used; for instance, polypropylene (PP)- or silicone-membrane would be an alternative to the PE membrane. Especially, PP membrane should be employed because of its similar physicochemical characteristics to PE. The PP may be feasible to modify its surface by RIGP. Therefore, we should take the use of PP alternative to PE into account in the future.

Classification of the membranes falls into two types: microporous membranes such as PE and PP or dense membranes such as polydimethylsiloxane (silicone). There is the difference of mass transfer between microporous and dense membranes. Mass transfer through porous membranes is facilitated by the diffusion through the gas-filled pores where the mass transfer coefficient is directly proportional to the porosity. With thin large-pore microporous membranes, the mass transfer resistance is usually negligible. However, a drawback is that if liquid penetrates into the pores, a phenomenon dependent on the liquid side pressure and the pore diameter, a severe reduction in the mass transfer coefficient is observed. Moreover, it has also been suggested that deposition of proteins

and cell lyses would cause the pore walls to become hydrophilic and fill with liquid, leading to microporous membranes unsuitable for long-term operation. An additional drawback of this type of membrane is their low bubble point, a feature that limits the maximum intramembrane pressure if bubble formation is to be prevented. On the other hand, the mechanism for the oxygen transport through dense membranes is that of solution diffusion. High permeability lies in the fact that oxygen is four to five times more soluble in silicone than in water. Unlike microporous membranes, pore clogging and the possibility of catastrophic liquid entry into pores is not a problem. Although silicone membranes have advantage of allowing very high intramembrane oxygen pressures to be applied, the wall thickness, which affects oxygen mass transfer critically, should be thinner and thinner for the achievement of high oxygen permeability, which would be costly. Furthermore, its surface is very smooth and hence unsuitable for biofilm formation on that. To overcome the problems that both the membranes have, a composite membrane has been developed. The composite membrane puts a 1 μm polymer coating without pores, *e.g.*, polyurethane, into microporous membranes (pore size 0.04-1.0 μm) to achieve bubbleless aeration at pressures of approximately 700 kPa. Composite membranes have the advantages of microporous and dense membranes.

Summarizing these issues, the use of such composite membrane would be effective for the application to a membrane-aerated biofilm reactor. Preferably, the composite membrane made of PP should be modified for enhancement of biofilm formation by RIGP. Therefore, parallel to the development of novel membrane-aerated biofilm process and the construction of mechanistic biofilm model, suitable membranes, which enables high oxygen permeability and capacity for rapid bacterial immobilization, should be developed in the future.

7.2.6 Applicability of membrane aerated biofilm to enhanced biological phosphorus removal

The introduction of denitrifying polyphosphate-accumulating organisms (DNPAOs) into biological nitrogen removal processes has recently increased. The capacity of DNPAOs to utilize either oxygen or nitrate as the terminal electron acceptor allows for the simultaneous nitrogen and phosphorus removal from wastewater, reducing TOC and aeration demand. Additionally, the utilization of nitrate rather than oxygen leads to a lower cell yield, resulting in a lower sludge production. If oxygen can be selectively supplied only to nitrifying bacteria in a reactor, such a novel BNR process, *i.e.*, simultaneous nitrogen and phosphorus removal in a single reactor, could be realized without the need for an additional control parameter.

  The best means to satisfy this constraint is the application of a membrane-aerated biofilm to the SBR. If nitrifying bacteria are immobilized onto the membrane surface, they can be supplied directly with oxygen, facilitating effective nitrification, which results in permeation of nitrite and nitrate that is electron acceptor for DNPAOs in the bulk. Therefore, oxygen is never utilized by DNPAOs theoretically, it means that this system does not require excess organic carbon; in other words, this system is very effective even in case of low C/N ratio wastewater. Currently, this study is under way and soon or later will validate the concept from both experiment and mathematical modeling. Such an application of membrane-aerated biofilm to conventional wastewater treatment system would be promising and quite useful because this biofilm can facilitate a potential of the treatment plant when removal performance is deteriorating.

7.2.7 Concluding remarks on the future perspective

Through this thesis, the author demonstrated the significance of surface physicochemical

properties on initial bacterial adhesion, subsequent biofilm formation and process performance with the biofilm reactor. The achievements lead to the development of a novel biofilm reactor with hollow-fibers applicable to simultaneous nitrification and denitrification in a single reactor vessel. Illustration on the future perspectives is shown in Figure 7.1. In the future, more practical consideration should be conducted for robust membrane biofilm reactor technology. In order to conduct the future study, mathematical modeling will be definitely helpful to support the experimental data. The combination of experimental results obtained from micro-, meso- and macro-scale investigations and modeling results would be powerful to pave the way for development of novel biofilm reactors and the proposition of strategy to control biofilm regarding physicochemical properties and microbial population, which will result in new paradigm regarding advanced and robust biofilm reactor technology.

Furthermore, the results from Chapters 2-4 provided with some clues how we can enhance or suppress biofilm formation. The combination of the experimental results with those of mathematical modeling will yield the generalization of initial bacterial adhesion and subsequent biofilm formation. Such generalization will pave the way for new interdisciplinary field, *e.g.*, biofilm prevention in the industrial and medical fields with use of surface modified materials.
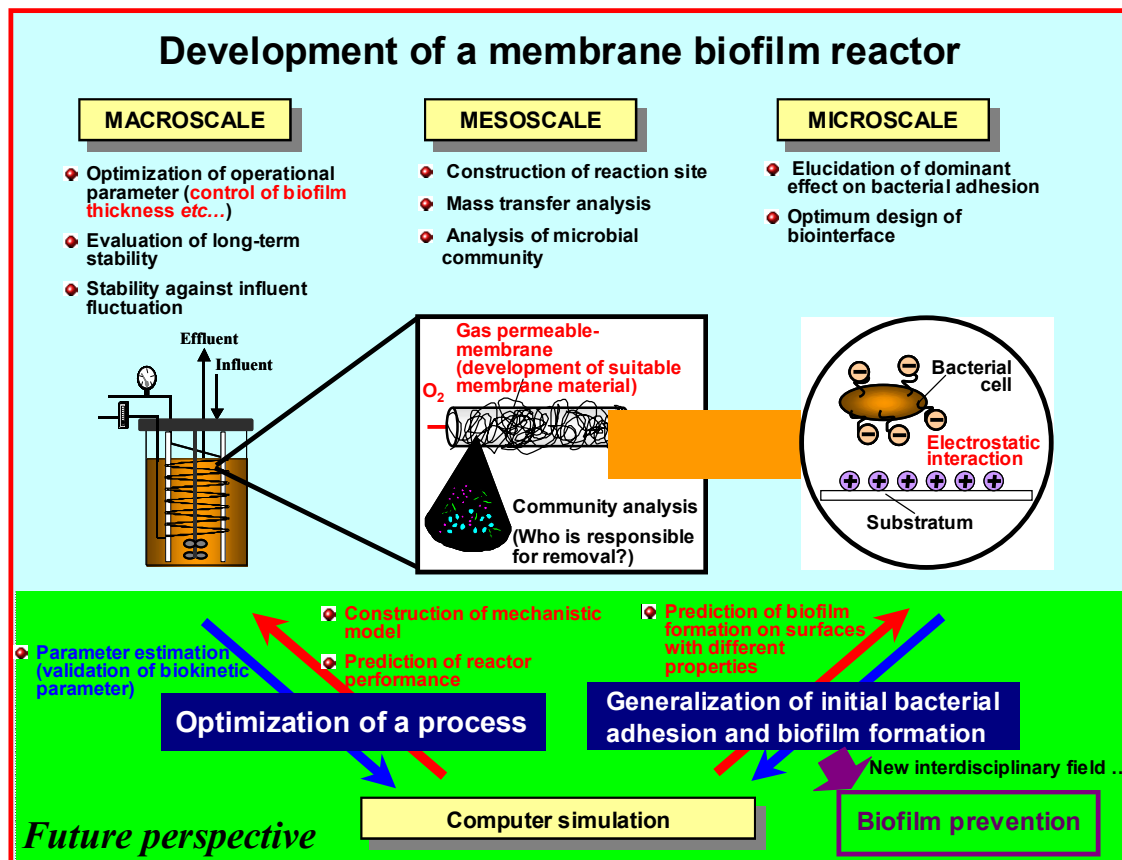
Figure 7.1 Illustration of the achievements in this research, 'development of a membrane reactor', and future perspectives.

Acknowledgement

Acknowledgement

The present thesis is the collection of the studies that have been conducted under the direction of Associate Professor Satoshi Tsuneda (Department of Chemical Engineering, Waseda University) as a supervisor. Although a PhD thesis is often seen as the author's own work, it is actually the result of many other people's helpful advice, useful suggestion and enthusiastic contribution.

I would like to express my deepest gratitude to my supervisor: Associate Professor Satoshi Tsuneda for all the valuable discussions, useful advice and encouragement through the study. Needless to say, his supervision and discussion brought me to have new insights and ideas in the field of not only environmental engineering but also surface science. I would also like to express my gratitude to Professor Emeritus Akira Hirata (Department of Chemical Engineering, Waseda University) for his heart-warming comment and supervision regarding my research.

I would like to thankful to Professor Kiyotaka Sakai, Professor Izumi Hirasawa and Assistant Professor Fukashi Kohori (Department of Chemical Engineering, Waseda University) for their constructive and useful comments.

I am grateful to Professor Masao Tamada and Mr. Akio Katakai (Takasaki Advanced Radiation Research Institute, Japan Atomic Energy Agency) for giving me an instruction about radiation-induced graft polymerization. Thanks to them, the experiments regarding

bacterial adhesion on surface modified polymer could be conducted without any problems.

I would like to my sincere gratitude to Professor Kyoichi Saito (Department of Applied Chemistry and Biotechnology, Chiba University) for his useful comment about physicochemical properties of grafted surfaces. I would also like to thank Dr. Hiroshi Hayashi (Applied Geoscience Department, Mitsubishi Material Corporation) for his useful comment regarding bacterial adhesion and great attitude toward a research. I am very grateful to Dr. Wako Takami (New Business Development Department, Asahi Kasei Chemicals) for providing us with flat sheet and hollow fiber membranes. I would also like to thank Associate Professor Takeo Yamaguchi (Department of Chemical System Engineering, University of Tokyo) and Dr. Taichi Ito (Department of Chemical Engineering, Massachusetts Institute of Technology) for providing me with measurement of membrane potential.

I am very grateful to the all members in the Tsuneda Laboratory, especially: Dr. Yoshiteru Aoi, Dr. Tatsuhiko Hoshino, Dr. Kazuaki Hibiya, Dr. Dzevo Alibegic, Mr. Naohiro Kishida, Mr. Koichi Soejima and Mr. Jun Nagai for very useful comments and advice, and Mr. Atsushi Yuasa, Mr. Ryota Igarashi, Mr. Syuichi Kaku, Mr. Tetsuya Yamamoto, Mr. Andrew Bell, Mr. Shinya Matsumoto, Ms. Maya Yamaguchi and Mr. Junpei Ito for their great help and contribution to carry out the study. Their comments and contribution brought me to finish up the thesis. I would like to express my gratitude to Ms. Hiroko Takeno, a secretary of the laboratory, for her kind and accurate support.

I have got new insights and ideas in Denmark, which leads to future researches. I have been working at Institute of Environment and Resources, Technical University of Denmark as a guest researcher from April to November 2005. I would like to express my gratitude to Professor Barth F. Smets for having fruitful discussions regarding adhesion,

biofilm formation, reactor and so on, and providing me with never-ending flow of ideas. I am also very grateful to Professor Mogens Henze, Dr. Jean-Philip Steyer, Dr. Arnaud Dechesne, Ms. Susanne Lackner, Ms. Irene Jubany Güell, Mr. Sanin Musovic, Mr. Axel Heimann and Ms. Larisa Maya Altamira (Institute of Environment and Resources, Technical University of Denmark) for having very useful comments and discussions, and sharing great time with them.

Although I could not write down all of the people who helped me a lot, I am sure that their support and encouragement lead me to finalize this thesis.

I was financially supported by a Research Fellowship for Young scientists from Japan Society for the Promotion of Science (JSPS) since 2003 to 2005 and by the Scandinavia Japan Sasakawa Foundation in 2005.

Finally, I would like to express my deepest gratitude to my family and Ms. Megumi Shimoda for their continuous encouragement and support. Without their help and cheer, I could not finish up this thesis.

January 2006

Akihiko Terada

Acknowledgement

Appendix

博士論文概要

水の世紀と言われている今日において，富栄養化の誘発因子である窒素化合物を無害化できる排水処理プロセスの開発が健全な水環境を維持していく上で重要になってきている。窒素化合物は主に微生物の代謝機能により窒素ガスに変換されて無害化されるが，硝化・脱窒反応という操作条件の全く異なる 2 つの反応を介さなければならないため，2 つの反応槽が必要である。一方で，微生物が固体表面上に付着して形成する厚い微生物細胞の層（バイオフィルム）内はその厚さ方向で全く異なる環境・微生物群集が存在し，この現象を利用することで単一槽内での硝化・脱窒反応を起こすことが可能になる。単一槽型硝化・脱窒システムを構築できれば，装置の飛躍的なコンパクト化，低コスト運転が実現できるため，環境負荷低減の観点からその意義は非常に大きい。上記システム構築のためにはバイオフィルム内にて安定した酸化・還元の反応場を創製することが必要であり，工学的課題として，迅速なバイオフィルム形成のために有利な材料表面の物理化学的性状の解明とその開発，バイオフィルム内への酸素供給の適切な制御が可能なバイオフィルムリアクターの開発の 2 点が挙げられる。

　本論文では迅速なバイオフィルムの形成および強固なバイオフィルムの創製を目指すためには材料表面の物理化学的性状と微生物細胞の初期付着の関係が非常に重要であることを鑑みて，様々な物理化学的性状を有する材料表面を作製し，その物理化学的性状と微生物細胞の付着特性および活性の評価を行った。材料表面を修飾する手段として，ラフネス・表面電荷を精密に制御可能な放射線グラフト重合（RIGP）法に着目した。また，微生物細胞が材料表面へ初期付着した後のバイオフィルム形成を追跡し，その関係解析を行った。以上より，バイオフィルム形成に有利な材料表面を用いたバイオフィルムリアクターの開発に取り組んだ。バイオフィルム内の制限物質である酸素を効率的に供給し，単一槽内で硝化・脱窒反応を安定して起こすために多孔性中空糸膜を用い，その外側のバイオフィルムに内側から酸素を供給可能な膜曝気型バイオフィルムリアクター（MABR）を構築した。最後に MABR により逐次的に硝化・脱窒反応が起こせることを水質およびバイオフィルムの解析により実証した。

　本論文は 7 章より構成されている。以下に各章の概要について述べる。

　第 1 章では，微生物細胞の界面特性および付着現象の物理化学に関する既往研究，バイオフィルム形成制御・促進のための表面修飾法，およびバイオフィルムリアクターによる窒素除去に関する既往研究を概説し，本研究の目的と意義を明らかにした。

　第 2 章では，ポリエチレン（PE）製の平膜に RIGP 法を用いてエポキシ基を有するグリシジルメタクリレート（GMA）をグラフト重合し，さらにジエチルアミン（DEA），亜硫酸ナトリウム（SS）を反応させることで材料表面を修飾した。得られた膜をそれぞれ GMA 膜，DEA 膜，SS 膜と命名した。表面修飾した材料のラフネス・膜電位はグラフト重合率に比例し，RIGP 法が材料表面の物理化学的性状を制御するのに有効な手法であることを証明した。微生物の材料表面への付着速度の評価として pH が中性付近でゼータ電位がマイナスであるグラム陰性細菌 *Escherichia coli, Pseudomonas aeruginosa, Pseudomonas putida, Pseudomonas*

fluorescens, *Paracoccus denitrificans* の 5 菌種を用いて付着試験を行ったところ，膜電位がプラスの DEA 膜に微生物は迅速に付着し，PE と比較して最大で約 30 倍の付着速度を得ることに成功した。さらに，材料の表面積あたりの微生物付着数を評価したところ，GMA 膜および SS 膜への付着促進は表面積の増加に起因すること，材料表面の膜電位が微生物細胞の付着速度を支配する主要な因子であることが明らかになった。

　第 3 章では，材料表面の膜電位に着目して，微生物細胞の付着特性および活性に関する検討を行った。RIGP 法により PE 製の平膜に GMA をグラフト重合し，1〜3 級アミンであるアンモニア（AM），エチルアミン（EA），DEA をそれぞれ反応させることで材料を作製した。得られた膜をそれぞれ AM 膜，EA 膜，DEA 膜と命名した。膜電位についてのキャラクタリゼーションを行った結果，EA 膜と DEA 膜の膜電位はそれぞれのアミノ基の密度に比例したが，AM 膜の膜電位はアミノ基の密度によらずほぼ一定であった。*E. coli* とそれぞれの材料表面への付着速度を評価したところ，付着速度は膜電位の増大により上昇すること，換言すれば静電的相互作用により微生物の付着が促進されることが統計的に示された。さらに，付着した *E. coli* の活性を核酸染色法によって評価した結果，静電的相互作用が大きくなるにつれ死菌の割合が増える傾向が得られ，特に膜電位が-8 mV 以上になると材料表面に付着している *E. coli* の生菌率が激減することが明らかになり，この閾値の前後で微生物細胞と材料表面の相互作用が大きく変化することを見出した。

　第 4 章では，材料表面の膜電位の違いがバイオフィルムの初期成長過程にどのような影響を与えるのかを検討した。PE 膜，GMA 膜，DEA 膜および SS 膜をフローセル内に設置し，*E. coli* を投入した。その後，培養基質を連続的に流入させ一定流速下のもとで形成したバイオフィルムを核酸染色し，蛍光顕微鏡下で観察した。その結果，DEA 膜には生菌と死菌が重なり合うように複雑な状態でバイオフィルムが形成されていることを確認した。一方で，PE 膜，GMA 膜および SS 膜の材料表面にはバイオフィルムの形成がほとんど確認されず，プラスに帯電している DEA 膜の材料表面と *E. coli* の細胞表面の静電的相互作用により強固なバイオフィルムが形成されることを明らかにした。以上の結果から，表面電荷がプラスに帯電した材料表面は，微生物細胞の初期付着促進のみならずバイオフィルムの形成促進に寄与している可能性が示された。

　第 5 章では，ジエチルアミノ基を導入した中空糸膜の外表面に硝化細菌を固定化し，中空糸膜内側からの酸素供給量に対する硝化速度の評価を行った。ジエチルアミノ基を有する膜表面への硝化細菌の付着速度は PE のそれと比較し約 10 倍高いことが明らかになった。また，中空糸膜内側から酸素を供給してバイオフィルム形成過程を追跡したところ，PE にはバイオフィルムがほとんど形成されなかったのに対し，ジエチルアミノ基を導入した膜には 1 ヶ月で 30 μm のバイオフィルムが形成され，表面修飾によるバイオフィルム形成促進効果が明らかとなった。無機アンモニア排水を対象として MABR の酸素供給を制御して連続運転した結果，約 1 ヶ月間亜硝酸酸化を抑えアンモニア酸化のみを起こすことに成功した。また，そのときの酸素利用効率は 100%に到達し，効率的なアンモニア酸化を達成したことから，酸素供給を精密に制御することで亜硝酸を経由する硝化・脱窒システムの構築への可能性を示唆

した。

　第 6 章では高濃度窒素含有排水の単一槽内有機物・窒素同時除去システムの開発を目指し，MABR の有機物・窒素除去特性，およびバイオフィルムの酸素濃度分布，微生物生態分布を確認し，バイオフィルム内の挙動解析および窒素除去経路の考察を行った。約 1 年間の連続運転により表面積当たりの平均窒素除去速度 4.48 g-N/(m^2·day)を達成し，高効率な窒素除去性能を有することが示唆された。微小電極を用いて測定したバイオフィルム内の溶存酸素濃度分布を解析した結果，約 1500 μm の厚みを有するバイオフィルム内にて中空糸膜の内側から供給された酸素が約 300-700 μm で完全に消費され，好気部位・無酸素部位の存在が確認された。また，Fluorescence *in situ* hybridization 法による微生物生態解析の結果より，好気部位にはアンモニアを亜硝酸に酸化するアンモニア酸化細菌が，無酸素部位には脱窒細菌を含むその他の細菌が存在していることを確認した。これらの事実から，異なる環境条件下で起こる硝化・脱窒という 2 つの反応を単一の MABR 内において起こせることを証明した。さらに，窒素除去経路の考察によりアンモニア酸化細菌は供給酸素の 86%を利用していることを確認した。この結果は硝酸を経由しないショートカットプロセスにて硝化・脱窒逐次反応が行われていた可能性を示唆するものであった。

　第 7 章では，本論文の総括および展望を記述した。

以上，本研究では微生物付着およびバイオフィルム形成促進のために材料を表面修飾し，微生物細胞との相互作用および微生物活性の評価を行った。そして，バイオフィルム形成促進のための材料開発の設計指針を明らかにし，これを硝化・脱窒逐次反応が可能な膜曝気型バイオフィルムリアクターへの開発に結びつけた。これらの研究成果は窒素除去プロセスの効率化のみならず，環境技術開発およびバイオインターフェイス開発に大きく貢献できるものと期待される。

履歴書

本籍(国籍)	東京都
現　住　所	〒192-0913　東京都八王子市北野台5-8-4 TEL　0426-35-6191
氏　　　名	てらだ　あきひこ 寺田　昭彦
生年月日	1977年5月28日

学歴

1996年　3月　都立町田高等学校　卒業

1997年　4月　早稲田大学理工学部応用化学科　入学

2001年　3月　　　　　　　同上　　　　　　卒業

2001年　4月　早稲田大学大学院理工学研究科修士課程　応用化学専攻　入学

2003年　3月　　　　　　　　同上　　　　　　　　　　修了

2003年　4月　早稲田大学大学院理工学研究科博士後期課程

　　　　　　　応用化学専攻　入学（化学工学研究）

　　　　　　　現在に至る

職歴

2003年4月　　　　日本学術振興会特別研究員（DC1）

　　　　　　　現在に至る

賞罰

2002年3月　　化学工学会　第67年会学生賞　受賞

研究業績

【論文】

(1)（報文）A. Terada, T. Yamamoto, S. Tsuneda, A. Hirata
Sequencing batch membrane biofilm reactor for simultaneous nitrogen and phosphorus removal: novel application of membrane-aerated biofilms
Biotechnology and Bioengineering (*in press*)

(2)（報文）A. Terada, T. Yamamoto, R. Igarashi, S. Tsuneda, A. Hirata
Feasibility of a membrane-aerated biofilm reactor to achieve controllable nitrification
Biochemical Engineering Journal (*in press*)

(3)（報文）A. Bell, Y. Aoi, A. Terada, S. Tsuneda, A. Hirata
Comparison of spatial organization in top-down- and membrane-aerated biofilms: A numerical study
Water Science and Technology 52 (7), 173-180 (2005)

(4)（報文）A. Terada, A. Yuasa, S. Tsuneda, A. Hirata, A. Katakai, M. Tamada
Elucidation of dominant effect on initial bacterial adhesion onto polymer surfaces prepared by radiation-induced graft polymerization
Colloids and Surfaces B: Biointerfaces 43 (2), 99-107 (2005)

(5)（報文）A. Terada, T. Yamamoto, K. Hibiya, S. Tsuneda, A. Hirata
Enhancement of biofilm formation onto surface-modified hollow-fiber membranes and its application to membrane-aerated biofilm reactor
Water Science and Technology, 49 (11-12), 263-268 (2004)

(6)（報文）寺田昭彦，日比谷和明，常田聡，平田彰
メンブレンエアレーション法を応用した単一槽内有機物・窒素同時除去システム
用水と廃水，46 (2), 148-155 (2004)

(7)（報文）A. Terada, K. Hibiya, J. Nagai, S. Tsuneda, A. Hirata
Nitrogen removal characteristics and biofilm analysis of a membrane-aerated biofilm reactor applicable to high-strength nitrogenous wastewater treatment
Journal of Bioscience and Bioengineering, 95 (2), 170-178 (2003)

(8)（報文）K. Hibiya, A. Terada, S. Tsuneda, A. Hirata
Simultaneous nitrification and denitrification by controlling vertical and horizontal microenvironment in a membrane-aerated biofilm reactor
Journal of Biotechnology, 100 (1), 23-32 (2003)

【解説】

(1) 寺田昭彦，日比谷和明，常田聡，平田彰
中空糸メンブレンを用いた新しい水処理技術
水処理技術, 44 (4), 153-164 (2003)

【講演（国際会議）】

(1) B. Andrew, Y. Aoi, <u>A. Terada</u>, S. Tsuneda, A. Hirata
Comparison of spatial organization in top-down- and membrane-aerated biofilms: A numerical study
IWA BIOFILMS 2004 Biofilm Structure and Activity, Las Vegas, USA (October, 2004)

(2) <u>A. Terada</u>, T. Yamamoto, R. Igarashi, S. Tsuneda, A. Hirata
Feasibility study of a membrane-aerated biofilm reactor to achieve controllable nitrification under oxygen-depleted conditions
IWA 4th World Water Congress, Marrakech, Morocco (September, 2004)

(3) <u>A. Terada</u>, T. Yamamoto, K. Hibiya, S. Tsuneda, A. Hirata
Enhancement of biofilm formation onto surface-modified hollow-fiber membranes and its application to membrane-aerated biofilm reactor
5th International Conference on Biofilm Systems, Cape Town, South Africa (September, 2003)

(4) <u>A. Terada</u>, R. Igarashi, S. Tsuneda and A. Hirata
Development of a membrane-aerated biofilm reactor applicable to ammonia removal from industrial wastewater
The 2nd Joint China/Japan Chemical Engineering Symposium, Shanghai, China (November, 2002)

(5) <u>A. Terada</u>, K. Hibiya, S. Tsuneda and A. Hirata
Structure and activity of a biofilm in a membrane-aerated biofilm reactor applicable to simultaneous nitrification and denitrification
Biofilms in Industry, Medicine and Environmental Biotechnology, Galway, Ireland (August, 2002)

【講演（国内）】

(1) 松本慎也，<u>寺田昭彦</u>，青井議輝，常田聡，平田彰
メンブレンエアレーションバイオフィルムにおける実験的解明およびシミュレーションモデルの構築
日本微生物生態学会第21回大会， 福岡（2005年10月発表）

(2) 松本慎也，<u>寺田昭彦</u>，青井議輝，常田聡，平田彰
バイオフィルム内の微生物生態構造の実験的解明およびシミュレーション解析
化学工学会関東支部50周年記念大会， 東京（2005年8月発表）

(3) <u>寺田昭彦</u>，湯浅敦，常田聡，平田彰
材料表面の物理化学的性質が微生物付着およびバイオフィルム形成に及ぼす影響の評価
化学工学会第70回大会， 名古屋（2005年3月発表）

(4) 松本慎也，Bell Andrew，<u>寺田昭彦</u>，青井議輝，常田聡，平田彰
トップダウンおよびメンブレンエアレーションバイオフィルムにおける硝化細菌群の生態構造の比較
化学工学会第70回大会， 名古屋（2005年3月発表）

(5) 寺田昭彦，山本哲也，常田聡，平田彰
メンブレンエアレーション型 SBR による窒素・リン同時除去
日本水環境学会第39回年会，千葉（2005年3月発表）

(6) 湯浅敦，寺田昭彦，常田聡，平田彰
材料表面の物理化学的性質と微生物付着性および付着時の活性との関係
日本微生物生態学会第20回大会バイオフィルム研究部会，仙台（2004年11月）

(7) 賀來周一，寺田昭彦，常田聡，平田彰
水素供与型メンブレン及び繊維状担体を用いた脱窒リアクターの開発
日本水処理生物学会第41回大会，つくば（2004年11月）

(8) 湯浅敦，寺田昭彦，常田聡，平田彰
材料表面の物理化学的性質と微生物の付着性との関係解析
化学工学会秋田大会，秋田　（2004年7月）

(9) 寺田昭彦，山本哲也，常田聡，平田彰
メンブレンエアレーション法による低 C/N 比からの有機物・栄養塩同時除去
日本水環境学会第37回年会，熊本（2003年3月）

(10) 寺田昭彦，永井潤，日比谷和明，常田聡，平田彰
メンブレンエアレーションリアクタの窒素除去特性と生物膜解析
化学工学会第67年会，福岡 (2002年3月)

(11) 永井潤，日比谷和明，寺田昭彦，常田聡，平田彰
生物膜内における基質・酸素浸透深さおよび微生物活性部位の流入負荷変動に対する応答性
化学工学会第66年会，広島 (2001年4月)

(12) 日比谷和明，永井潤，寺田昭彦，常田聡，平田彰
微小電極法を用いた生物膜内基質濃度分布の測定
化学工学会第33回秋季大会，浜松 (2000年9月)

【特許】

(1) 　常田聡，平田彰，寺田昭彦
排水処理装置及び排水処理槽
特願 2004・274386